THE HYDRAULIC JUMP AT AN ABRUPT ENLARGEMENT

A THESIS SUBMITTED TO
THE GRADUATE SCHOOL OF NATURAL AND APPLIED SCIENCES
OF
THE MIDDLE EAST TECHNICAL UNIVERSITY

BY

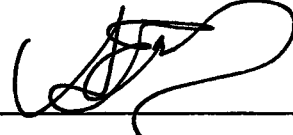TUNCAY KAAN ALBAYRAK

IN PARTIAL FULFILLMENT OF THE REQUIREMENTS

FOR THE DEGREE OF

MASTER OF SCIENCE

IN

THE DEPARTMENT OF CIVIL ENGINEERING

NOVEMBER 1997

Approval of the Graduate School of Natural and Applied Sciences

Prof.Dr. Tayfur Öztürk
Director

I certify that this thesis satisfies all the requirements as a thesis for the degree of Master of Science

Prof.Dr Fuat Erbatur
Head of Department

This is to certify that we have read this thesis and that in our opinion it is fully adequate, in scope and quality, as a thesis for the degree of Master of Science

Assoc. Prof.Dr. Nuray Denli Tokyay
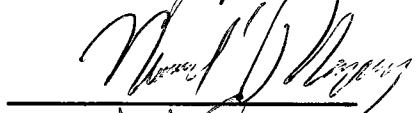Supervisor

Examining Committee Members

Prof.Dr. Metin Ger

Prof. Dr. Tülay Özbek

Prof. Dr. Mustafa Göğüş

Assoc. Prof. Dr. Nuray Denli Tokyay

Asst. Prof. Dr. Zafer Bozkuş

ABSTRACT

HYDRAULIC JUMP AT AN ABRUPT ENLARGEMENT

Albayrak,Tuncay Kaan

M.S., Department of Civil Engineering

Supervisor : Assoc. Prof. Dr. Nuray Denli Tokyay

November 1997, 108 pages

The hydraulic jump at an abrupt enlargement may occur in two different forms namely R-jump and S-jump depending on the upstream Froude number, the relative magnitudes of the tailwater depth and the width ratio with respect to the initial depth of the jump. The characteristics of the R- and S-jumps at an abrupt enlargement have been investigated both experimentally and theoretically. To predict the relative depth ratio for known upstream conditions, the momentum equation is written for the outlet section and the end of the jump. For R-jumps, a coefficient of friction is introduced to estimate the friction force. For S-jumps, to calculate the pressure force on the expanded walls, the backed-up depth is simply estimated as the arithmetic mean of the depths of the jet at the outlet and tailwater. The data obtained from the experiments on R- and S-jumps are compared with the new approaches introduced in the present study and the approaches in the literature. For practical design purposes, a scaling factor called as modified Froude number, is introduced.

Key Words: Hydraulic Jump, Abrupt enlargement, R-Jump, S-Jump, Modified Froude Number

ÖZ

ANİ KANAL GENİŞLEMELERİNDE OLUŞAN HİDROLİK SIÇRAMA

Albayrak, Tuncay Kaan

Yüksek Lisans, İnşaat Mühendisliği Bölümü

Tez Yöneticisi : Doç. Dr. Nuray Denli Tokyay

Kasım 1997, 108 sayfa

Ani kanal genişlemelerinde hidrolik sıçrama, menba suyu Froude sayısına, kuyruk suyu ve genişleme oranına bağlı olarak iki değişik şekilde oluşur. Bu oluşumlar, R-tipi sıçrama ve S-tipi sıçrama olarak adlandırılmaktadır. R- ve S-tipi sıçramalar hem deneysel hem de teorik olarak incelenmiştir. Belirli menba suyu Froude sayısına ve genişleme oranına bağlı olarak,her iki sıçrama için, genişlemenin hemen başı ile sıçramanın sonu arasında momentum denklemleri kurularak kuyruk suyu yüksekliği hesaplanmasında teoriler geliştirilmiştir. R-tipi sıçramada sürtünme kuvvetinin, S-tipi sıçramada ise genişleme duvarlarında oluşan kuvvetin hesaplanması için yeni yaklaşımlar geliştirilmiştir. Deney verileri, literatürdeki yaklaşımlar ve yeni yaklaşımlar ile kıyaslanmıştır. Pratik tasarım yöntemleri için, uyarlanmış Froude sayısı ölçek faktörü olarak tanımlanmıştır.

Anahtar Kelimeler:Hidrolik Sıçrama, Ani Kanal Genişlemeleri, R-tipi Sıçrama, S-tipi Sıçrama, Uyarlanmış Froude Sayısı

To My Family

ACKNOWLEDGMENTS

TABLE OF CONTENTS

LIST OF FIGURES

Figures

LIST OF TABLES

LIST OF SYMBOLS

y	the depth of flow ;
u	the mean velocity of flow;
b	the width of the supercritical stream;
t	subscript to denote the tailwater;
o	subscript to denote the upstream flow;
B	the width of the expanded section;
Y	relative depth ratio;
α	relative width ratio;
F_r	Froude number;
Q	discharge;
q	unit discharge;
g	gravitational acceleration;
F_f	the bed shear force;
C_s	consolidated shear force coefficient;
F_w	the pressure force on the channel enlargement;
F	the specific force;
γ	the specific weight of fluid;
E	energy of the flow;
E_l	head loss through the jump;
L_j	length of the jump;
L_r	length of the surface roller;
L_o	length of separation zone in R-jump;
L_l	length between outlet and the toe of R-jump;
ρ	mass density of fluid;
θ	parameter used for backed-up depth.
F_M	Modified Froude Number

CHAPTER I

INTRODUCTION

1.1   General

Hydraulic jump is a local phenomenon which transfers a supercritical flow into a subcritical one, accompanied by considerable turbulence and energy loss. Therefore, the hydraulic jump may be practically used to dissipate energy in water flowing over dams, weirs, and other hydraulic structures. When a flow takes place over a spillway or under a sluice gate, it becomes supercritical and has a tremendous kinetic energy. As a result, erosion of the channel downstream from the structure may take place. Hence, for such flows, in order to prevent erosion, a considerable portion of kinetic energy of the flow must be dissipated. Various methods of energy dissipation might be used.

One of the most effective methods for the energy dissipation is to form a hydraulic jump. As the flow becomes subcritical after the jump, the velocity of the flow will reduce and hence it becomes incapable of scouring the downstream channel bed.

There are other practical applications of the hydraulic jump, (Chow, 1958), such as; "(i) to recover head or raise the water level on the downstream side of a measuring flume and thus maintain high water level in the channel for irrigation or other water distribution purposes. (ii) to increase weight on an apron

1

and thus reduce uplift pressure under a masonry structure by raising the water depth on the apron. (iii) to increase the discharge of a sluice by holding back tailwater, since the effective head will be reduced if the tailwater is allowed to drawn the jump. (iv) to indicate special flow conditions, such as the existence of supercritical flow or the presence of a control section so that a gaging station may be located; (v) to mix chemicals used for water purification; (vi) to aerate water for city water supplies; and (vii) to remove air pockets from water-supply lines and prevent air locking."

Whenever a hydraulic jump is used as an energy dissipater, it is usually confined to a paved channel section which is known as the stilling basin. In practice, to reduce the size and hence the cost of the stilling basin, some accessories such as sills, baffle blocks, abrupt and gradual channel bottom variations (positive and negative steps) or channel enlargements are used. Such controls have additional advantages for it improves the dissipation function of the basin, stabilizes the jump action and in some cases increases the factor of safety.

Although the simple hydraulic jump has been studied in literature for about 150 years, the hydraulic jump at an abrupt expansion has been studied only during the last two decades. Former researches show that although the hydraulic jump at an abrupt enlargement requires smaller tailwater depths than that of simple hydraulic jump with the same upstream conditions, the energy dissipation is much greater than that of simple jump. This means hydraulic jump at an abrupt enlargement is a powerful energy dissipater and needs a shallower basin which may reduce the cost.

Moreover, hydraulic jump at sudden expansion may also take place if only one of the gate is open in a flow through many gated overflow spillways. In these respects, the hydraulic jump forming at an abrupt enlargement needs to be studied. In the present study, the hydraulic jumps at abrupt enlargements have been studied both experimentally and theoretically.

1.2 Formation Of A Hydraulic Jump At An Abrupt Enlargement

The hydraulic jump at an abrupt enlargement may occur in two different forms depending on the upstream Froude number, the relative magnitudes of the tailwater depth and the width ratio with respect to the initial depth of the jump.

Consider a supercritical flow in a rectangular channel which has an abrupt symmetrical expansion in width. As the supercritical flow enters the abrupt enlargement, it expands freely until it occupies the full width of the channel and then creates a system of diagonal surface waves due to successive reflections. However, if the flow at a downstream section of the enlargement is subcritical, a hydraulic jump with an oblique front is formed somewhere downstream. With an increase in the tailwater depth, the jump moves upstream and its front gradually becomes normal. However, the jump soon reaches a *limiting position*. Any further increase in the tailwater depth causes the jump to collapse and the tailwater spills on the upstream supercritical flow, the jet twists and deflects to one side of the expanded section, creating an unstable nonuniform flow situation. The jump formed under this tailwater condition is termed the *repelled jump* and is designated as *R-JUMP*, (Rajaratnam, 1968).

With a further increase in the tailwater level, the outlet gradually submerges, but the jet still be unstable, oscillating rather violently. However, at a certain higher tailwater level, the jet ceases to oscillate, the flow becomes stable and phenomenon resembles the familiar hydraulic jump with small submergence. The minimum tailwater situation at which the stable flow takes place after the collapse of the R-jump is designated as *stable (spatial) jump or S-JUMP*,(Rajaratnam, 1968). Further increase in the tailwater causes greater submergence and the flow resembles a submerged jump.

1.3   Review of Literature

In 1961, *Unny* investigated the spatial hydraulic jumps in a channel expansion. His paper deals with a fundamental physical analysis of the spatial jump. He thought that the existing formula for the depth ratio in a spatial jump are more or less empirical in nature and contain many inconsistencies. By putting proper boundary conditions to the well known formula for the classical jump, he has developed a new formula. As a result of experiments, he showed that the factors introduced into the general formula were absolute constants and supported his theoretical analysis.

In 1964, *Kuznetsov* investigated the free horizontal spread of the streamflow in the tailwater of hydro structures, which is useful for the selection of the best shape of the chute outlets. As a result of the tests performed, Kuznetsov (1964) gave an equation for the computation of the sequent depth of the R-jump which includes an empirical coefficient to take into account the nonuniform

4

distribution of velocity and discharge across the cross section of the channel.

In 1968, *Rajaratnam and Subramanya* investigated the hydraulic jump at an abrupt expansion both theoretically and experimentally. They defined the jumps as R-Jump and S-Jump. They derived the expressions related with R-Jump and S-Jump. They saw that at the tailwater ranges between R-Jump and S-Jump, unstable and undesirable flow conditions occurred. For R-Jump, the momentum equation which neglects the total bed shear force could not predict the sequent depth and an empirical equation to predict the sequent depth had been developed. For S-Jump, they compared their experimental results with the equations of Abramov and Unny, and an equation obtained from simple momentum equation, and stated that all was unsatisfactory for predicting the sequent depth. The length characteristics of both jumps had also been studied.

In 1972, *Herbrand* studied the spatial hydraulic jump both theoretically and experimentally. A simple, usable relationship was established for designing a laterally expanded stilling basin. No consideration was made for wall friction influence or for the coefficients of velocity and pressure distribution in the end sections. The investigator showed that a shallower stilling basins is occurred and the spatial hydraulic jump tends to augment the instability and asymmetry of the discharge, and for spatial jumps, energy dissipation is greater than in regular basins.

In 1984, *Hager* analyzed the hydraulic jump in non-prismatic, rectangular, horizontal channels. Distinction is made between the cases in which flow is non-separated and separated from the

5

channel side-walls, respectively. Results included a rational prediction of the sequent depth ratio in terms of the inflow Froude number and the channel width ratio, the relative energy dissipation and the length characteristics of the roller and the jump. His study aimed to establish rational hydraulic approaches for hydraulic jump in gradual and abrupt channel enlargements. The results were compared with each other and with the classical jump in prismatic rectangular channels. Several advantages of the channel enlargements was discussed in Hager's studies. He also observed that Herbrand investigated jumps located just at the transition zone while Rajaratnam considered jumps downstream of the abrupt enlargement.

1.4 Scope of The Present Study

In the present study, the characteristics of the hydraulic jumps at abrupt enlargements are studied both theoretically and experimentally for different width ratios. General one-dimensional momentum equation is used for the analysis of the jump. For R-jumps, a coefficient of friction is introduced to predict the relative depth ratio for a given geometry and upstream flow conditions. The case, in which friction force is neglected, is also studied. For S-jumps, to predict the relative depth ratio, it is important to estimate the force on the expanded walls, and hence the backed-up depth. The backed-up depth is approximated as a simple arithmetic mean of the depth of the jet at the outlet section and the tailwater and a prediction formula for the relative depth ratio is obtained from momentum equation. The results are compared with the data obtained in the present study and the data available in literature. A modified Froude number is introduced as a scaling factor both for R- and S-jumps. The relative depth ratio

both for R- and S-jumps are obtained as a function of modified Froude number. The length characteristics and the energy dissipation in both jumps are also studied.

The theoretical considerations in the literature and the new approaches are given in Chapter II. Experiments done for R-Jump and S-Jump are explained in Chapter III. The observations on the flow and the results, and the discussion of the results are given in Chapter IV. Conclusions and recommendations are presented in Chapter V. The data obtained in the present study and the available data in literature are given in Appendix.

CHAPTER II

THEORETICAL CONSIDERATIONS

2.1 General

At an abrupt enlargement, hydraulic jump occurs in two different forms, depending on the upstream Froude number, relative magnitudes of the tailwater depths and the width ratio. These two forms which are designated as R-Jump and S-Jump, are shown in Fig. (2.1) and Fig. (2.2).

In Fig. (2.1) and Fig. (2.2) ; y_o and u_o are the depth and the mean velocity at the outlet section, respectively; y_t and u_t are the tailwater depth and the corresponding velocity, respectively, b is the width of the supercritical stream and B is the width of the expanded section where the jump takes place.

At an abrupt expansion in width, either R-Jump or S-Jump will occur depending on the relative depth ratio, $Y = y_t/y_o$, for a given relative width ratio, $\alpha = b/B$, and the Froude number of the upstream supercritical flow, $F_{ro} = q_o / \sqrt{g y_o^3}$

8

Surface Roller

y_t

u_t

y_g u_o y_o

(1)

Outlet Section

(2)

End of the Jump

Sectional View

L_1

L_o

L_r

y_g b y_o

y_t
B

L_j

Plan View
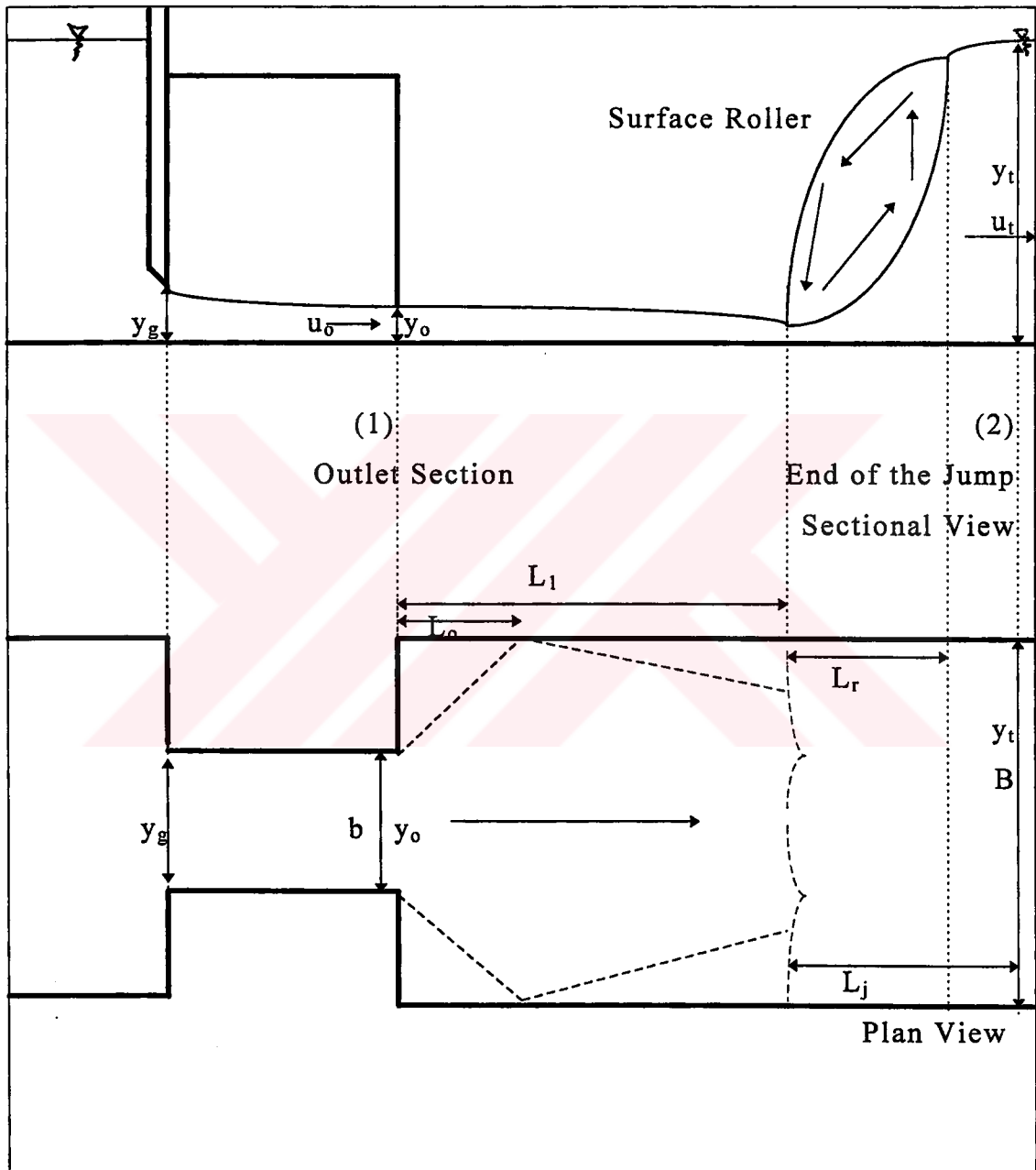
Fig. (2.1)   Definition Sketch For R-Jump.

9
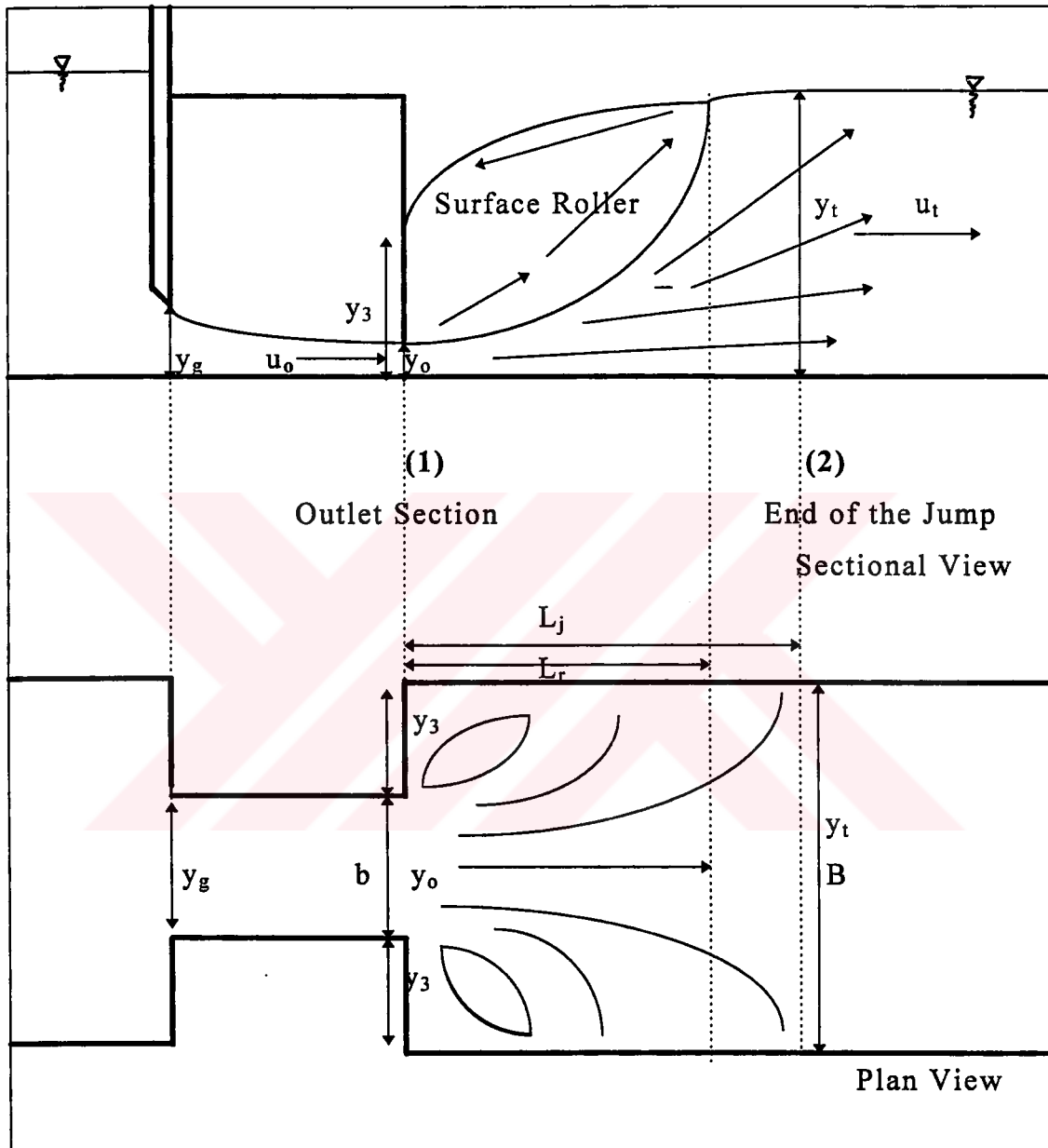
Fig. (2.2)   Definition Sketch For S-Jump.

10

2.2 Occurrence Of A Hydraulic Jump At An Abrupt Enlargement

If a supercritical flow in a rectangular channel enters to a channel section where the width is enlarged abruptly, it expands freely until it occupies the full width of the channel and forms oblique surface waves which reflect and appear as a system of diagonal surface waves. If this supercritical flow encounters a tailwater depth of a subcritical flow, then a hydraulic jump with an oblique front is formed somewhere downstream. With an increase in the tailwater depth, the jump moves upstream and its front gradually becomes normal. Under this tailwater condition, R-Jump is formed. If the tailwater depth is slightly greater than the sequent depth of the R-jump, an unstable nonuniform flow is created and backward flow sets in and the jet twists and deflects to one side of separation zone. If the tailwater depth is further increased, the outlet gradually submerges, but the jet still be unstable, oscillating rather violently. At a certain higher tailwater depth, the flow becomes stable and S-Jump with small submergence is occurred. Further increase of tailwater causes greater submergence and the flow resembles a submerged jump.

For the given upstream conditions of a hydraulic jump, to obtain the downstream condition, one dimensional linear momentum equation has successfully been used in literature. In the application of the momentum equation to a hydraulic jump at an abrupt enlargement, it is necessary to estimate the pressure distribution and magnitudes of the forces acting on the corners of the enlargements and the wall shear stresses.

11

2.3 General Momentum Equation Applied To Hydraulic Jump At An Abrupt Enlargement

To predict the tailwater depth, y_t, for the hydraulic jump at an abrupt enlargement, the momentum equation can be written between the sections (1) and (2) as shown in Fig. (2.3).
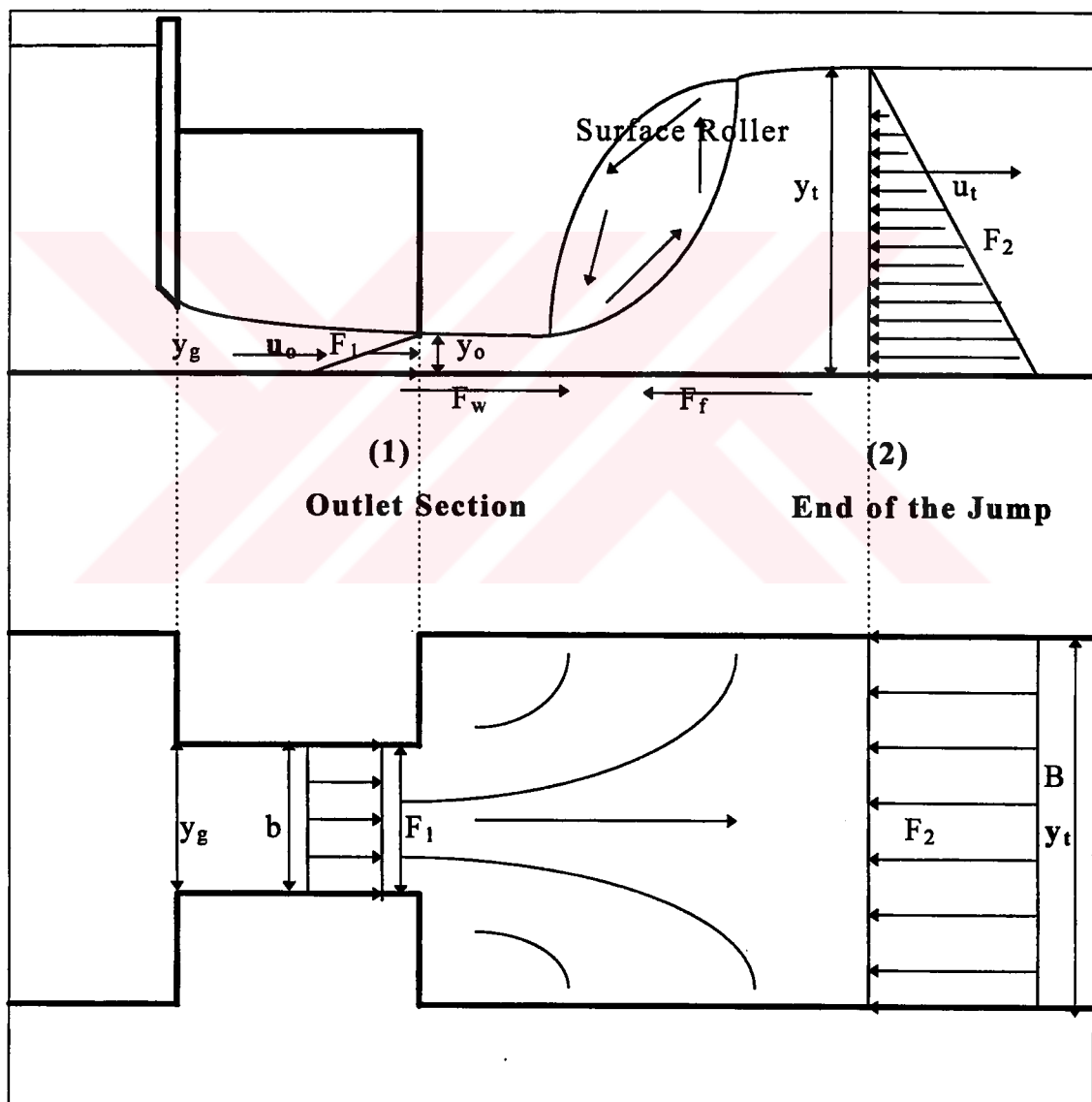
Figure (2.3.a)   Forces Acting On The Fluid Body For R-Jump.
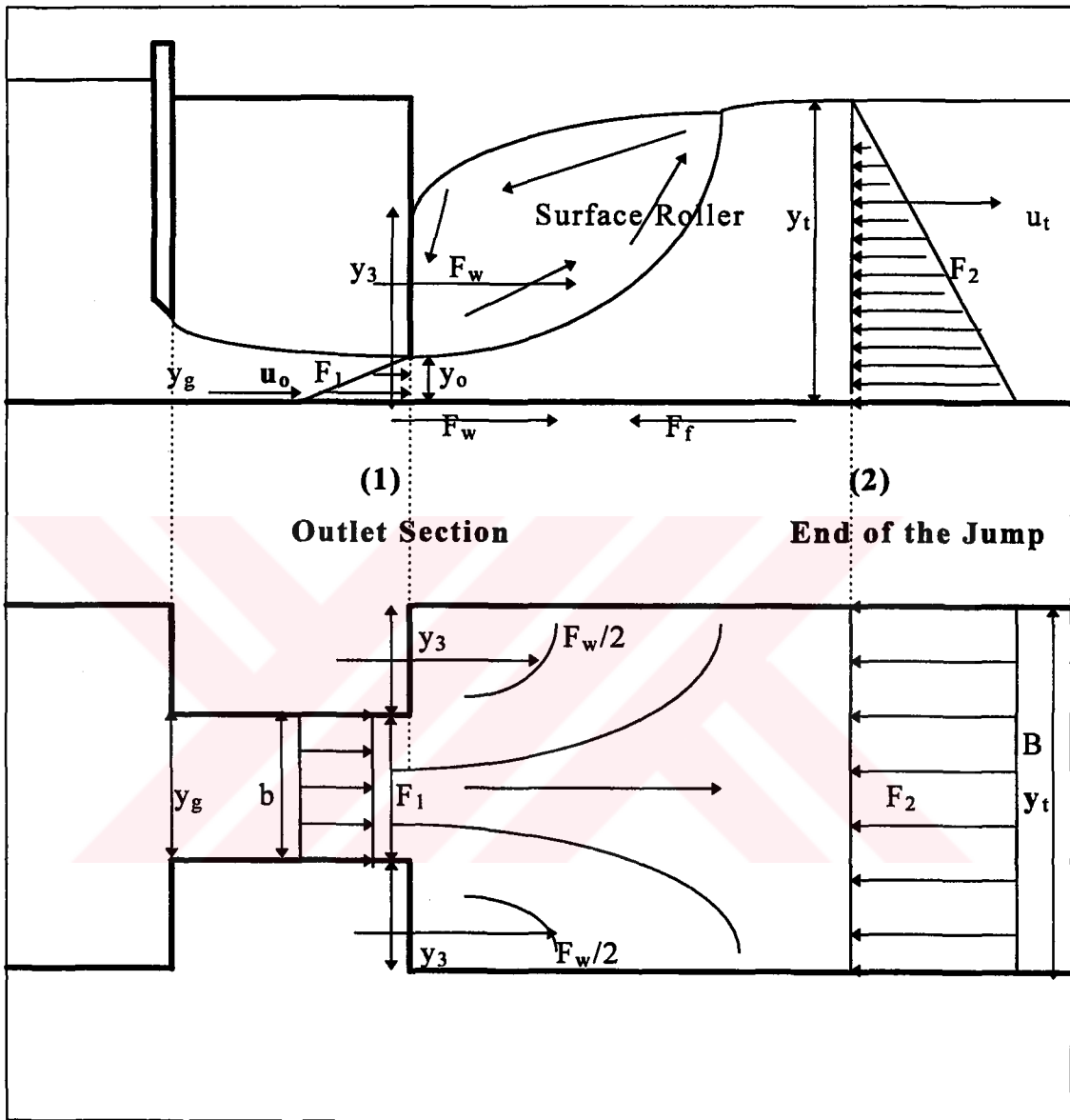
Figure (2.3.b)   Forces Acting On The Fluid Body For S-Jump.

By assuming that the pressure distribution at sections (1) and (2) are hydrostatic and the momentum correction factors, β_1 and β_2, may be taken as unity, the momentum equation between section (1) and section (2) can be written as

$$bF_1 + \frac{F_w}{\gamma} = BF_2 + \frac{F_f}{\gamma} \quad\dotfill(2.1)$$

where;

F_f :the bed shear force between sections (1) and (2),

F_w :the pressure force on the water due to channel enlargement,

γ : the specific weight of fluid.

F_i :the specific force at i^{th} section, i =1,2 and defined as

$$F_i = \frac{1}{2} y_i^2 + \frac{q_i^2}{gy_i}, \qquad i=1,2 \qquad \dotfill(2.2)$$

where;

y_i :the depth of flow at i^{th} section,

q :the unit discharge,

g :the acceleration of gravity,

Substitution of Eq. (2.2) into Eq. (2.1) yields that

$$b(\frac{1}{2}y_o^2 + \frac{q_o^2}{gy_o}) - B(\frac{1}{2}y_t^2 + \frac{q_t^2}{gy_t}) = \frac{(F_f - F_w)}{\gamma} \quad\dotfill(2.3)$$

Dividing both side of Equation (2.3) by $(\frac{1}{2}By_o^2)$, the equation can be written as

$$\frac{b}{B}(1 + \frac{2q_o^2}{gy_o^3}) - (\frac{y_t^2}{y_o^2} + \frac{2q_t^2}{gy_t}\frac{1}{y_o^2}) = \frac{2(F_f - F_w)}{B\gamma y_o^2} \quad\dotfill(2.4)$$

14

Let $Y = y_t/y_o$ be the depth ratio and $\alpha = b/B$ be the relative width ratio, and $F_{ro}^2 = q_o^2/gy_o^3$ be the Froude number of the upstream supercritical flow. In terms of these variables defined, and by using the equation of continuity, $q_t = \alpha q_o$, Eq. (2.4) can be written as

$$\alpha(1 + 2F_{ro}^2) - (Y^2 + \frac{2\alpha^2 F_{ro}^2}{Y}) = \frac{2(F_f - F_w)}{B\gamma y_o^2} \qquad \dots\dots\dots(2.5)$$

For the known upstream flow conditions (F_{ro} and y_o) and the channel geometry (α), Eq. (2.5) can be solved for the depth ratio Y, provided that the values of F_f and F_w are known.

The friction force F_f and the force on the expanded walls, F_w, take different values depending on the type of jump, that is whether an R-jump or S-jump takes place.

2.3.1 R-Jump

Experiments show that, the two triangular areas (Fig. 2.1) formed at the corners of the abrupt enlargement contain almost no water. Hence, in case of R-jumps F_w can be taken as zero. On the other hand, the friction force can be written as (Rajaratnam and Subramanya, 1968).

$$F_f = C_s \rho Q u_o \qquad \dots\dots\dots\dots\dots\dots\dots\dots\dots\dots\dots\dots\dots\dots\dots(2.6)$$

where C_s = a consolidated shear force coefficient.

15

By taking $F_w = 0$, and using Eq. (2.6), the right-hand side of the Eq. (2.5) can be written as

$$\frac{2F_f}{\gamma By_o^2} = 2C_s\alpha F_{ro}^2 \qquad\qquad ....(2.7)$$

By inserting Eq. (2.7) into Eq. (2.5) and rearranging it, the following equation can be obtained ;

$$Y^3 - \alpha (\ 1 + 2F_{ro}^2\ (1-C_s))Y + 2F_{ro}^2\ \alpha^2 = 0 \qquad ....(2.8)$$

Solution of Eq. (2.8) depends on the form and the value of C_s.

The approximations on estimation of the force F_f and/or C_s , and hence the solution of Eq. (2.8) in literature can be summarized as follows:

(i) Kuznetsov Approach :

Kuznetsov (1964) studied the formation of a hydraulic jump at an abrupt enlargement experimentally, and gave a relation to compute the sequent depth of the jump as

$$Y = \frac{K}{2}(\sqrt{(\alpha^2 + 8F_{ro}^2\alpha)} - \alpha) \qquad\qquad ....(2.9)$$

where $K = f(\alpha)$, and it is given as

$$K = 0.8-(0.9-\ \alpha)0.15 = 0.665+0.15\ \alpha \qquad ....(2.10)$$

16

(ii)   Rajaratnam and Subramanya Approach :

Rajaratnam and Subramanya (1968) investigated the hydraulic jump at an abrupt enlargement both theoretically and experimentally. They introduced the definitions of R- and S-jumps. In their theoretical analysis, the momentum equation was written between the outlet section and the section where the jump ends. The pressure distribution at the two sections is assumed to be hydrostatic and the momentum correction factors taken as unity. The force on the expanded walls F_w are taken as zero. On the other hand, by neglecting the friction force, an approximate solution of Eq. (2.8) is given as

$$Y = \frac{1}{2}(\sqrt{(\alpha^2 + 8F_{ro}^2\alpha)} - \alpha) \qquad \qquad \ldots\ldots\ldots\ldots\ldots(2.11)$$

When $\alpha=1$, Eq. (2.11) becomes the well-known solution of simple hydraulic jump.

Rajaratnam and Subramanya (1968) stated that the coefficient K in Kuznetsov approach is apparently used to account for the neglect of friction force. They also tested the validity of Eq. (2.10), by using the data collected in their study. Their results show that K is a function of both F_{ro} and α; only beyond a certain value of F_{ro} does K become independent of F_{ro}. It is also stated that the values of K obtained in their study are considerably larger than those predicted by Eq. (2.10).

The friction force F_f is approximated by introducing a consolidated shear force coefficient as given in Eq. (2.6). It is

also shown that for a given value of α, C_s increases with F_{ro} to a certain value beyond which it is constant. The constant value of C_s increases with decreases in the value of α.

The depth ratio Y is expressed by an empirical relation for the values of α in the range 0.30 to 0.90 as

$$Y = 0.75 + (\alpha+0.30)(F_{ro} -0.85) \quad \ldots\ldots\ldots\ldots\ldots\ldots(2.12)$$

(iii) New Approach

In the present study, for the solution of Eq. (2.8), two approaches are considered; the first approach assumes that the friction force, F_f, is negligible and hence $C_s = 0$; in the second approach, the consolidated shear force coefficient C_s is considered as a function of α.

a) If friction force, F_f is negligible, then $C_s = 0$. Therefore Eq. (2.8) reduces to:

$$Y^3 - \alpha (1+ 2F_{ro}^2)Y + 2F_{ro}^2 \alpha^2 = 0 \quad \ldots\ldots\ldots\ldots\ldots(2.13)$$

The solutions of third-degree polynomial given by Eq. (2.13) are quite complicated. However, an approximate solution can be obtained with an error in the order of $(\alpha^2-\alpha^3)$. By adding a term $(\alpha^2-\alpha^3)$, Eq. (2.13) can be written as :

$$Y^3 - \alpha (1+ 2F_{ro}^2)Y + \alpha^2 (1+ 2F_{ro}^2) - \alpha^3 = 0 \quad \ldots\ldots\ldots(2.14)$$

Y=α is a solution of Eq. (2.14). Therefore it can be reduced to a second degree polynomial as

$$Y^2 + \alpha Y - \alpha(1+ 2F_{ro}^2) + \alpha^2 = 0 \qquad \text{.......................(2.15)}$$

The positive root of Eq. (2.15) is :

$$Y = \frac{1}{2}(\sqrt{(4\alpha(1+2F_{ro}^2)-3\alpha^2)} - \alpha) \qquad \text{.................(2.16)}$$

When α=1, it reduces to the well-known simple hydraulic jump relation.

b) If F_f is not negligible, then it is necessary to know the value of C_s. Rajaratnam and Subramanya (1968) noted that $C_s = C_s\ (\alpha, F_{ro})$, and that as α decreases, C_s increases. Also, the increase in C_s with the increase in F_{ro} is quite small. In the present study, considering all these arguments, C_s is taken to be a function of α only. A simple relation for C_s , enhancing convenience for the solution and in agreement with the aforementioned physical aspects, may be assumed as

$$C_s = 1 - \sqrt{\alpha} \qquad \text{...(2.17)}$$

By substituting Eq. (2.17) , Eq.(2.8) can be written as

$$Y^3 - \alpha\ (1+ 2\sqrt{\alpha}F_{ro}^2)Y + 2\alpha^2 F_{ro}^2 = 0 \qquad \text{...............(2.18)}$$

$Y = \sqrt{\alpha}$ is a solution of Eq.(2.18). Therefore it can be reduced to a second degree polynomial as

$$Y^2 + \sqrt{\alpha}Y - 2\alpha\sqrt{\alpha}\ F_{ro}^2 = 0 \qquad \text{.............................(2.19)}$$

The positive root of Eq. (2.19) is then given by

$$Y = \frac{1}{2}\sqrt{\alpha}\left(\sqrt{(1 + 8\sqrt{\alpha}\,F_{ro}^2)} - 1\right) \qquad \ldots\ldots\ldots\ldots(2.20)$$

When $\alpha=1$, it reduces to the simple hydraulic jump relation.

Modified Froude Number for Abrupt Enlargement

The momentum equation for hydraulic jump occurring at an abrupt enlargement reduces to Eq. (2.13) if the right-hand side of Eq.(2.5) is negligible.

Considering that the friction force F_f and the force on the wall have an effect to cancel each other, the following analysis can be done:

Let $v=1/Y$, then Eq. (2.13) can be written as

$$v^3 - \frac{(1+2F_{ro}^2)\alpha v^2}{2\alpha^2 F_{ro}^2} + \frac{1}{2\alpha^2 F_{ro}^2} = 0 \qquad \ldots\ldots\ldots\ldots(2.21)$$

as Y becomes very large, v^3 will approach to zero. Therefore Eq.(2.21) will reduce to

$$(1+ 2\,F_{ro}^2)\alpha v^2 = 1 \qquad \ldots\ldots\ldots\ldots\ldots(2.22)$$

Now replacing v^2 by $1/Y^2$ and solving for Y, one can get that

$$Y = \sqrt{\alpha(1+2F_{ro}^2)} \qquad \ldots\ldots\ldots\ldots\ldots\ldots(2.23)$$

Let us define the modified Froude number as

$$F_M = \sqrt{\alpha(1 + 2F_{ro}^2)} \qquad \dots\dots\dots\dots\dots\dots\dots\dots\dots(2.24)$$

In order to take into account the terms neglected the relative depth ratio may be considered as a function of F_M, i.e.

$$Y = f(F_M) \qquad \dots\dots\dots\dots\dots\dots\dots\dots\dots\dots(2.25)$$

2.3.2 S-Jump Studies

When an R-jump takes place at an abrupt enlargement, any increase in the tailwater causes the jump to collapse and the tailwater spills on the upstream supercritical flow, and a backward flow sets in and the jet twists and deflects to one side forming an unstable flow. Further increase in tailwater will submerge the outlet and at a certain tailwater level , a kind of submerged stable jump will occur. This type of jump is named as S-jump.

In formulating the general momentum equation for a simple hydraulic jump, friction force is neglected and average cross sectional values are used without any correction to account for nonuniform velocity distribution. This approach has been justified for all practical purposes, because the effects of the local and time variations of velocity as well as that of the non-hydrostatic pressure and the air entrainment on the depth ratio are small and, in part, tend to cancel each other out. By the same reasoning the friction force may be disregarded in case of S-jumps.

In case of S-jumps, although the friction force may be neglected, the force on the expanded walls must be considered. By neglecting the friction force in Eq. (2.8) and solving it for F_{ro} , one can obtain that

$$F_{ro}^2 = \frac{Y^3 - \alpha Y - \dfrac{2F_w}{\gamma B y_o^2} Y}{2\alpha(Y - \alpha)} \qquad \dots\dots\dots\dots\dots\dots(2.26)$$

The solution of Eq. (2.26) depends on the value of F_w.

There are several investigations on S-jump in literature which may be summarized as follows:

(i) Unny Approach :

Unny (1961) has obtained a semiempirical formula for the case of $\alpha = 0.50$,

$$Y = \frac{1}{2}(1 + 2.2\frac{y_1}{b}F_{ro}^2)(\sqrt{(1 + \frac{8F_{ro}^2}{1 + 2.2\frac{y_1}{b}F_{ro}^2})} - 1) \qquad \dots\dots\dots\dots(2.27)$$

where y_1 is the mean supercritical depth before spatial jump.

(ii) Abramov Approach:

The sequent depth ratio in an S-jump, is given by Abramov(1966), (from Rajaratnam and Subramanya(1968)), as

$$Y = \frac{K_1 + 14}{10(K_1 + 2)}(\sqrt{(1 + 600\frac{K_1 + 2}{(K_1 + 14)^2}F_{ro}^2)} -) \qquad \dots\dots\dots(2.28)$$

in which K_1 is an empirical factor which could be taken as 3 to 4 for B/b<10 and 5 to 6 for B/b>10.

(iii)   Rajaratnam and Subramanya Approach :

In S-jumps, the forward flow occupies the whole width of the channel at the end of the jump. Further, the backed-up depth at the outlet is almost constant in the lateral direction. With these observations and neglecting the integrated bed-shear stress, Rajaratnam and Subramanya (1968) writes the momentum equation between the outlet and the end of the jump as

$$\frac{1}{2}\gamma By_3^2 - \frac{1}{2}\gamma By_t^2 = \rho Qu_t - \rho Qu_o \qquad ....(2.29)$$

where y_3 is the backed-up depth. If $y_3 = \theta y_o$, Eq. (2.29) can be reduced to the form:

$$Y^3 - Y(2F_{ro}^2 \alpha + \theta^2) + 2F_{ro}^2 \alpha^2 = 0 \qquad ....(2.30)$$

Rajaratnam and Subramanya (1968) stated that "based on the experimental results, as a first approximation θ was given an average value of 4.0, and Eq. (2.27), Eq.(2.28) and Eq.(2.30) was evaluated for all runs and is compared with the experimental results and have all been found to be unsatisfactory for predicting the sequent depth. It is suggested that to write a reasonably correct equation, it is necessary to predict the backed-up depth, the width and the nature of the forward flow at the end of the jump, and the shear force on the bed. As an alternate method, a

simple formula based on the dimensional analysis and using the present experimental results is developed."

They have introduced the concept of the characteristic length of the outlet which is nothing but the hydraulic radius at the outlet section given by

$$r' = \frac{by_o}{b + 2y_o} \qquad \dots\dots\dots\dots\dots\dots\dots\dots\dots(2.31)$$

They obtained a simple relation for the sequent depth of S-jumps by using data fit as

$$\frac{y_t}{r'} = 1.08F'_{ro} + 1.40 \qquad \dots\dots\dots\dots\dots\dots\dots\dots(2.32)$$

where $F'_{ro} = \dfrac{u_o}{\sqrt{gr'}}$.

(iv)   Herbrand's Approach:

Herbrand (1972) studied the S-jumps experimentally and tried to obtain a relation for the sequent depth by using one-dimensional momentum equation.

In Eq.(2.26) , the force on the expanded walls may be obtained by considering a hydrostatic pressure distribution on the expanded walls as :

$$F_w = \frac{1}{2}\gamma y_3^2(B - b) \qquad \dots\dots\dots\dots\dots\dots\dots\dots(2.33)$$

By inserting Eq. (2.33) into Eq.(2.26) , and rearranging, one can obtain that:

$$Y^3 - Y\ (\alpha + (1-\alpha)\theta^2 + 2\alpha F_{ro}{}^2) + 2\alpha^2 F_{ro}{}^2 = 0 \quad \ldots\ldots\ldots\ldots(2.34)$$

To solve Eq. (2.34) for the given upstream conditions, It is necessary to estimate the value of backed-up depth y_3.

Herbrand (1972) states that it is quite difficult to draw general conclusions as to the size of y_3 due to the non-hydrostatic pressure distribution in the separation zone and the strong air entrainment. Consequently, he introduced further simplifying assumptions as $\theta = 1$ and $F_w = 0$, which reduces the S-jump equation, Eq.(2.34) into R-jump equation, Eq.(2.8).

Herbrand (1972) also stated that "if one also recognizes that on the tailwater side the momentum is small in comparison with the static water pressure force and that the change in momentum which results from expanding the basin is even smaller, then one is lead to the conclusion that the pressure must be the same in the classical and in the expanding stilling basin, i.e."

$$\frac{1}{2}\gamma B y_s^2 = \frac{1}{2}\gamma b y_c^2 \qquad \ldots\ldots\ldots\ldots\ldots\ldots\ldots\ldots\ldots\ldots\ldots\ldots(2.35)$$

where y_s is the depth of S-jump in the expanding stilling basin and y_c is the depth of classical jump. With these considerations, Eq. (2.35) yields

$$\frac{y_s}{y_c} = \sqrt{\alpha} \qquad\qquad \dots\dots\dots\dots\dots\dots\dots\dots\dots(2.36)$$

He concluded that "the application of Eq. (2.36) to sizing a spatial stilling basin implies that the basin has to be widened by the square of the factor by which the actual depth is smaller than the calculated depth. If one obeys this rule then the hydraulic preconditions for the jump are still valid."

(v)   Hager Approach :

Hager (1985) studied S-jumps theoretically by using one-dimensional momentum equation given by Eq.(2.26). He gave upper, intermediate and lower limits for Eq. (2.26) by using different approximations on the estimation of F_w.

For upper limit, Hager assumes that the force on the expanded walls is given by

$$F_w = \frac{1}{2}\gamma \, (B\text{-}b){y_t}^2 \qquad\qquad \dots\dots\dots\dots\dots\dots\dots\dots\dots(2.37)$$

If Eq. (2.37) is substituted into Eq.(2.26), it becomes

$$F_{ro}^2 = \frac{Y(Y^2 - 1)}{2(Y - \alpha)} \qquad\qquad \dots\dots\dots\dots\dots\dots\dots\dots(2.38)$$

An intermediate case is given by assuming that the force on the expanded walls can be computed by using the depth of the jet, y_o as

$$F_w = \frac{1}{2}\gamma (B\text{-}b)y_o{}^2 \quad \dots\dots\dots\dots\dots\dots\dots\dots\dots\dots\dots(2.39)$$

for which Eq. (2.26) becomes

$$F_{ro}^2 = \frac{Y(Y^2 - 1)}{2\alpha(Y - \alpha)} \quad \dots\dots\dots\dots\dots\dots\dots\dots\dots(2.40)$$

For the lower limit, the minimum condition is $F_w = 0$. Therefore Eq.(2.26) becomes

$$F_{ro}^2 = \frac{Y(Y^2 - \alpha)}{2\alpha(Y - \alpha)} \quad \dots\dots\dots\dots\dots\dots\dots\dots\dots\dots(2.41)$$

(vi)   New Approach

All the discussions on S-jumps in literature (Rajaratnam and Subramanya (1968), Herbrand (1972), Hager (1985)) show that it is quite important to estimate the force on the expanded walls, F_w.

In the present study, the force on the expanded wall is estimated by using two approaches:

i) F_w can be assumed to be given by hydrostatic pressure distribution due to backed-up depth y_3.
ii) Analogous to the abrupt expansion in a pipe, F_w may be obtained by assuming uniform pressure distribution γy_3 within the separation zone.

Whichever approach is used , it is necessary to estimate the value of backed-up depth y_3 . The simplest model is to assume that y_3 is the arithmetic average of y_o and y_t , i.e

$$y_3 = \frac{1}{2}(y_o + y_t) = \frac{1}{2}y_o(1 + \frac{y_t}{y_o}) \qquad \dots\dots\dots\dots\dots\dots(2.42)$$

or

$$\theta = \frac{y_3}{y_o} = \frac{1}{2}(1 + Y) \qquad \dots\dots\dots\dots\dots\dots\dots(2.43)$$

Case i) The force F_w is considered as given by hydrostatic pressure distribution as:

$$F_w = \frac{1}{2}\gamma \, (B\text{-}b)y_3^2 \qquad \dots\dots\dots\dots\dots\dots\dots\dots\dots(2.44)$$

or

$$\frac{2F_w}{\gamma By_o^2} = \theta^2(1-\alpha) \qquad \dots\dots\dots\dots\dots\dots\dots\dots\dots(2.45)$$

Substution of Eq. (2.45) into Eq.(2.26) yields a relation between F_{ro} and Y as

$$F_{ro}^{\ 2} = \frac{Y^3 - \alpha Y - \theta^2(1-\alpha)}{2\alpha(Y-\alpha)} \qquad \dots\dots\dots\dots\dots(2.46)$$

If θ may be approximated by Eq.(2.43) , Eq.(2.46) becomes

$$F_{ro}^{\ 2} = \frac{Y^3 - \alpha Y - \dfrac{1}{4}(Y+1)^2 Y(1-\alpha)}{2\alpha(Y-\alpha)} \qquad \dots\dots\dots\dots(2.47)$$

28

Case ii) If the pressure distribution within the separation pocket is assumed to be uniform and equal to γy_3, then the force F_w becomes:

$$F_w = \gamma(B-b)y_3{}^2 \quad \dots\dots\dots\dots\dots\dots\dots\dots\dots(2.48)$$

or in the non-dimensional form:

$$\frac{2F_w}{\gamma B y_o^2} = 2\theta^2(1-\alpha) \quad \dots\dots\dots\dots\dots\dots\dots\dots(2.49)$$

Hence, by substituting Eq. (2.49) into Eq.(2.26), the relation between F_{ro} and Y becomes

$$F_{ro}{}^2 = \frac{Y^3 - \alpha Y - 2\theta^2(1-\alpha)}{2\alpha(Y-\alpha)} \quad \dots\dots\dots\dots\dots(2.50)$$

Again, if θ is assumed to be given by Eq.(2.43) , Eq.(2.50) will take the form:

$$F_{ro}{}^2 = \frac{Y^3 - \alpha Y - \dfrac{1}{2}(Y+1)^2 Y(1-\alpha)}{2\alpha(Y-\alpha)} \quad \dots\dots\dots(2.51)$$

All the approaches in the literature and new approaches in this study derived from momentum equation for R- and S-jumps are tabulated in Table (2.1), and Table (2.2), respectively.

Table 2.1   The Approaches For R-Jump

	R-Jump
Kuznetsov Approach (1964)	$Y = \dfrac{K}{2}(\sqrt{(\alpha^2 + 8F_{ro}^2\alpha)} - \alpha)$ (2.9) $K = 0.8-(0.9-\alpha)0.15$ (2.10)
Rajaratnam & Subramanya Approach (1968)	Approximate Solution; (by neglecting F_f) $Y = \dfrac{1}{2}(\sqrt{(\alpha^2 + 8F_{ro}^2\alpha)} - \alpha)$ (2.11) Empirical Formula; $Y= 0.75 + (\alpha+0.30)(F_{ro} -0.85)$ (2.12)
New Approach	If F_f is negligible, $Y = \dfrac{1}{2}(\sqrt{(4\alpha(1+2F_{ro}^2) - 3\alpha^2)} - \alpha)$ (2.16) If F_f is not negligible, $Y = \dfrac{1}{2}\sqrt{\alpha}(\sqrt{(1 + 8\sqrt{\alpha}F_{ro}^2)} - 1)$ (2.20)

Table 2.2   The Approaches For S-Jump

	S-Jump
Rajaratnam & Subramanya Approach (1968)	If $y_3 = \theta y_0$ $Y^3 - Y(2F_{ro}^2\,\alpha + \theta^2) + 2F_{ro}^2\,\alpha^2 = 0$ (2.30) By using data fit as $\dfrac{y_t}{r^{'}} = 1.08F_{ro}^{'} + 1.40$ (2.32) where $F_{ro}^{'} = \dfrac{u_0}{\sqrt{gr^{'}}}$, $r^{'} = \dfrac{by_0}{b+2y_0}$.
Herbrand Approach, (1972)	$Y^3 - Y\,(\alpha + (1-\alpha)\theta^2 + 2\alpha F_{ro}^2) + 2\alpha^2 F_{ro}^2 = 0$ (2.34)
Hager Approach, (1985)	For upper limit, $F_w = \dfrac{1}{2}\gamma\,(B-b)y_t^2$ $F_{ro}^2 = \dfrac{Y(Y^2-1)}{2(Y-\alpha)}$ (2.38) For intermediate case, $F_w = \dfrac{1}{2}\gamma\,(B-b)y_0^2$ $F_{ro}^2 = \dfrac{Y(Y^2-1)}{2\alpha(Y-\alpha)}$ (2.40) For the lower limit, $F_w = 0$, $F_{ro}^2 = \dfrac{Y(Y^2-\alpha)}{2\alpha(Y-\alpha)}$ (2.41)
New Approach	Hydrostatic pressure, $F_w = \dfrac{1}{2}\gamma\,(B-b)y_3^2$, $\theta = \dfrac{y_3}{y_0} = \dfrac{1}{2}(1+Y)$ $F_{ro}^2 = \dfrac{Y^3 - \alpha Y - \dfrac{1}{4}(Y+1)^2 Y(1-\alpha)}{2\alpha(Y-\alpha)}$ (2.47) Uniform Pressure, $F_w = \gamma(B-b)y_3^2$, $\theta = \dfrac{y_3}{y_0} = \dfrac{1}{2}(1+Y)$ $F_{ro}^2 = \dfrac{Y^3 - \alpha Y - \dfrac{1}{2}(Y+1)^2 Y(1-\alpha)}{2\alpha(Y-\alpha)}$ (2.51)

2.4 Energy Dissipation Characteristics

The energy dissipation due to a hydraulic jump may be found by application of the one-dimensional energy equation between Sections (1) and (2). If E_o is the energy of the supercritical stream at the outlet,

$$E_o = y_o + \frac{u_o^2}{2g} \qquad\qquad \dots\dots\dots\dots\dots\dots\dots\dots\dots\dots(2.52)$$

and E_t is the energy at the end of the jump,

$$E_t = y_t + \frac{u_t^2}{2g} \qquad\qquad \dots\dots\dots\dots\dots\dots\dots\dots\dots(2.53)$$

the energy dissipation in the hydraulic jump is

$$h_l = E_o - E_t \qquad\qquad \dots\dots\dots\dots\dots\dots\dots\dots\dots\dots\dots\dots\dots(2.54)$$

and the relative energy dissipation is

$$\frac{h_l}{E_o} = 1 - \left(\frac{y_t}{y_o + \frac{u_o^2}{2g}} + \frac{\frac{u_t^2}{2g}}{y_o + \frac{u_o^2}{2g}} \right) \qquad \dots\dots\dots\dots\dots\dots(2.55)$$

The relative energy dissipation is a function of F_{ro}, α and can be written as

$$\frac{h_l}{E_o} = 1 - \left(\frac{\alpha^2 F_{ro}^2 Y^2 + 2Y}{2 + F_{ro}^2} \right) \qquad \dots\dots\dots\dots\dots\dots(2.56)$$

32

In previous investigations given by Rajaratnam and Subramanya (1968) and Herbrand (1972), it is observed that abrupt enlargements possess substantially higher relative energy dissipation than that of simple hydraulic jump for a given F_{ro}. $\alpha=1.0$ is the case of simple hydraulic jump. Eq.(2.56) shows also that the relative energy dissipation increases as α decreases. Consequently, the stilling basins with abrupt enlargements are powerful energy dissipaters.

2.5 Length Characteristics

The length of jump may be defined as the distance measured from the front face of the jump to a point on the surface immediately downstream from the roller and the length of the roller may be defined as the distance from the face of the jump to the point where the surface roller ends. These lenghts can not be determined easily by theory, but it has been investigated experimentally in the present study and also in Rajaratnam's studies.

CHAPTER III

EXPERIMENTS AND EXPERIMENTAL APPARATUS

3.1 Description of Apparatus

The experimental work was conducted in a horizontal open channel, 50 cm deep, 25 cm wide and 10.5 m long schematically represented in Fig.(3.1). The channel was made of concrete and fiberglass. The walls of the middle section, which was about 3.53 m long, was made of fiberglass. The remaining parts at the entry and outlet of the channel were made of concrete. To form an abrupt enlargement in the channel, three different fiberglass apparatus were used in the fiberglass part of the rectangular channel by contracting the channel width. Two adjustable sluice gates were used to control the upstream and downstream water depths. These sluice gates were made of fiberglass. The upstream sluice gate was placed 3.80 m from the channel entry and the width of the gate was changed by changing the downstream channel width. The downstream sluice gate was placed at the end of the channel over the free fall.

Water was supplied from a constant head tank through a 18 cm pipe which was regulated by a valve. Water issuing out from the downstream sluice gate was collected in a basin connected to a return channel. Discharge was measured, by a triangular weir placed at the end of the return channel. The maximum capacity of the channel was 23.5 lt/sec. The surface elevations were measured by a movable point gage.

Another point gage was used to measure the head over the triangular weir. The lengths of the jumps were measured by engineering steel tape and milimetric papers placed along the channel.

3.2 Discharge Measurements

The discharge measurements were regulated with a valve at the supply pipe, and the flow rate was measured by using a triangular weir which had 30° notch angle. The head on the triangular weir was measured by a point gage located 3.60 m upstream of the weir. The discharge was obtained from the calibration curve of the weir, shown in Fig. (3.2).
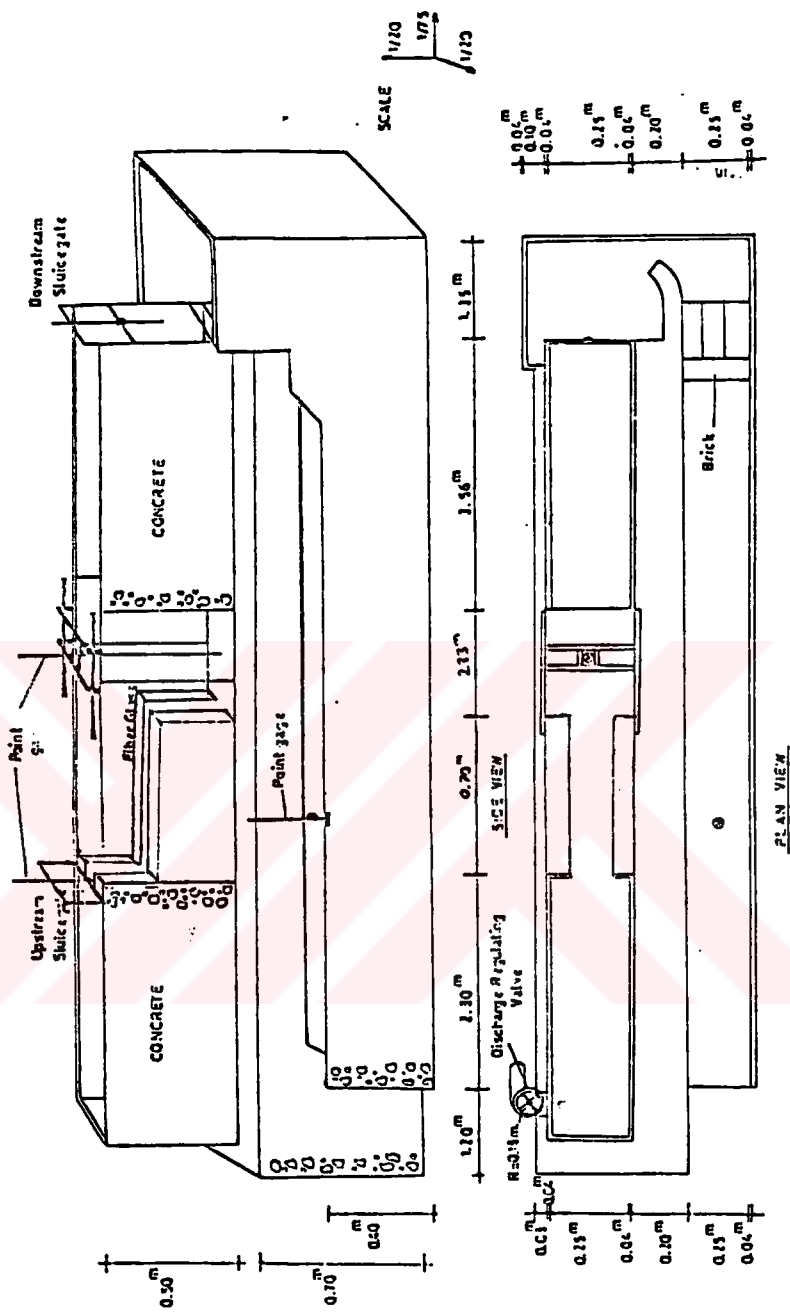
Fig.(3.1) Schematic Representation of The Experimental Arrangement

36
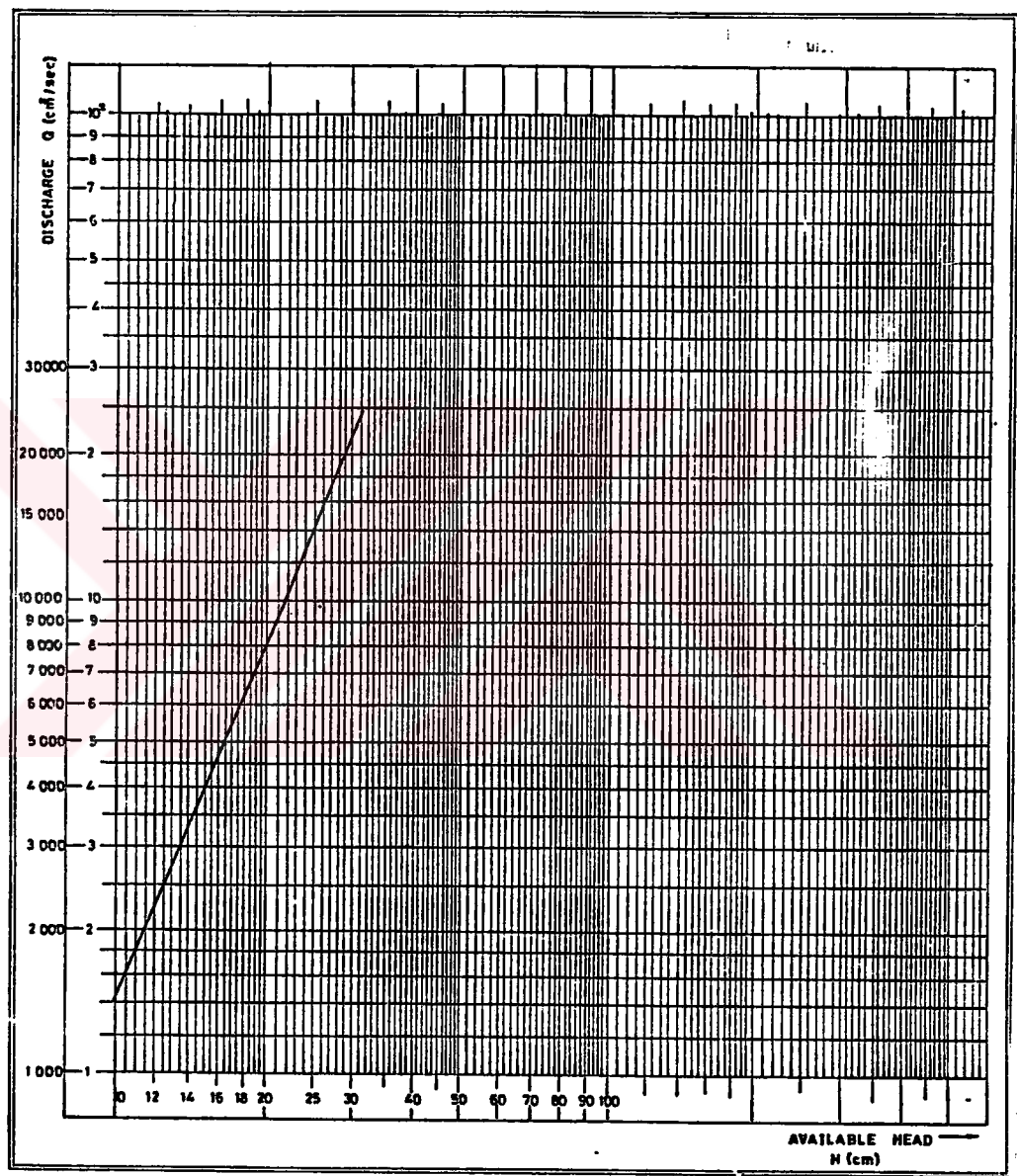
Fig. (3.2)   Calibration Curve

37

3.3 Experimental Procedure

The experiments were conducted for four values of the width ratios $\alpha = b/B = 1$, 0.80, 0.50, and 0.30 for R-Jump and $\alpha = b/B = 0.80$ and 0.50 for S-Jump. On the whole 174 experiments were done, 33 of them belonged to simple hydraulic jump, 92 of them belonged to R-jumps and the remaining 49 belonged to S-jumps.

The following measurements were taken for each experimental run; (i) Measurement of discharge from the supply tank by using the calibration curve; (ii) measurement of the distance of the toe and the heel of the jump from the beginning of the transition designated as L_l and L_j, respectively and length of the surface roller, L_r; (iii) depth of flow at the beginning of the transition and depth of water at the separation zones of both sides designated as y_0 and y_3, respectively; (iv) tailwater depth, y_t and depth of water at the toe of the jump could not be measured directly because of the oscillating nature of the toe of the jump; (v) length of the separation zone from the transition and designated as L_o ; (vi) the width of the channel ,B and the width of the supercritical stream at the outlet, b. All measurements were made along the longitudinal center line. All of the data are given in Appendix.

For a certain width ratio, and discharge, upstream flow conditions were fixed by adjusting the upstream sluice gate. The depth of water under the upstream sluice gate is changed in the ranges of 1.5 cm to 6 cm for the values of the upstream Froude number. Then, by changing the setting of the downstream sluice gate, the downstream depths of water, the depths of tailwater, were adjusted to obtain R-Jump or S-Jump.

In the experiments, for the fixed upstream supercritical flow conditions, first the supercritical stream occupied the full width of the channel and a system of diagonal surface waves were formed. Then, by adjusting the downstream sluice gate to a relatively high tailwater level somewhere downstream, a hydraulic jump with an oblique front was formed. The depth of tailwater was controlled by the downstream sluice gate. With the increase in the tailwater, the jump moved upstream and its front gradually became normal. Then the tailwater depth was increased till the limiting position was reached. All measurements for the characteristics of the jump (y_o, y_t, L_l, L_o, L_r, L_j), and the head on the weir were made. If the tailwater depth was slightly increased, the jump moved upstream and an unstable nonuniform flow was observed. The backward flow set in and deflected to one side. The depth of the deflected wave was deeper than the tailwater depth.

The tailwater depth was increased by the downstream gate and the outlet gradually submerged, but the jet was still unstable and oscillated violently. However, at a certain tailwater level, the jet ceased to oscillate and the flow became stable and a hydraulic jump with a small submergence was formed. That was S-Jump. The characteristics of the jump and the discharge measurements were made.

CHAPTER IV

RESULTS AND DISCUSSION OF RESULTS

4.1 Observations

When a supercritical flow in a rectangular channel enters a wider channel at an abrupt symmetrical enlargement, the supercritical stream expands freely until it occupies the full width of the channel and then creates a system of diagonal surface waves due to successive reflections as shown in Fig. 4.1.
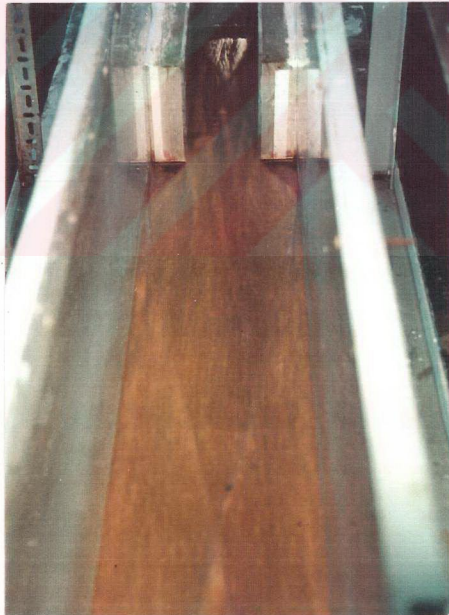
Fig. 4.1.a   A System of Diagonal Surface Waves
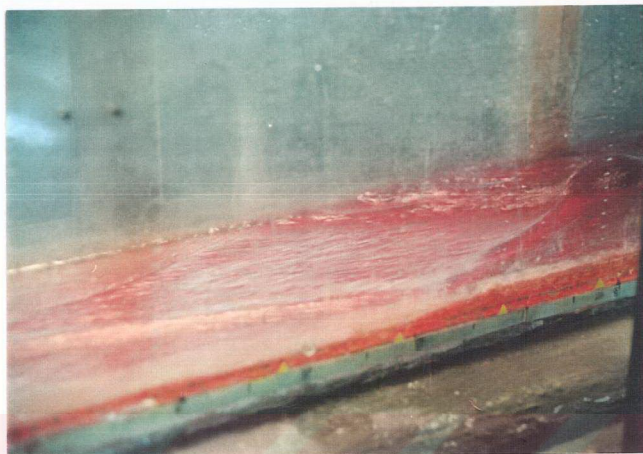
Fig. 4.1 (b,c)   A System of Diagonal Surface Waves

Kuznetsov (1964) describes the different regions in a free horizontal spread of a supercritical flow at an abrupt expansion and the formation of the jump quite well. For this reason, this description is given below:

Kuznetsov (1964) explains the free horizontal spread of a streamflow as "the movement in which water mass in the tailrace does not affect the spread of the upper part of the spilling jet", and he shows the pattern of the free horizontal spread of a water stream schematically as reproduced in Fig. 4.2.

In Fig. 4.2, Kuznetsov (1964) divides the whole stream arbitrarily into three regions:

A - inside, leaf-shaped, spreading region;

B - outside region separated from A by bottom rollers;

C - region at the corner of the structure,(separation zone)
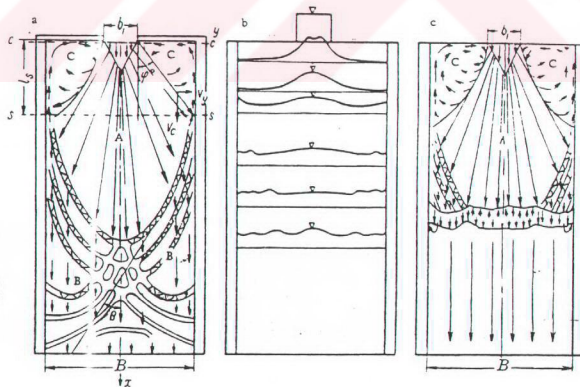
Fig. 4.2   Free Horizontal Spread of A Streamflow

42

Kuznetsov (1964) states that their results showed that " in region B a series of bottom rollers are formed. The upstream rollers form a boundary which separates regions A and B. The bottom rollers have a rotational and translational (helical) movement. With the increase in angle θ the translational movement decreases whereas the rotational movement increases (Fig. 4.2.a). The liquid mass coming from the region A flows over the bottom rollers, inducing a wave motion, and changes the direction of the velocities toward the stream axis. In region B the directions of the bottom and surface currents coincide. Thus, region B constitutes the zone of junction between the flashy stream of region A and the calm stream in the tailrace. At the junction there is a series of slanting wave-jumps in which the bottom rollers are analogous to the rollers of slanting wave-jumps in the two dimensional problem. As the tailwater level increases, a hydraulic jump with a surface roller forms gradually at the end of region A."

Later, in 1968 Rajaratnam and Subramanya defined the jump formed in this way as R-jump. In the present study similar flow patterns have been observed. A typical cross sectional and longitudinal profiles of the free horizontal spread of supercritical jet is shown in Figs.4.3 and 4.4, respectively.

In Fig. 4.3, a typical cross sectional profile of the jet for $\alpha=0.30$ and $F_{ro}=2.83$ is shown at distances 0, 5 cm, 10 cm, 20 cm, 40 cm, 60 cm, 80 cm downstream of outlet section, where abrupt enlargement takes place. The corresponding typical longitudinal profiles of the jet along the centerline and sidewalls of the channel and also along sections A, B, C, D, E and F which are 2.5 cm apart each other are shown in Fig. 4.4.
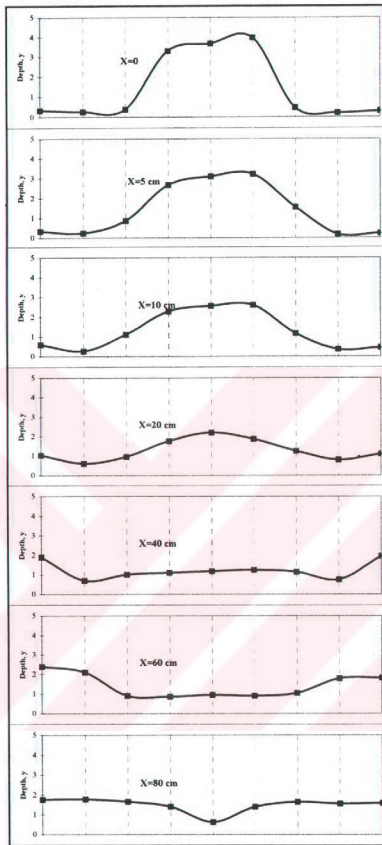
Fig. 4.3   Cross sectional Profiles of The Jet.
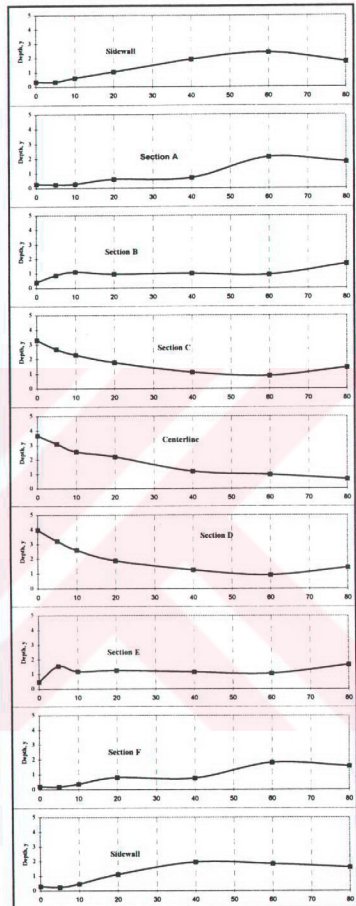
Fig. 4.4   Longitudinal Profiles of The Jet.

44

If the supercritical flow spreading at an abrupt expansion encounters a tailwater depth for which flow is subcritical, a hydraulic jump with an oblique front is formed somewhere downstream as shown in Fig. 4.5.

Fig. 4.5   Hydraulic Jump With An Oblique Front

An increase in the tailwater depth will cause the jump to move upstream and its front gradually becomes normal, as shown in Fig.4.6.
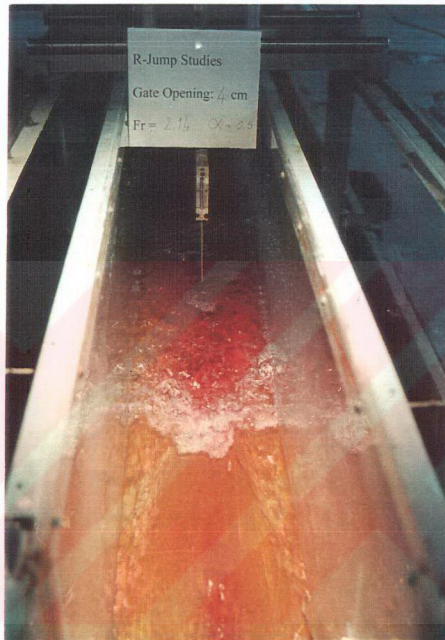
Fig. 4.6   Hydraulic Jump With Normal Front

However, the jump soon reaches a limiting position. Any further increase in the tailwater depth causes the jump to collapse and the tailwater spills on the upstream supercritical flow on one side and an unstable nonuniform flow is observed. The stable jump forming with a normal front at this limiting tailwater level (just before the unstable nonuniform flow occurs) is called repelled or R-jump. Typical examples of R-jump are shown in Fig. 4.7
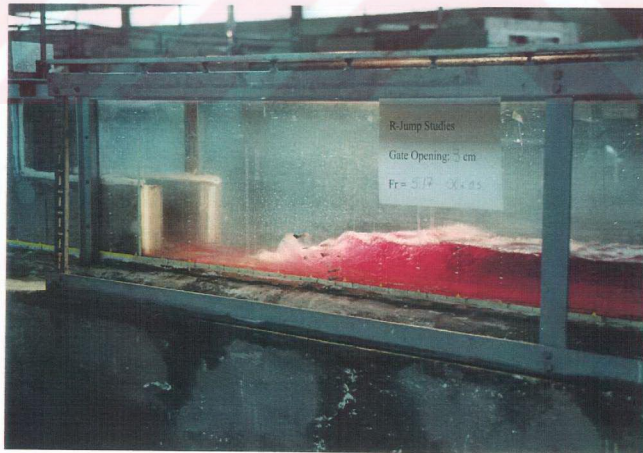
Fig. 4.7 (a,b) A View of R-Jump
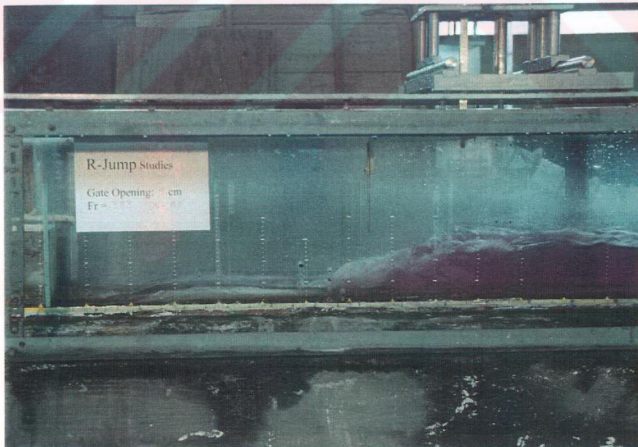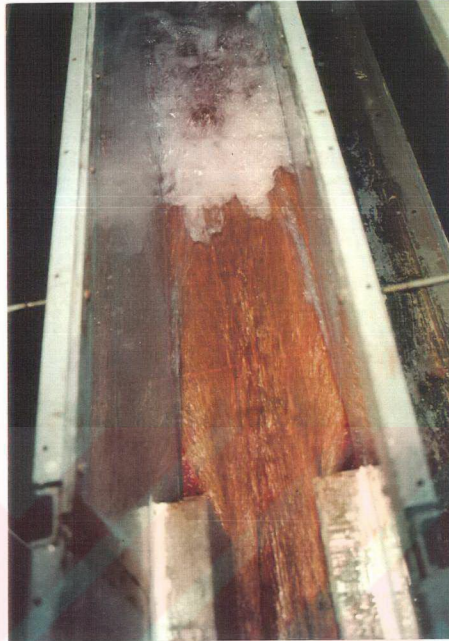
Fig. 4.7 (c,d) A View of R-Jump

If the tailwater is slightly greater than the sequent depth of the R-jump, the perfect jump in region A and the slanting wave-jumps in region B move upward, backward flow sets in and the jet twists and deflects to one side of separation zone C, creating an unstable nonuniform flow situation as shown in Fig. 4.8.
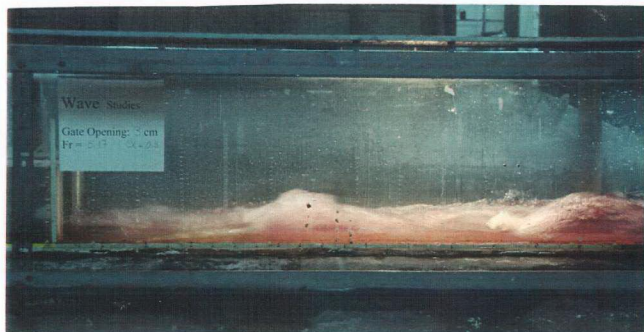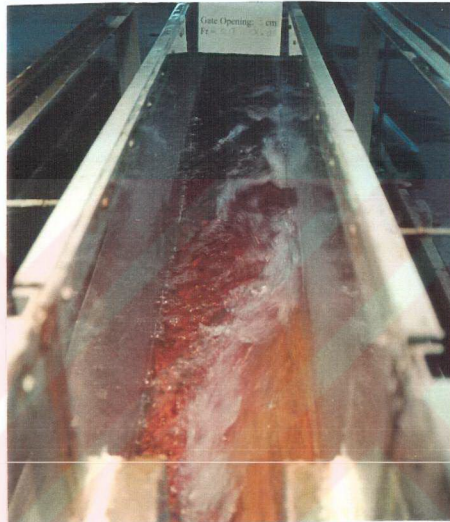
Fig. 4.8 (a,b)   Unstable Nonuniform Flow

49

The outlet gradually submerges with a further increase in the tailwater level, but the jet still be unstable, oscillating rather violently. However, at a certain higher tailwater level, the jet ceases to oscillate, the flow becomes stable and phenomenon resembles the familiar hydraulic jump with small submergence. The minimum tailwater situation at which the stable flow takes place after the collapse of the R-jump is S-Jump as shown in Fig.4.9. Further increase of tailwater causes greater submergence and the flow resembles a submerged jump.
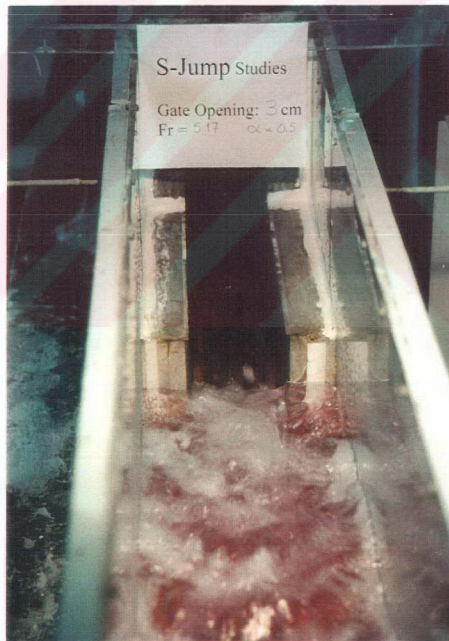
Fig. 4.9.a A View of S-Jump
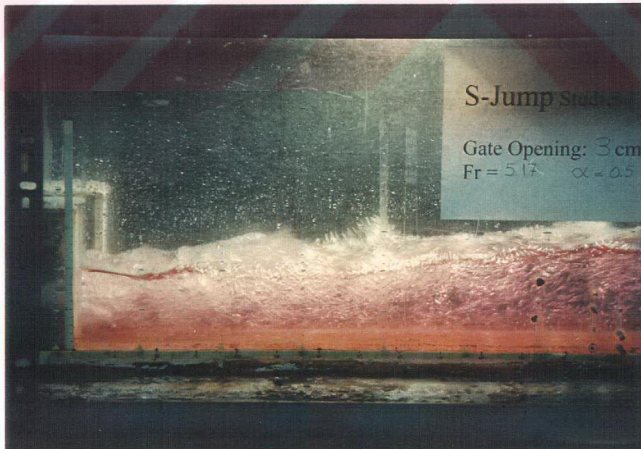
Fig. 4.9 (b,c) A View of S-Jump

4.2   Results and Discussion of Results For R-Jumps.

4.2.1 Sequent Depth For R-Jumps

For all the series, having $\alpha = 0.80$, 0.50 and 0.30, in the entire range of F_{ro} tested, R-Jump had an essentially normal front with a strong surface roller. The jump was stable and the stability improved with increase in the Froude number. The ranges of the Froude number of the upstream supercritical flow in the experiments performed for three different width ratios are given below:

$$\alpha = 0.80 \qquad 1.89 \le F_{ro} \le 6.33$$
$$\alpha = 0.50 \qquad 1.94 \le F_{ro} \le 6.63$$
$$\alpha = 0.30 \qquad 1.45 \le F_{ro} \le 3.21$$

The variation of the relative sequent depth, Y with F_{ro} and α for all the experiments done in the present study is shown in Fig. 4.10. In each case, the value of α was kept constant and the values of discharge, Q and the supercritical flow depth, y_o were variable. Fig. 4.10 shows that for a given α, the relative depth versus F_{ro} values fall on a single line in the range tested, indicating the insignificant effect of b/y_o ratio.

The comparison of the R-jump data with the classical jump ($\alpha = 1.0$) data is also given in Fig.4.10, together with $\alpha = 0.80$, 0.50, 0.30. Fig.4.10 shows that for a given value of F_{ro}, the relative depth ratio, Y decreases with a decrease in the value of α.
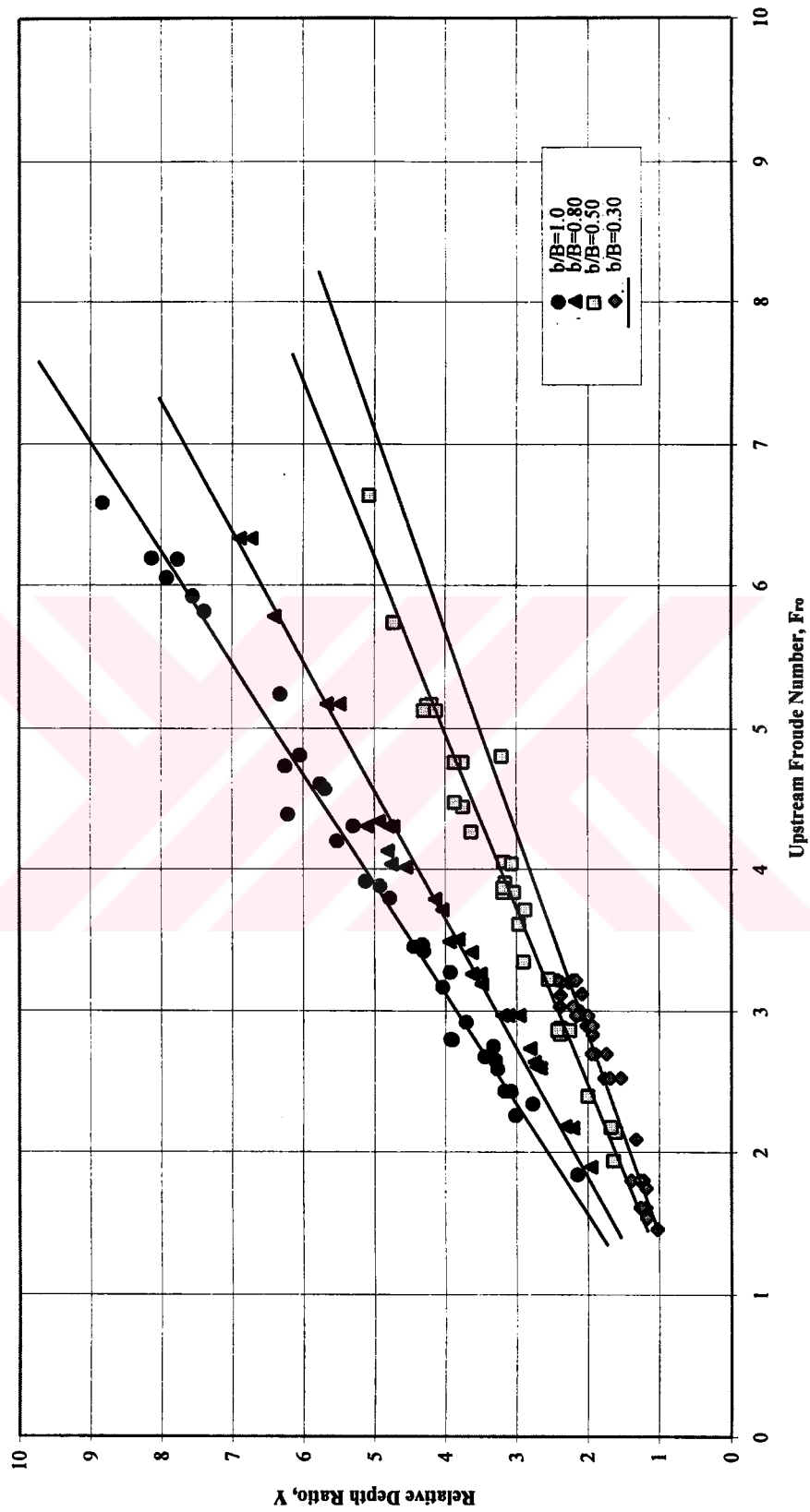
Fig. 4.10   Variation of The Relative Depth Ratio, Y With F_{ro}

53

Prediction of Y:

The R-jump data taken in the present study and in the literature are compared with the new approaches in Fig.4.11 and 4.12, respectively.

Fig. 4.11 and 4.12 show that the new approach which considers the friction force as given by Eq.(2.6) and Eq.(2.17) gives good results for all α values tested except $\alpha=0.30$ and $\alpha=0.33$. For $\alpha=0.30$, the new approach which takes $F_f=0$ (Eq.2.16) gives better results. However, this is not conclusive, because in the present study for $\alpha=0.30$, the range of the Froude number is quite small, because of the capacity of the channel used in the experiments. On the other hand, Rajaratnam's data for $\alpha=0.33$ is in between two approaches as shown in Fig.4.12.d. Fig.4.12.d shows the same trend with the data taken in the present study; when $F_{ro}\leq4$, the data is closer to the line given by Eq.(2.16) which considers $F_f=0$, as F_{ro} becomes larger than 4, it approaches to Eq.(2.20) which considers $F_f\neq0$, with a maximum error of 16%.

Present data with the approaches in the literature (Kuznetsov (1964) and Rajaratnam and Subramanya (1968)) is also compared in Fig.4.13. These figures show that Rajaratnam and Subramanya's empirical relation (Eq. 2.12) predicts the relative depth ratio values better than their approximate solution (Eq.2.11) and also better than Kuznetsov approach (Eq. 2.9) in the range of $\alpha=0.80$, 0.50 and 0.30 measured.

At section 2.3.1, a modified Froude number is introduced which assumes that the relative depth ratio is a function of modified Froude number, F_M. The present data and Rajaratnam's data (which is the only available data for R-jumps in the literature) are plotted as Y versus F_M in Fig. 4.14. The values of α in Fig. 4.14 are α=0.30, 0.33, 0.50, 0.67, 0.80 and 0.83. This figure shows that the modified Froude number is a good scaling factor for hydraulic jumps at abrupt enlargements. The best line passing through these data points is $Y=0.83F_M$ with a correlation coefficient of 99%.

Therefore, for all practical design purposes the relative depth ratio for R-jumps can be written as

$$Y=0.83 \sqrt{\alpha(1+2F_{ro}^2)} \qquad \dots\dots\dots\dots(4.1)$$

4.2.2   Length Characteristics of R-Jump

As explained at section 2.3.2, Herbrand (1972) discusses that in sizing a spatial stilling basin the value of $\sqrt{\alpha}$ becomes an important scaling factor. In fact the previous discussions shows that modified Froude number and hence $\sqrt{\alpha}$ are the important factors for hydraulic jumps occurring at abrupt enlargements. Therefore, the length of the surface roller and the length of the jump are plotted as $\sqrt{\alpha}\, L_r/y_t$ versus F_M and $\sqrt{\alpha}\, L_j/y_t$ versus F_M in Figs. 4.15 and 4.16, respectively. The mean curve through the data shows that $\sqrt{\alpha}\, L_r/y_t$ reaches a limit value about 3.0 for $F_M \cong 8.0$ in the range of α studied as shown in Fig. 4.15. Regarding the length of the jump, Fig. 4.16 shows considerable scatter as expected. Because the measurement of the length of the jump is a difficult task. In general, R-jump requires a longer stilling basin than the

corresponding simple hydraulic jump. In fact Fig. 4.16 shows that $\sqrt{\alpha}\, L_j/y_t$ approximately approaches a limit as 6.7. For simple hydraulic jumps, L_j/y_t is about 6.0. On the other hand, the tailwater depth ratio for simple hydraulic jump to R-jump is about $\sqrt{\alpha}$. Therefore, for R-jumps, L_j/y_t is approximately 6.7. This indicates that the jump length for R-jump is about 11% larger than that of simple hydraulic jump. In fact Rajaratnam and Subramanya (1968) states also that for R-jumps L_j/y_t is about 15% larger than that of a simple jump.

4.2.3   Energy Dissipation in R-Jumps

The energy dissipation in R-jump is computed by using Eq.(2.56) and it is plotted against F_{ro} for $\alpha=0.30$, 0.50, 0.80 and 1.0 in Fig. 4.17. This plot shows that the relative energy dissipation is a function of F_{ro} and α. It is observed that abrupt enlargements possess substantially higher relative energy dissipation than that of simple hydraulic jump for equal F_{ro}. Eq.(2.56) shows also that the relative energy dissipation increases as α decreases. Consequently, the stilling basins with abrupt enlargements are powerful energy dissipaters.
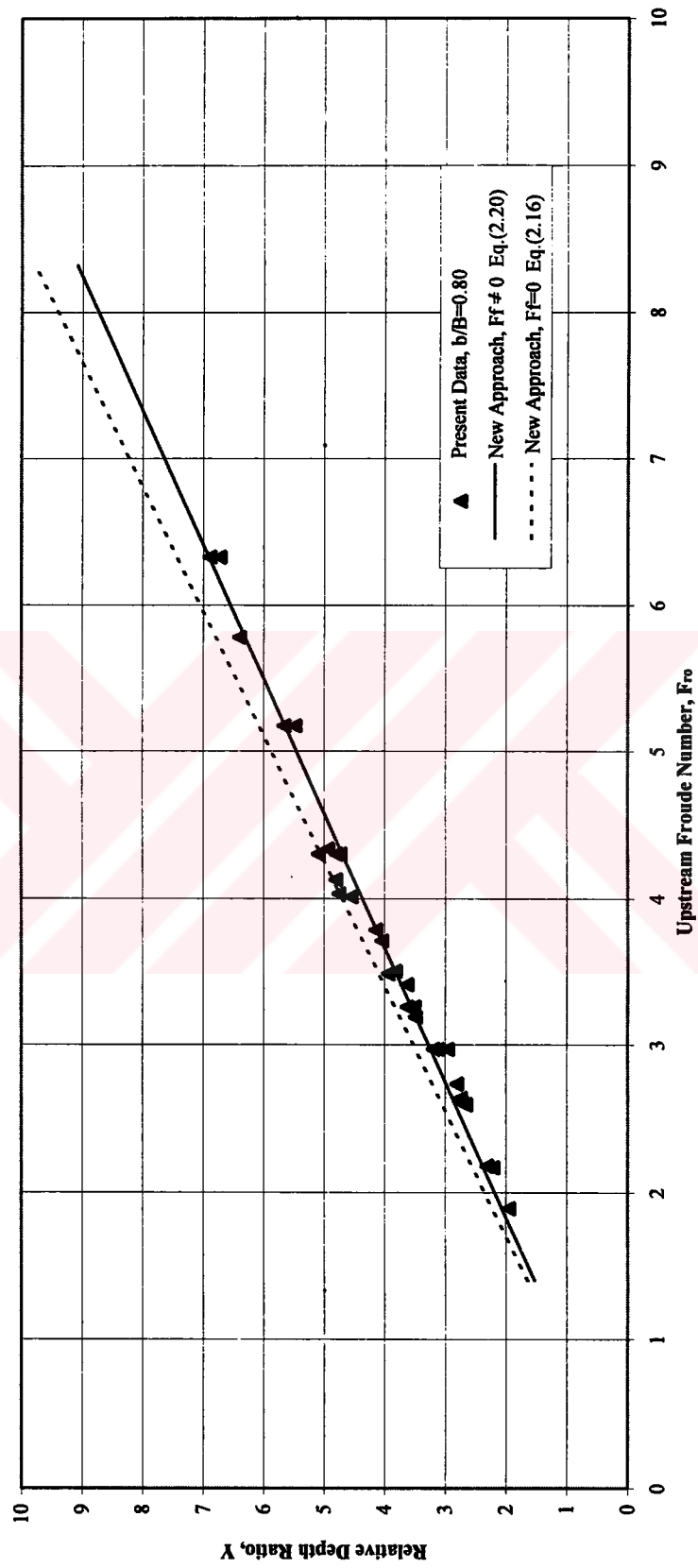
Fig. 4.11.a   Comparison of Present Data With New Approaches, α=0.80

57
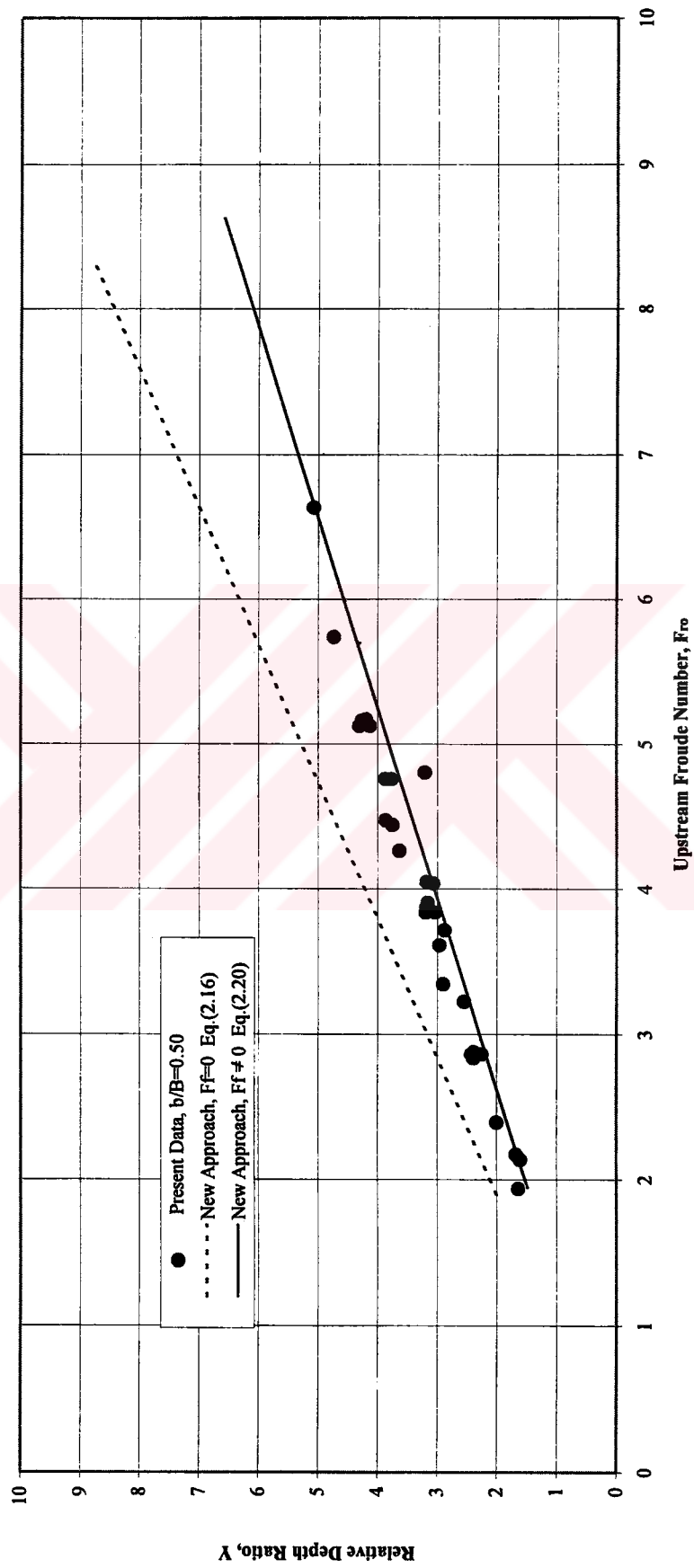
Fig. 4.11.b   Comparison of Present Data With New Approaches, α=0.50

58
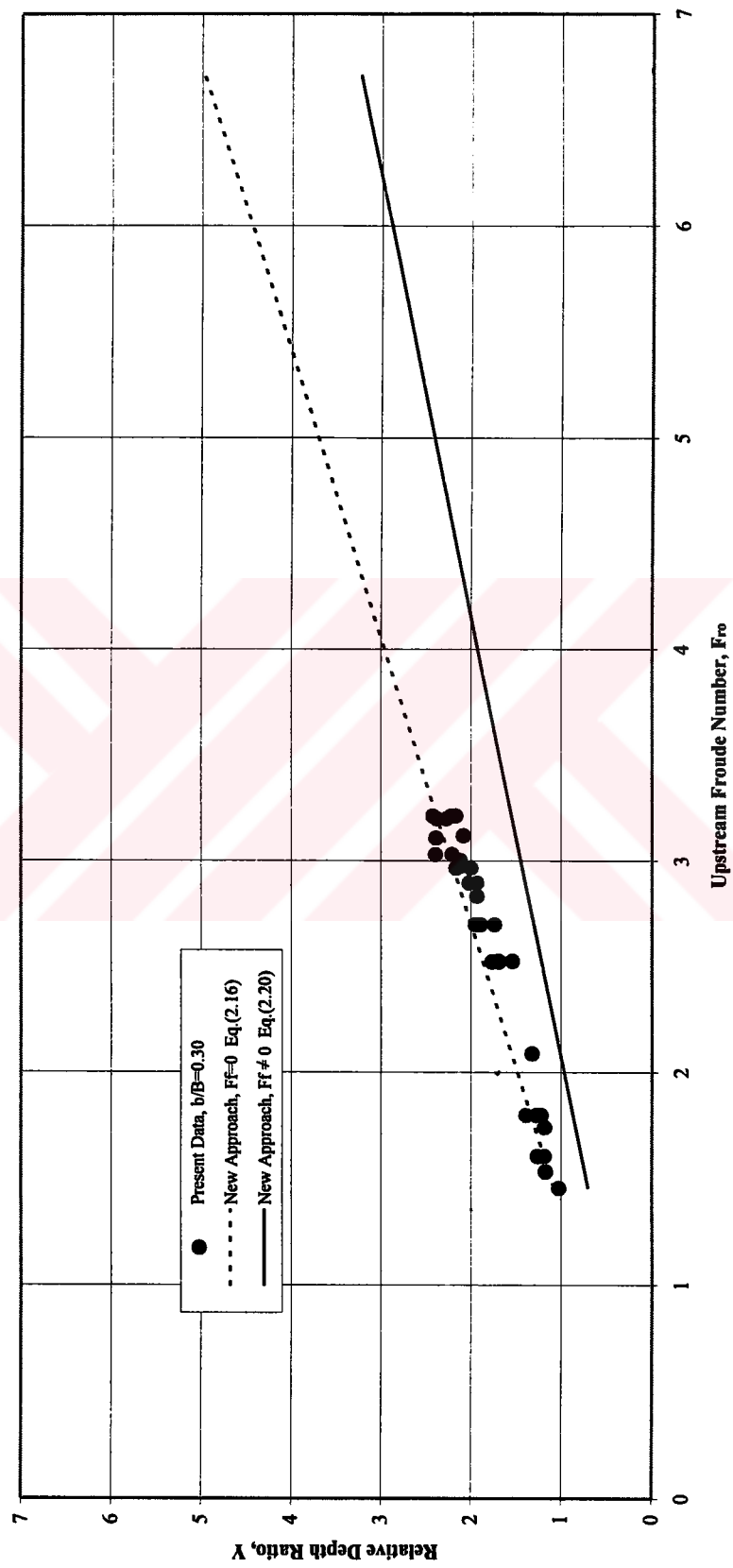
Fig. 4.11.c   Comparison of Present Data With New Approaches, $\alpha = 0.30$

59
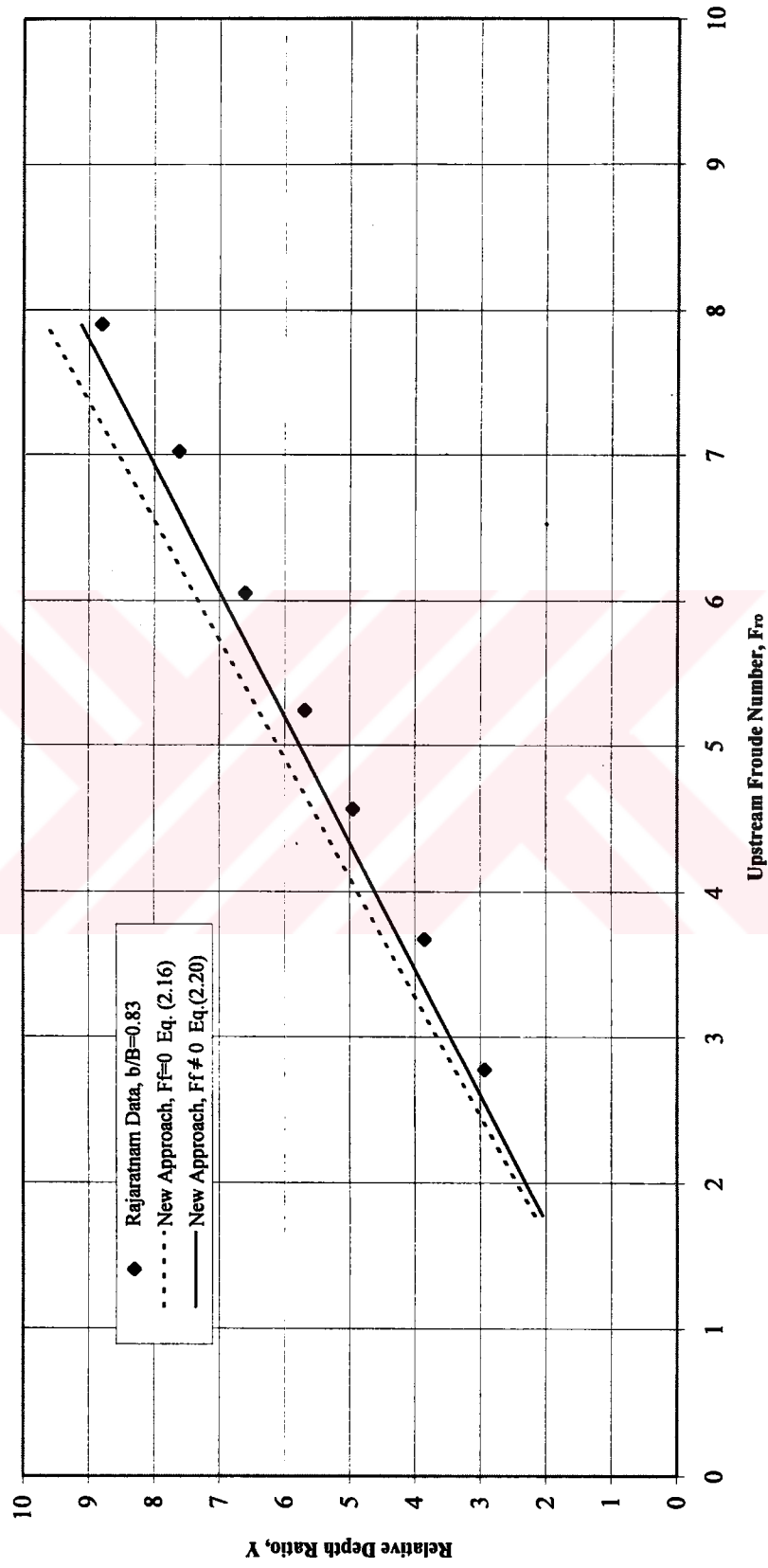
Fig. 4.12.a   Comparison of Rajaratnam's Data With New Approaches, $\alpha = 0.83$

60
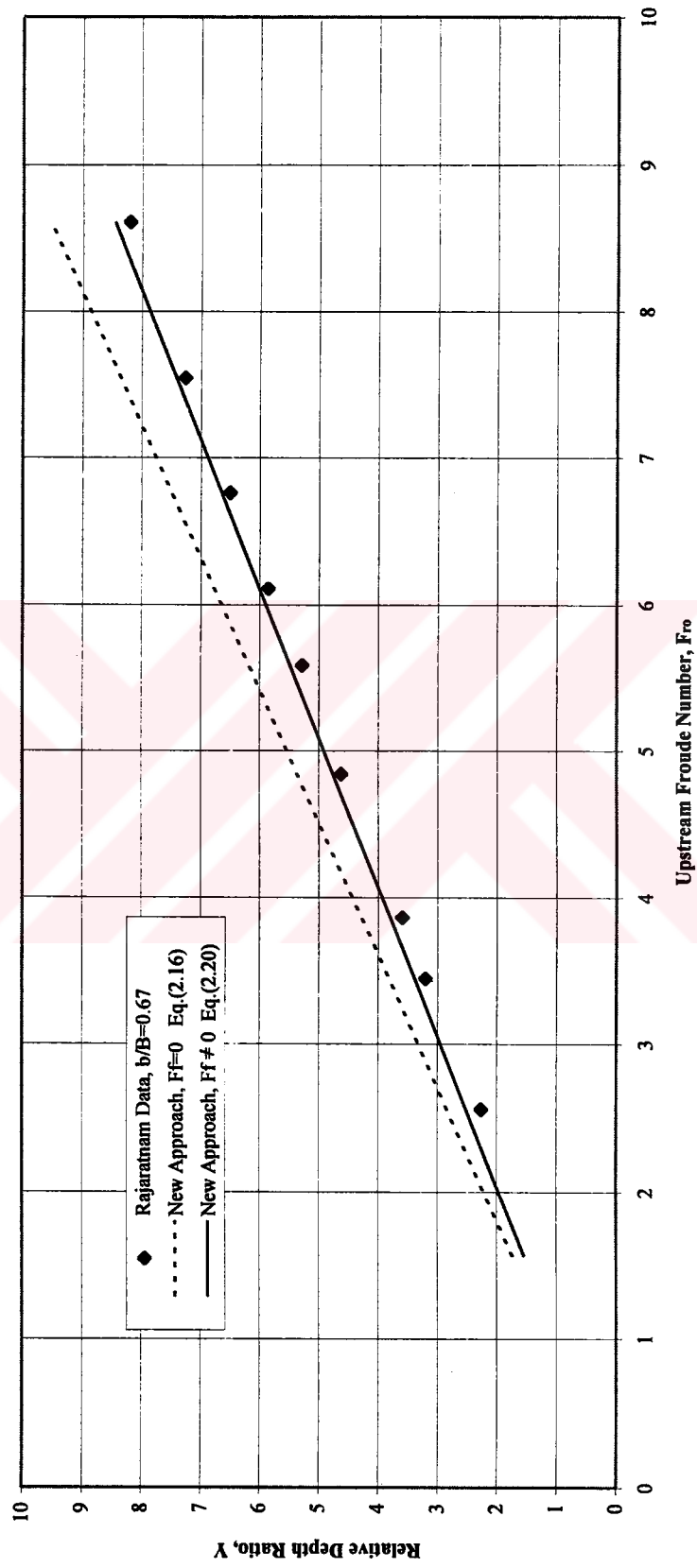
Fig. 4.12.b   Comparison of Rajaratnam's Data With New Approaches, $\alpha=0.67$

61
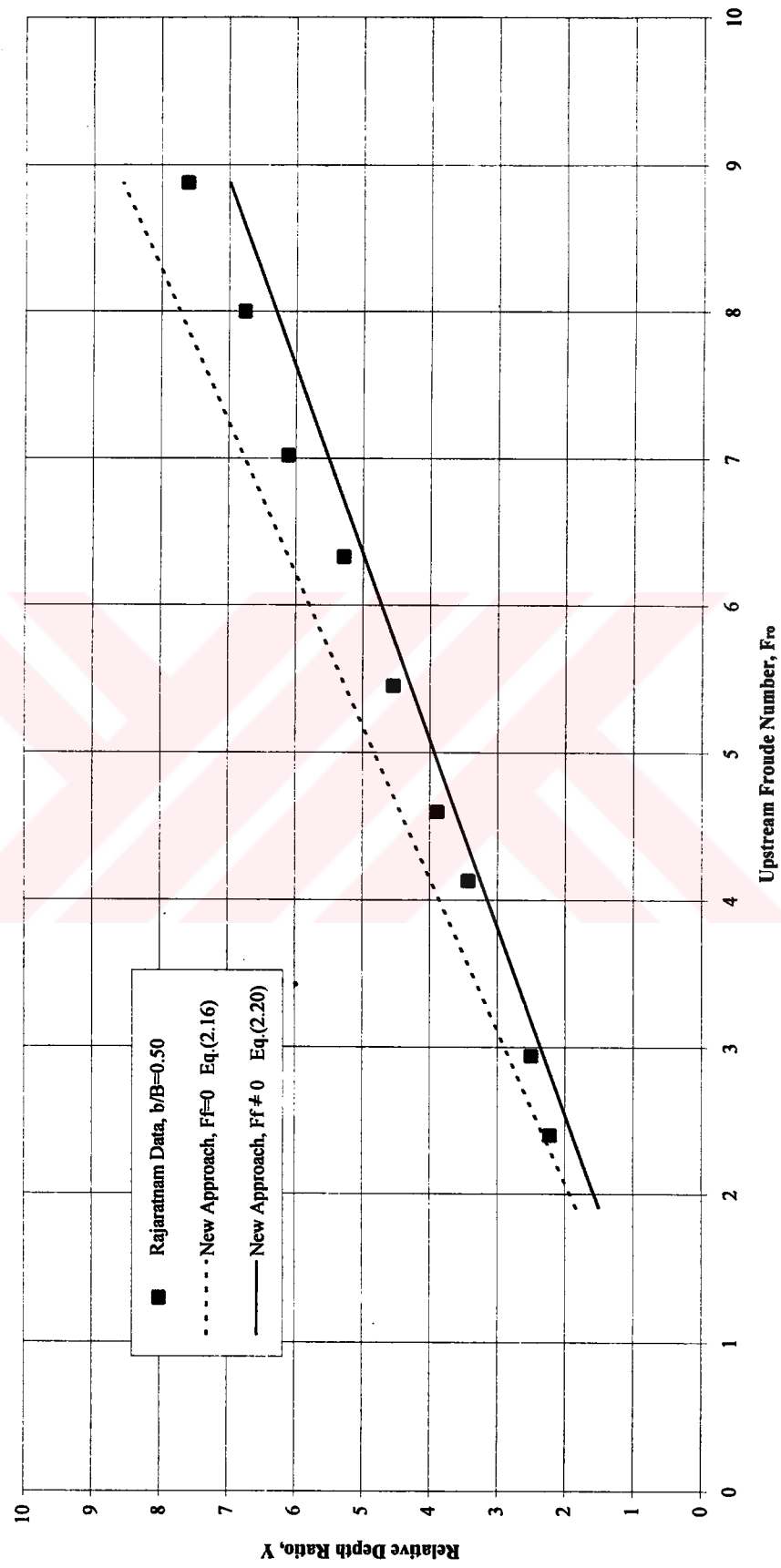
Fig. 4.12.c   Comparison of Rajaratnam's Data With New Approaches,   α=0.50
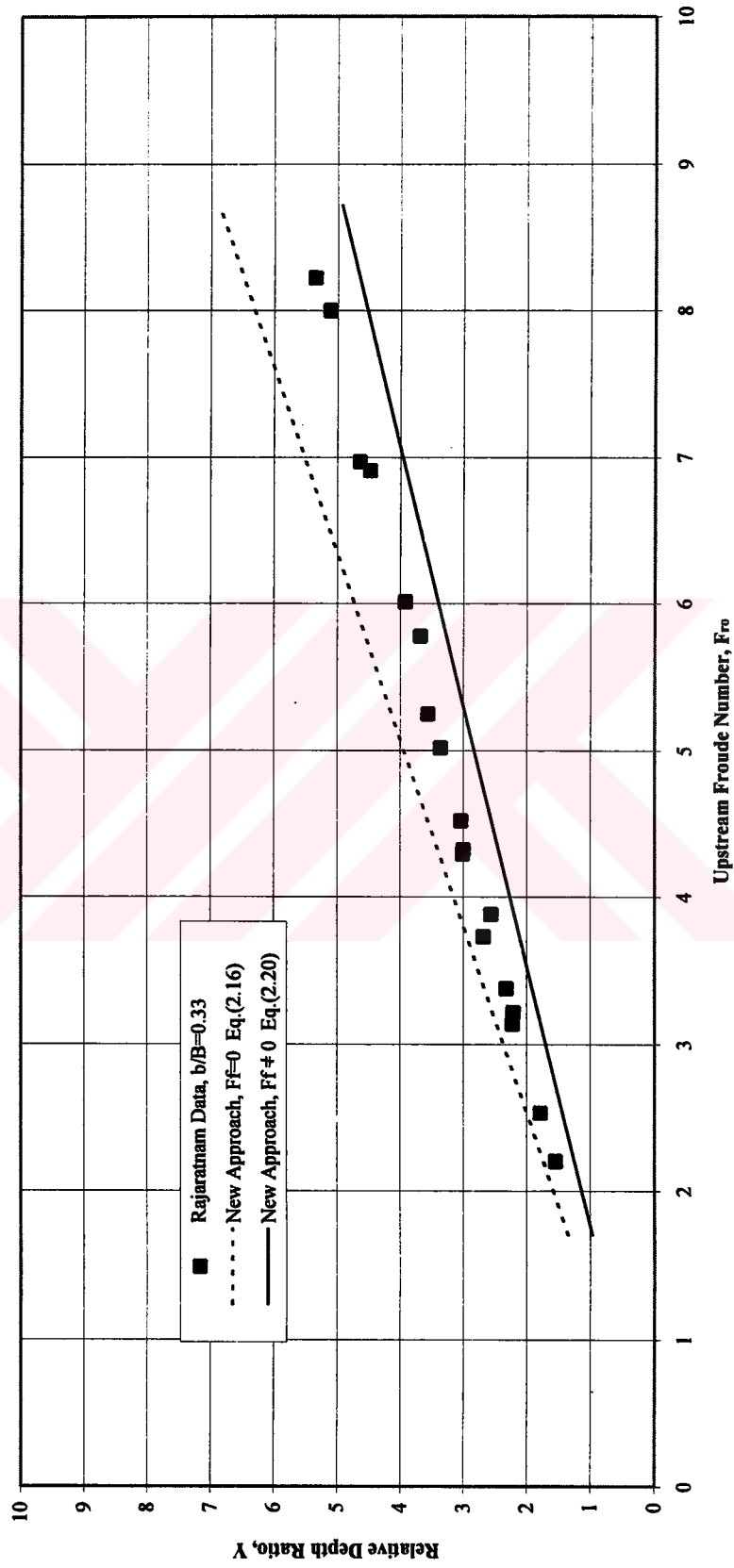
Fig. Fig. 4.12.d   Comparison of Rajaratnam's Data With New Approaches, α=0.33

63
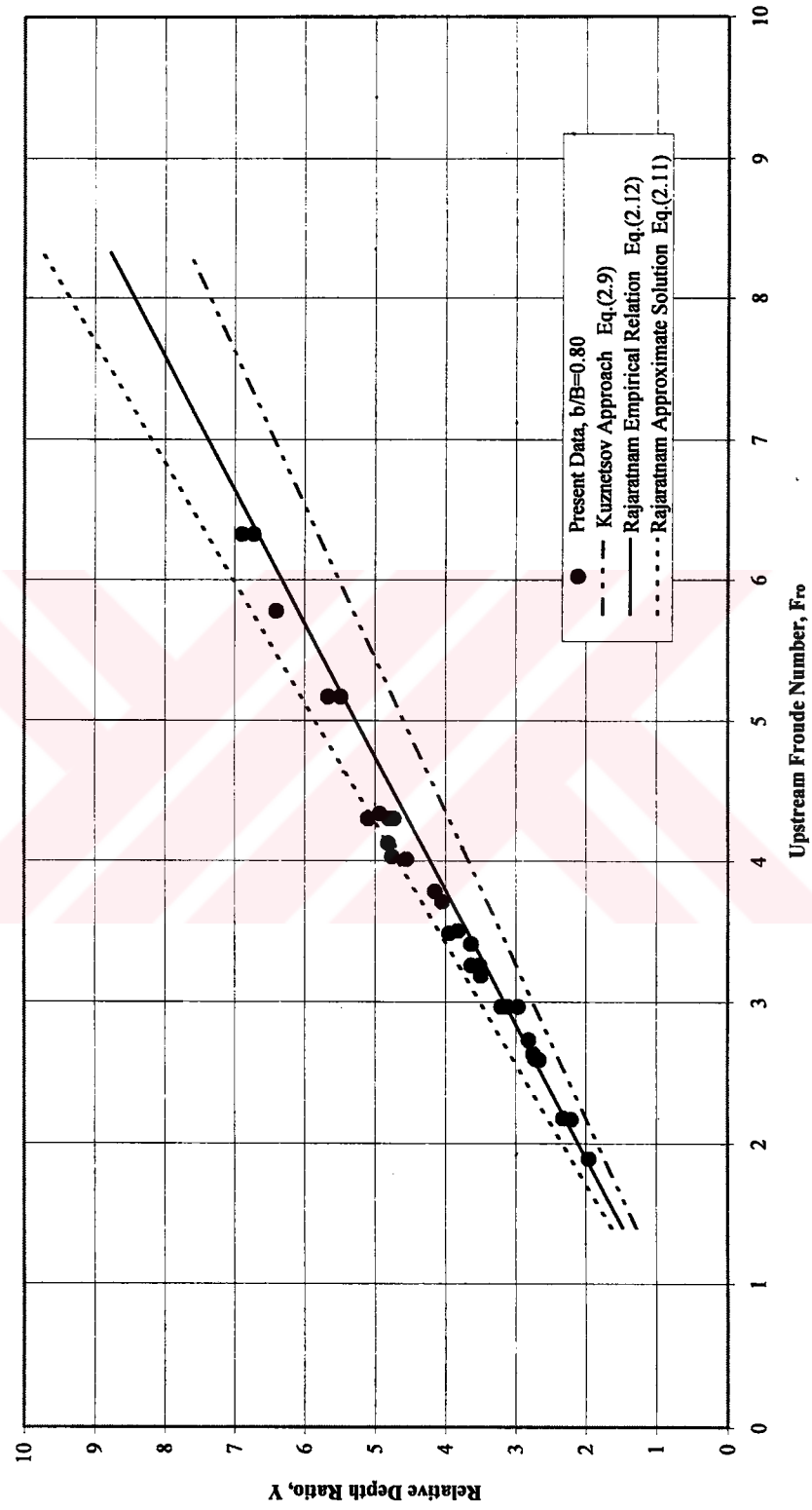
Fig. 4.13.a   Comparison of Present Data With The Approaches in The Literature, α=0.80

64
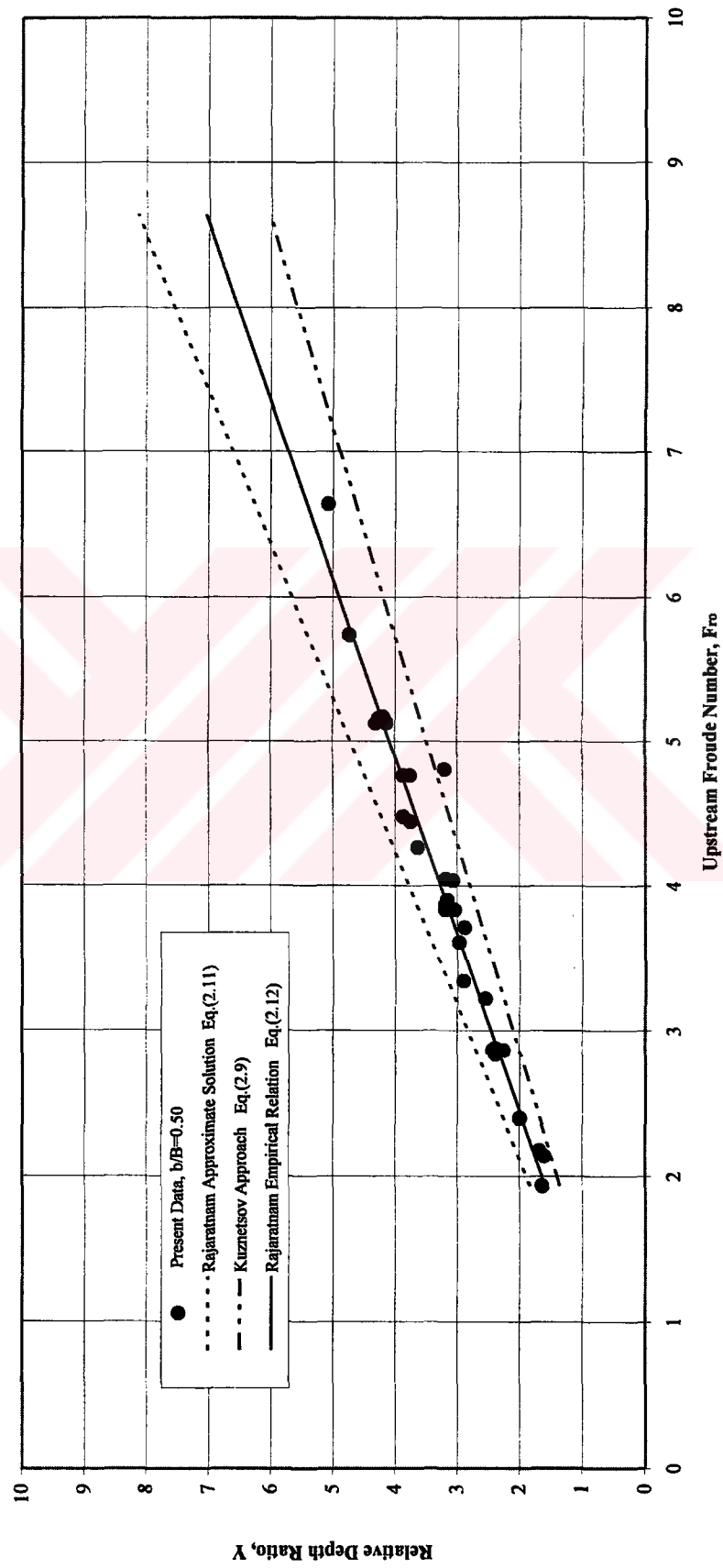
Fig. 4.13.b   Comparison of Present Data With The Approaches in The Literature, α=0.50

65
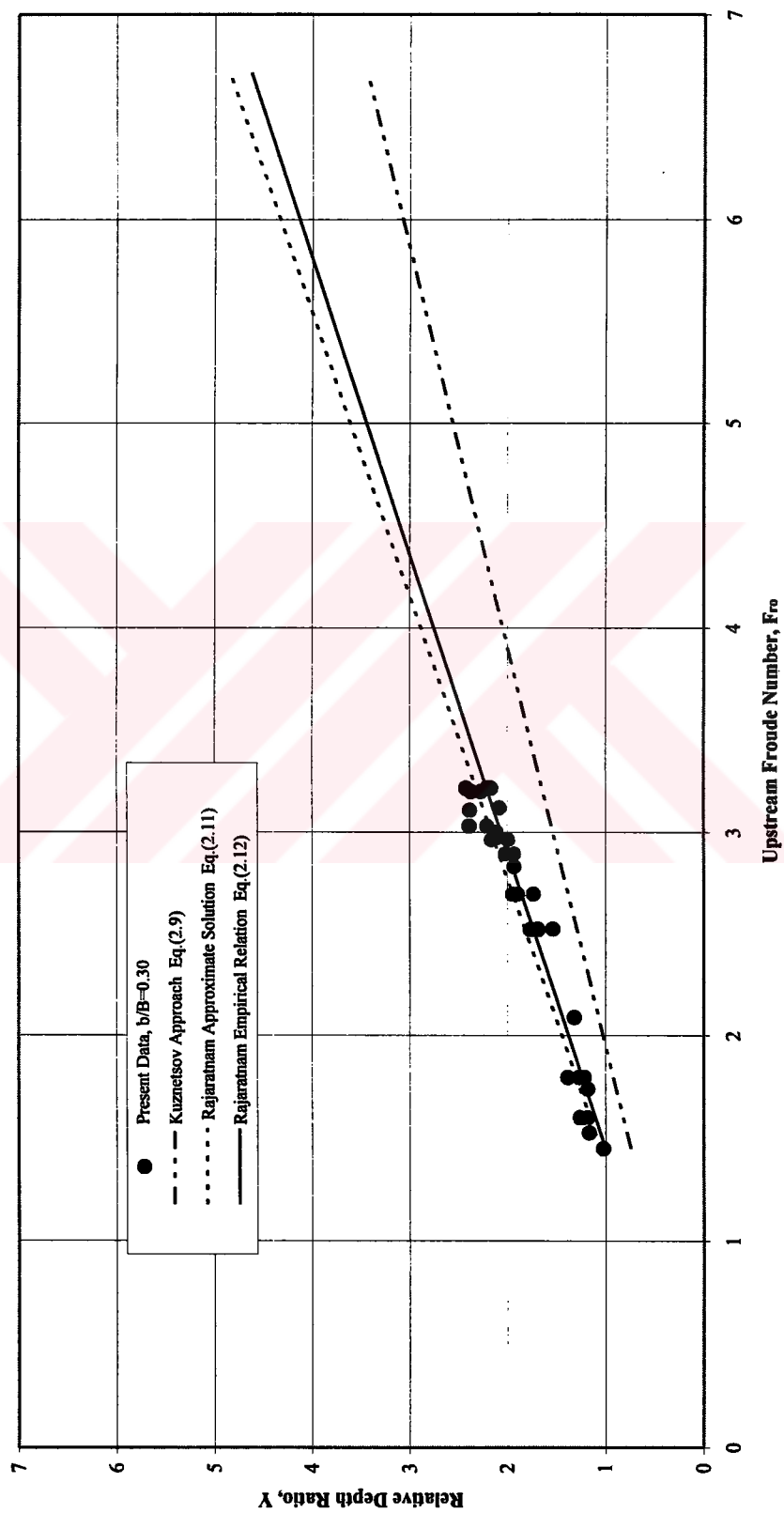
Fig. 4.13.c   Comparison of Present Data With The Approaches in The Literature, α=0.30
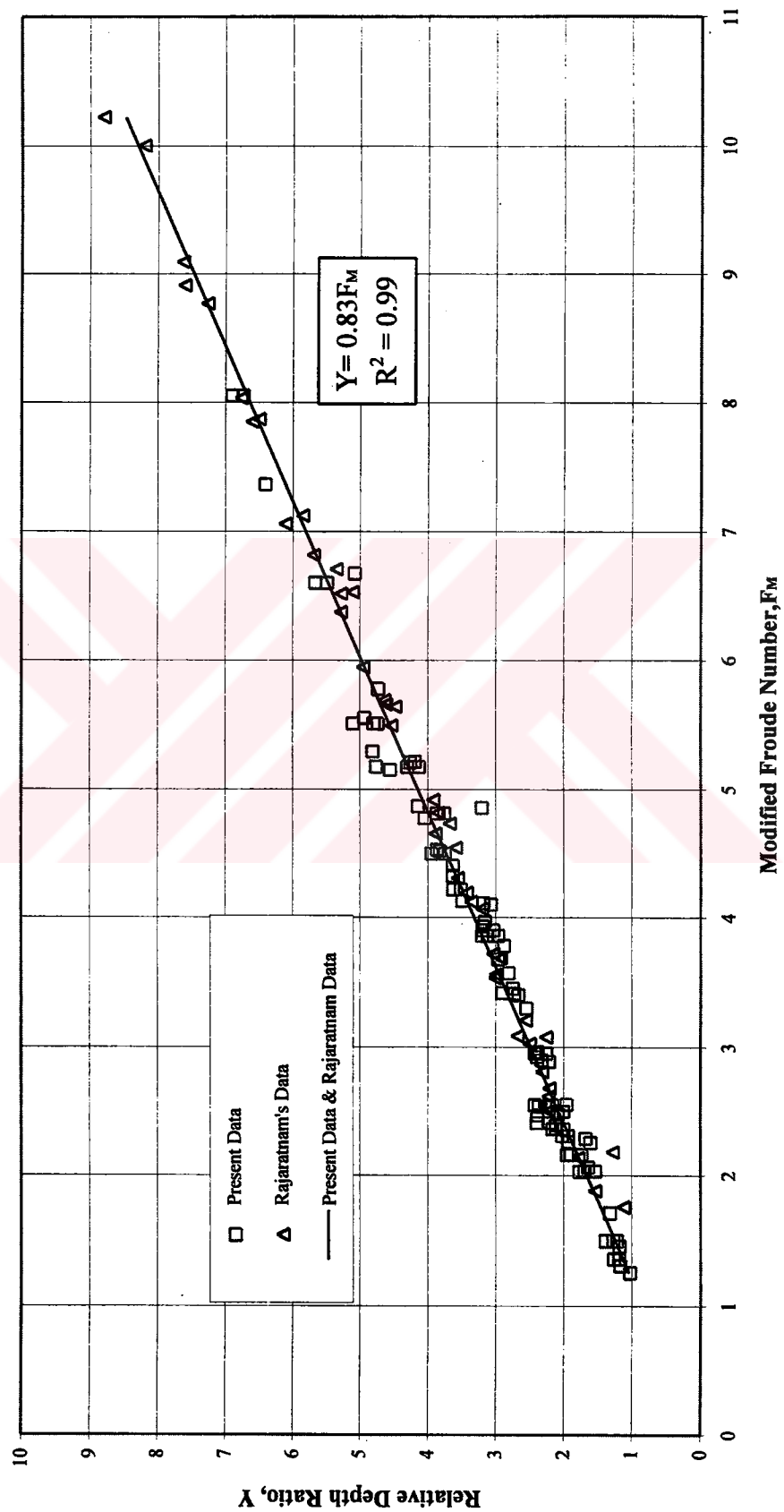
Fig. 4.14 Variation of The Relative Depth Ratio, Y With F_M, R-Jump.

The chart legend contains:
- Present Data
- Rajaratnam's Data
- Present Data & Rajaratnam Data

$Y = 0.83F_M$
$R^2 = 0.99$

X-axis: Modified Froude Number, F_M

Y-axis: Relative Depth Ratio, Y
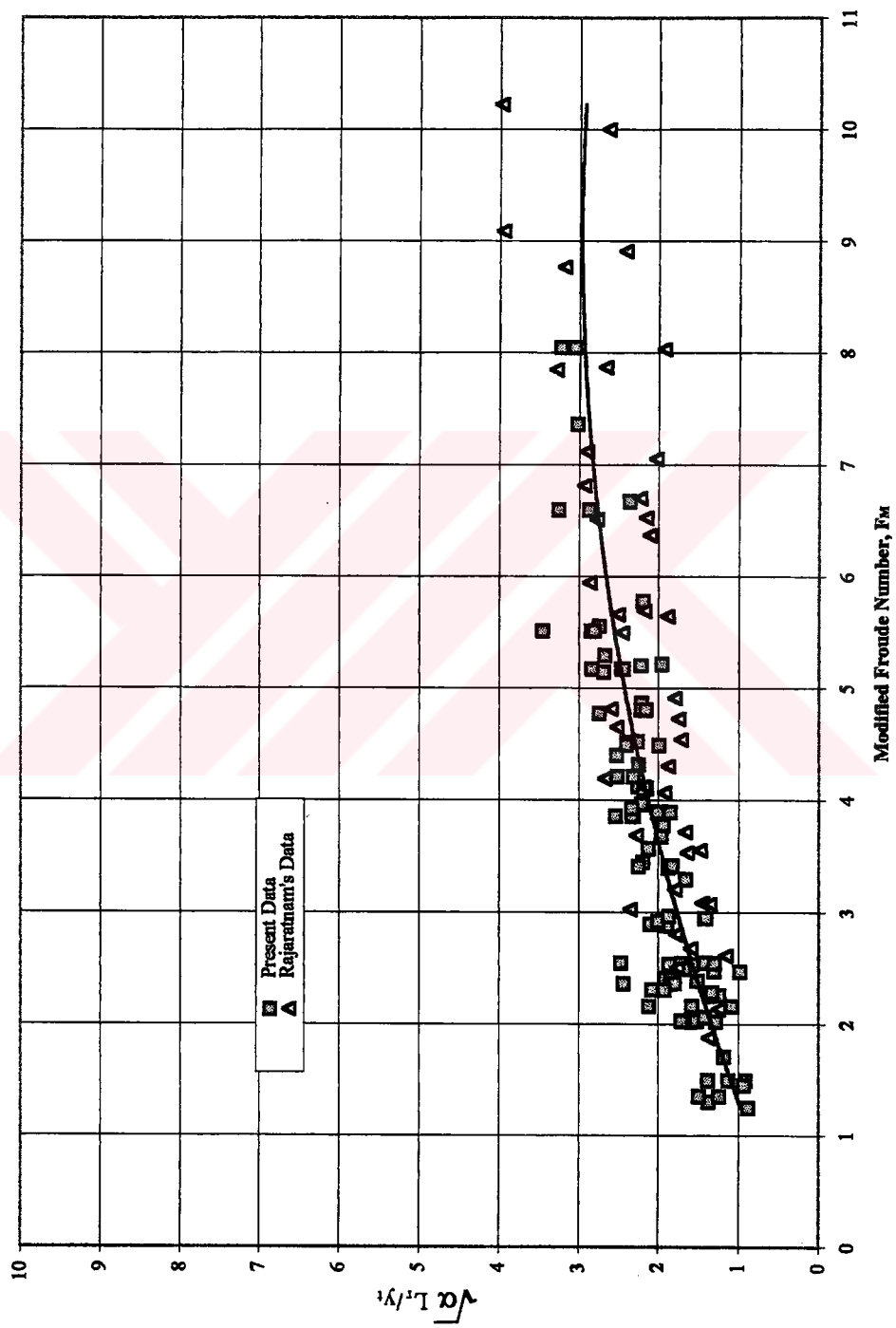
Fig. 4.15 Variation of The Length of Surface Roller of R-Jump.
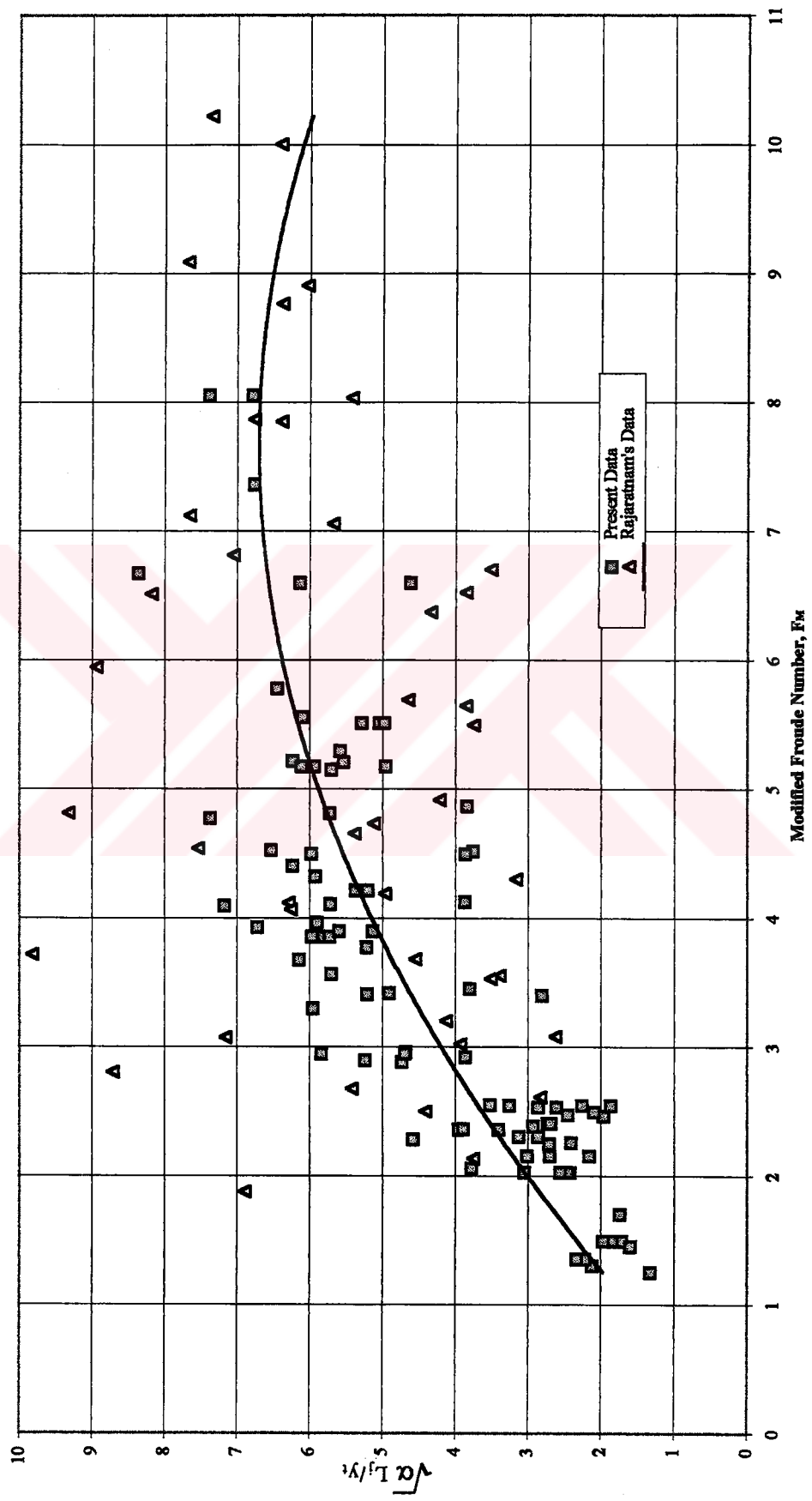
Fig. 4.16   Variation of The Length of R-Jump .
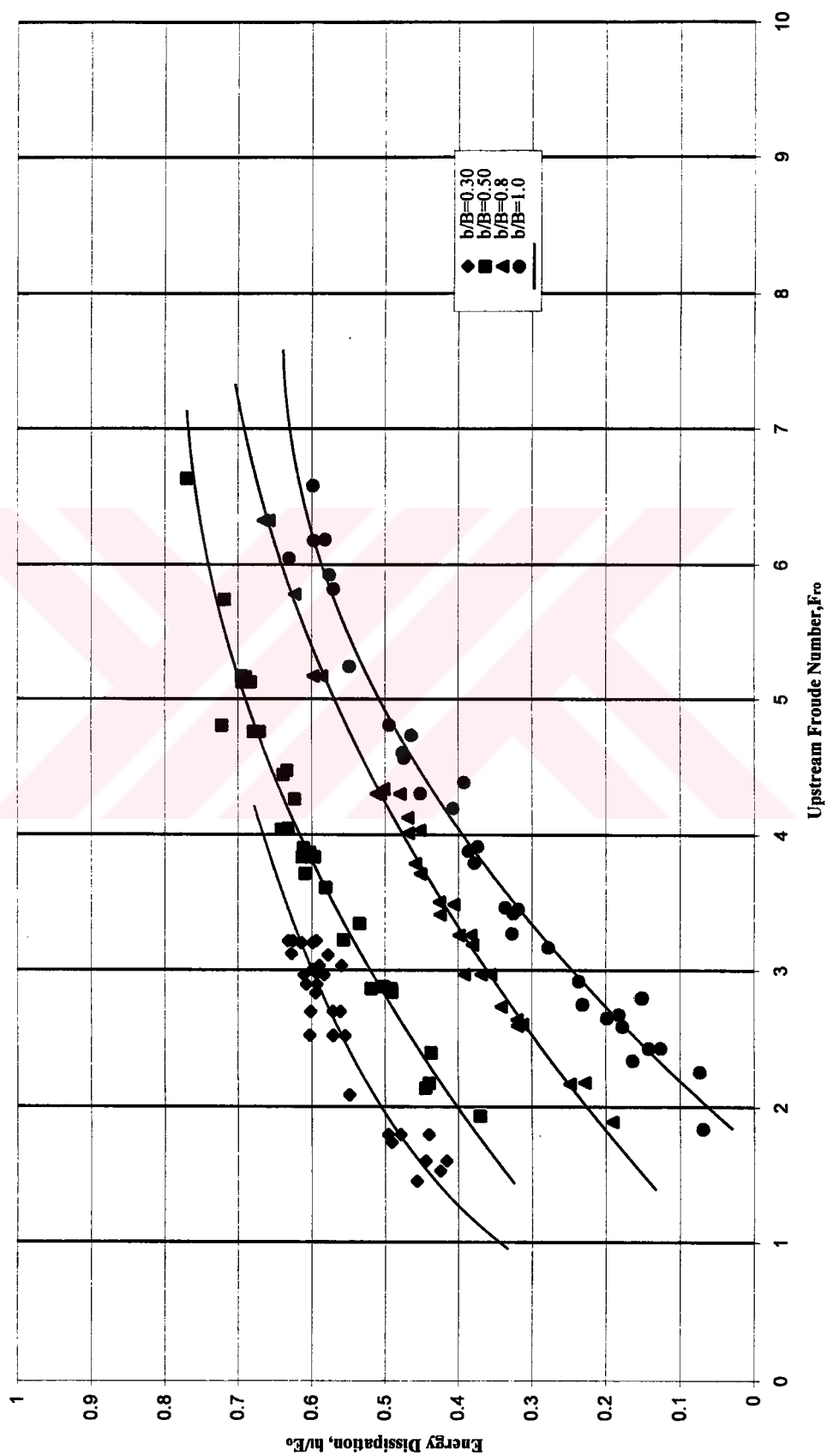
Fig. 4.17   Energy Dissipation Characteristics For R-Jump.

70

4.3   Results and Discussion of Results For S-Jumps

4.3.1 Sequent Depth for S-Jumps

The ranges of the Froude number of the upstream supercritical flow in the experiments performed for $\alpha = 0.80$ and 0.50 are given below:

$$\alpha = 0.80 \qquad 1.89 \leq F_{ro} \leq 6.33$$
$$\alpha = 0.50 \qquad 1.94 \leq F_{ro} \leq 9.12$$

Fig. 4.18 shows the variation of the relative depth ratio, Y with F_{ro} and α for all the experiments done in the present study.

The comparison of the S-jump data ($\alpha = 0.80$ and 0.50) with the simple hydraulic jump ($\alpha = 1.0$) data is also shown in Fig.4.18 and it is observed that the relative depth ratio, Y decreases with a decrease in the value of α for a given value of F_{ro}.
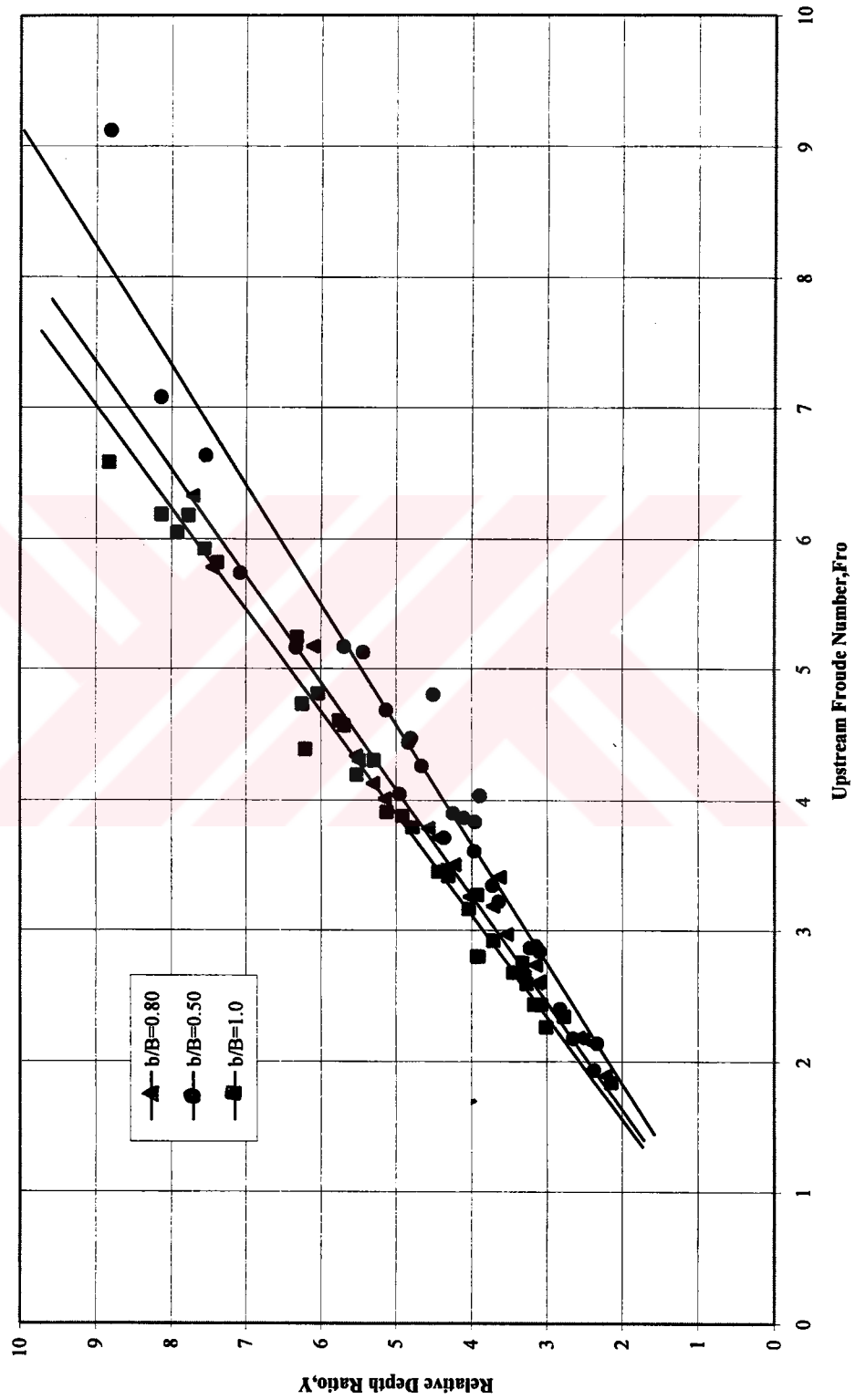
Fig. 4.18 Variation of The Relative Depth Ratio, Y With F_{ro} , S-Jump

Prediction of Y:

At section 2.3.2, two new approaches are introduced for the estimation of the force on the expanded walls. In the first approach given by Eq.(2.46), F_w is considered as given by hydrostatic pressure distribution due to backed-up depth, y_3. In the second approach given by Eq. (2.50), F_w is considered as given by uniform pressure distribution due to γy_3. The values of the backed-up depth are measured in the experiments. The Y values computed by using Eq.(2.46) and Eq.(2.50) and the measured y_3 values are compared with the data in Figs. 4.19.a and 4.19.b, respectively.

Figs. 4.19 show that Eq.(2.46) which assumes that the force on the wall, F_w can be computed by using hydrostatic pressure distribution due to the backed-up depth, y_3 , gives quite good results. However, to use Eq.(2.46), one needs to know the backed-up depth, y_3.

On the other hand, at section 2.3.2, the backed-up depth, y_3 is approximated simply as the arithmetic average of y_0 and y_t as given by Eq.(2.37) and (2.38). With this assumption Eq.(2.46) yields Eq.(2.47) and Eq.(2.50) yields Eq.(2.51).

The prediction of Y by using Eqs.(2.47) and (2.51) are compared with the data taken in the present study and data of Herbrand and data of Rajaratnam and Subramanya in Figs.4.20, 4.21 and 4.22, respectively.

Figs.4.20 show that Eq.(2.47) and Eq.(2.51) have the same trend and two approaches give quite good results for $\alpha=0.80$. However, for $\alpha=0.50$, when $F_{ro} >5$, the present data is getting away from the

line given by Eq.(2.47) and (2.51), respectively with a maximum error of 16%.

In Figs.4.21, Herbrand(1972)'s data is compared with the new approaches (Eq. 2.47 and Eq.2.51) for $\alpha=0.714$, 0.50, 0.286. It is observed that Eq.2.47 gives better results than Eq. (2.51) for $\alpha=0.714$. However, for $\alpha=0.50$ and 0.286, Eq.(2.47) has the same trend with Herbrand's data but with a maximum error of 10%.

In Figs. 4.22, Rajaratnam and Subramanya(1968)'s data is also compared with the new approaches (Eq. 2.47 and Eq.2.51) for $\alpha=0.83$, 0.67, 0.50, 0.33. It is observed that Eq.2.47 gives better results than Eq. (2.51) for $\alpha=0.83$ and 0.67. However, for $\alpha=0.50$, when $F_{ro} \leq 5$, the data has the same trend with the line given by Eq.(2.47), as F_{ro} becomes larger than 5, it approaches to Eq.(2.51) with a maximum error of 6% due to the change in the value of b/y_o from 8.3 to 3.4. Also, for $\alpha=0.33$, when $F_{ro} \leq 4.5$, the data approaches to Eq.(2.51) with a maximum error of 22%, as F_{ro} becomes larger than 4.5, the data has a trend through Eq.(2.47) with a maximum error of 7%.

Present data with the approaches in the literature (Hager (1985)) is also compared in Fig.4.23. These figures show that, for $\alpha=0.80$, when $F_{ro} \leq 4$, Hager's intermediate and lower limits (Eq.2.40 and Eq.2.41) predict the relative depth ratio values better than upper limit approach (Eq.2.38), as F_{ro} becomes larger than 4, the trend of the data could not be predicted. For $\alpha=0.50$, the data is in between Hager's three approaches, (Eq.2.38, Eq.2.40, Eq.2.41). Three approaches have all been found to be unsatisfactory for predicting the sequent depth.

At section 2.3.1, a modified Froude number is introduced which assumes that the relative depth ratio is a function of modified Froude number, F_M. The present data, Rajaratnam's data and Herbrand's data are plotted as Y versus F_M in Fig. 4.24. The values of α in Fig. 4.24 are α=0.286, 0.30, 0.33, 0.50, 0.67, 0.714, 0.80 and 0.83. This figure shows that the modified Froude number is a good scaling factor for hydraulic jumps at abrupt enlargements. Fig. 4.24 show that Rajaratnam's data separates from the present data and Herbrand's data and it is parallel to the best fit. It is important to note in the experimental set up used by Rajaratnam (1968), the jet is issuing out from a nozzle.

Therefore, the same plot is repeated by excluding Rajaratnam's data in Fig. 4.25, for which the best fit line is $Y=1.006F_M$ with a correlation coefficient of 95%.

Therefore, for all practical design purposes the relative depth ratio for S-jumps can be written as

$$Y=\sqrt{\alpha(1+2F_{ro}^2)} \qquad \dots\dots\dots\dots\dots\dots\dots(4.2)$$

4.3.2 Length Characteristics of S-Jump

In sizing the length characteristics of S-jump, the value of $\sqrt{\alpha}$ and modified Froude number are used as scaling factors. Therefore, the length of the surface roller and the length of the jump are plotted as $\sqrt{\alpha}\, L_r/y_t$ versus F_M and $\sqrt{\alpha}\, L_j/y_t$ versus F_M in Figs. 4.26 and 4.27, respectively. Regarding the length of the roller and the jump, Figs. 4.26 and 4.27 show considerable scatter as expected.

4.3.3 Energy Dissipation in S-Jumps

The energy dissipation in S-jump is obtained by the application of Eq.(2.56) and it is plotted against F_{ro} for $\alpha=0.50$, 0.80 and 1.0 in Fig. 4.28. This plot shows that the relative energy dissipation is a function of F_{ro} and α. It is observed that abrupt enlargements possess substantially higher relative energy dissipation than that of simple hydraulic jump for equal F_{ro}. Eq.(2.56) shows also that the relative energy dissipation increases as α decreases. Consequently, the relative energy dissipation relating to the reduced depth is greater than in the regular basins.
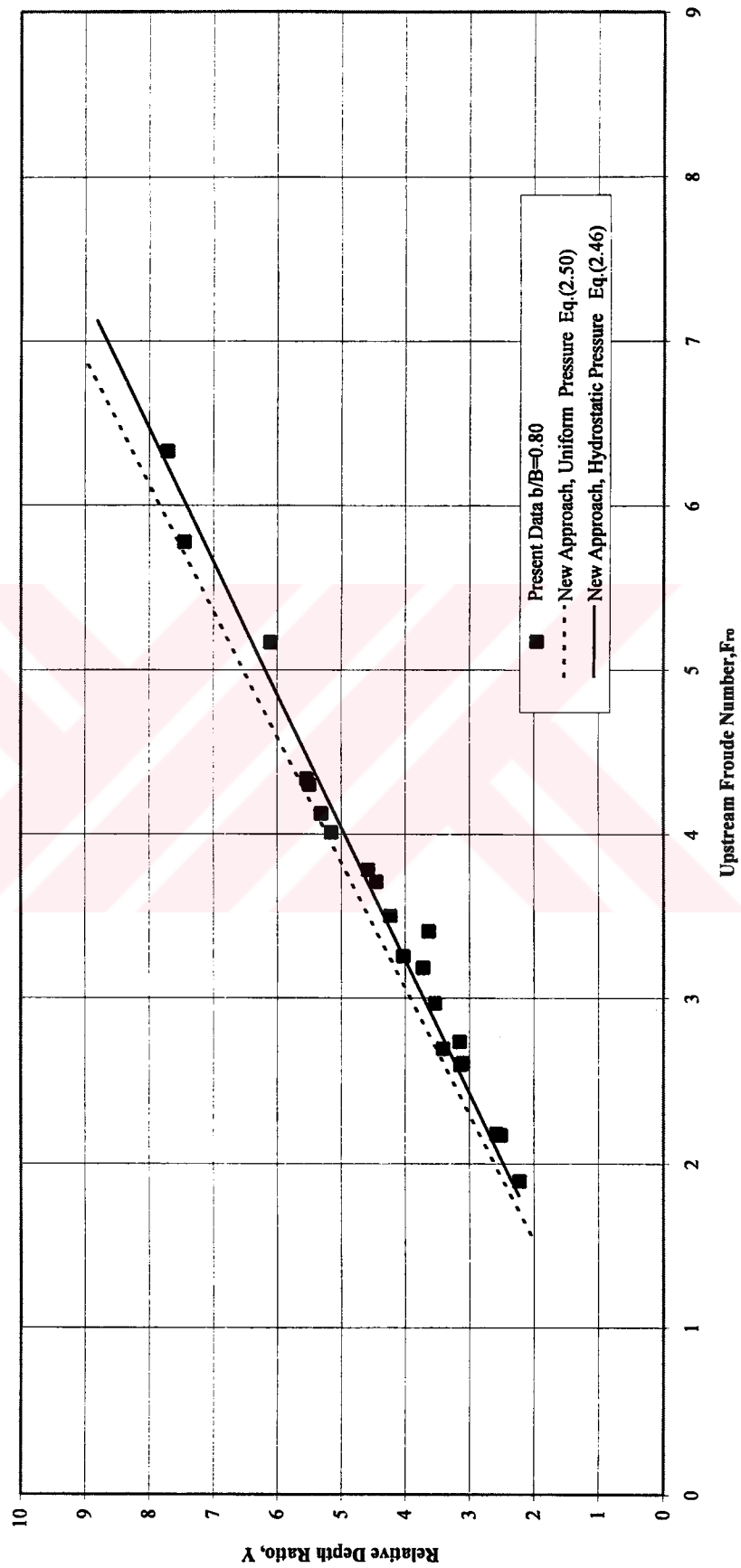
Fig. 4.19.a   Comparison of Present Data With New Approaches, α=0.80

77
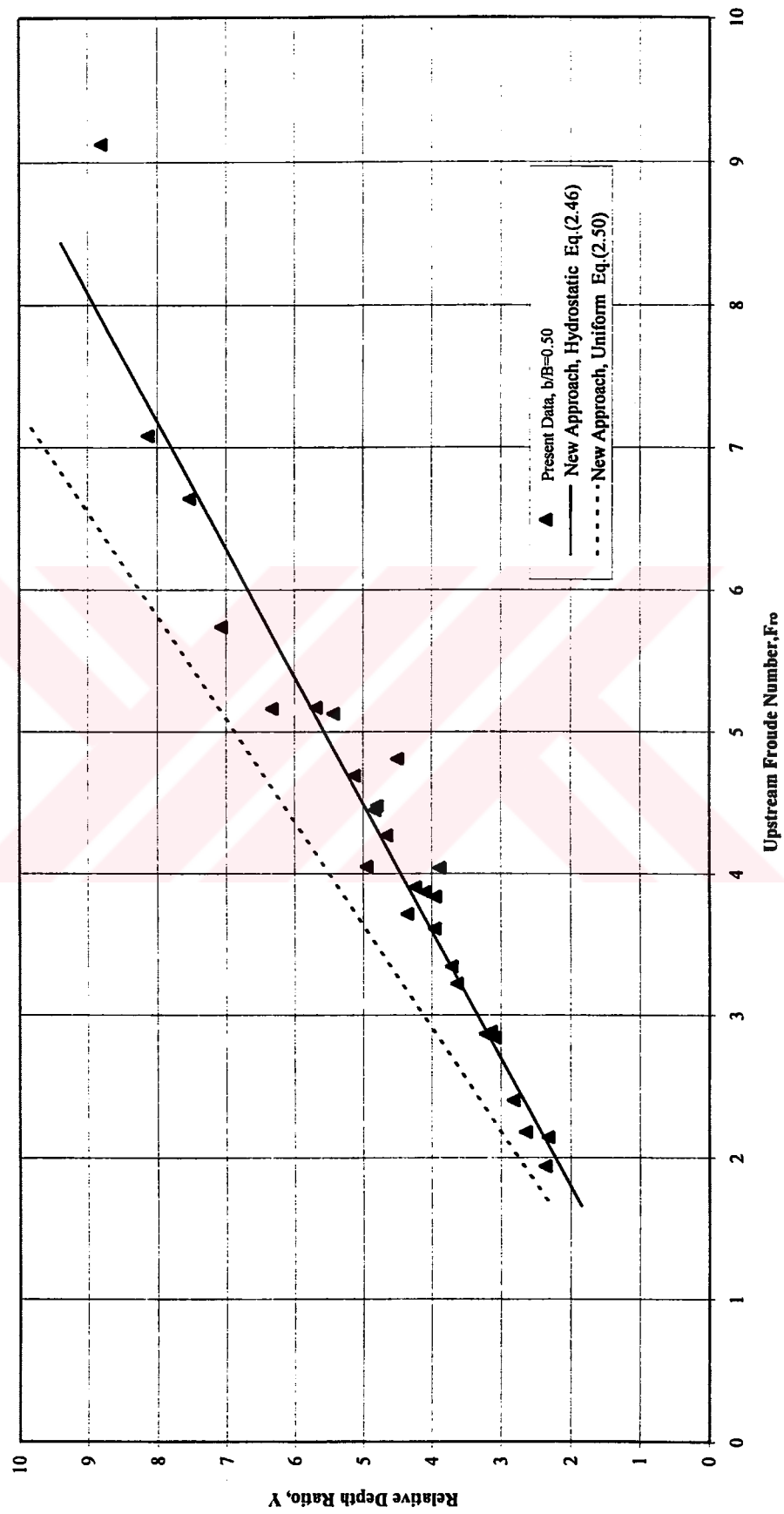
Fig. 4.19.b   Comparison of Present Data With New Approaches, $\alpha=0.50$

78
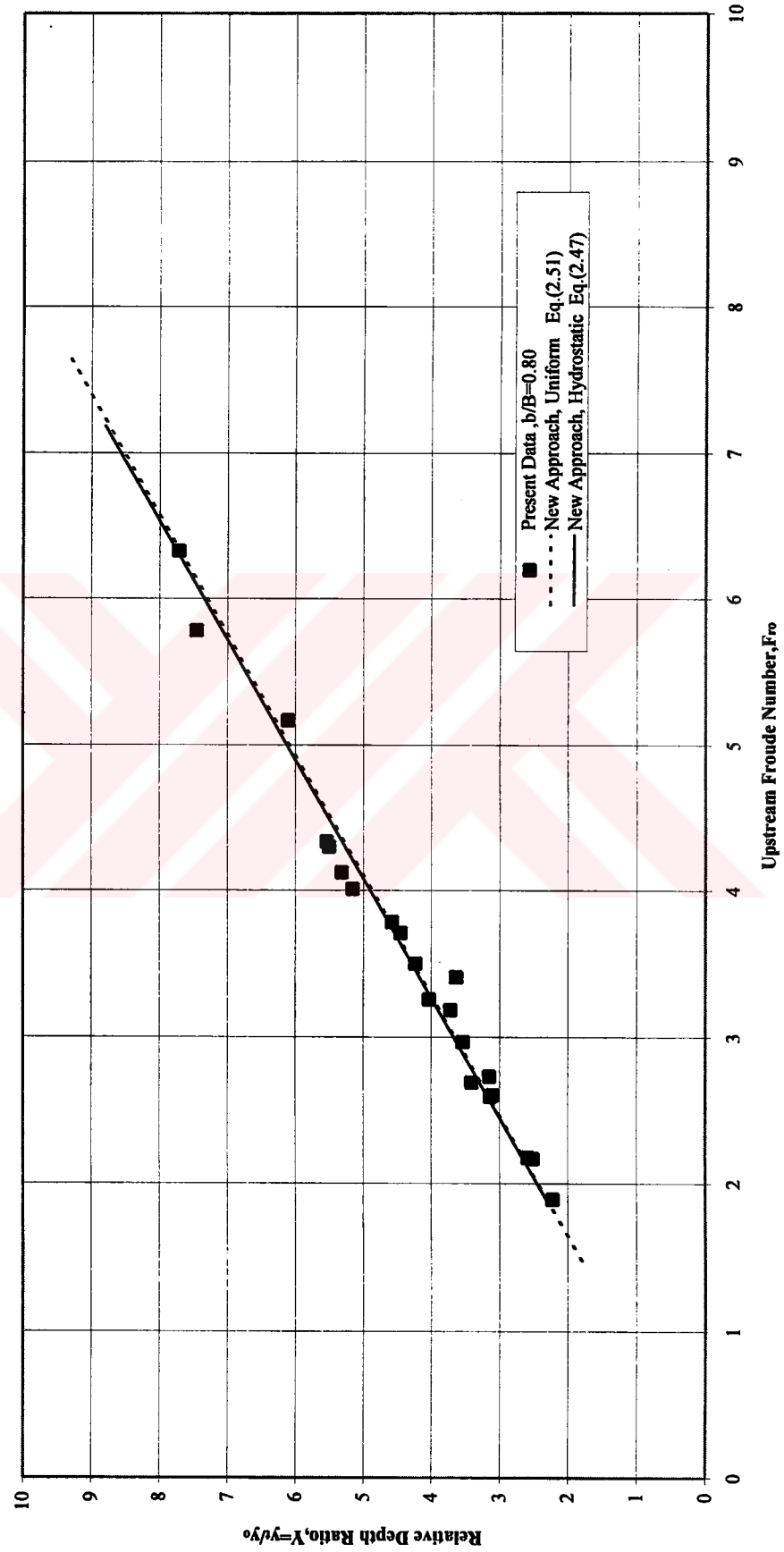
Fig. 4.20.a   Comparison of Present Data With New Approaches, α=0.80

79
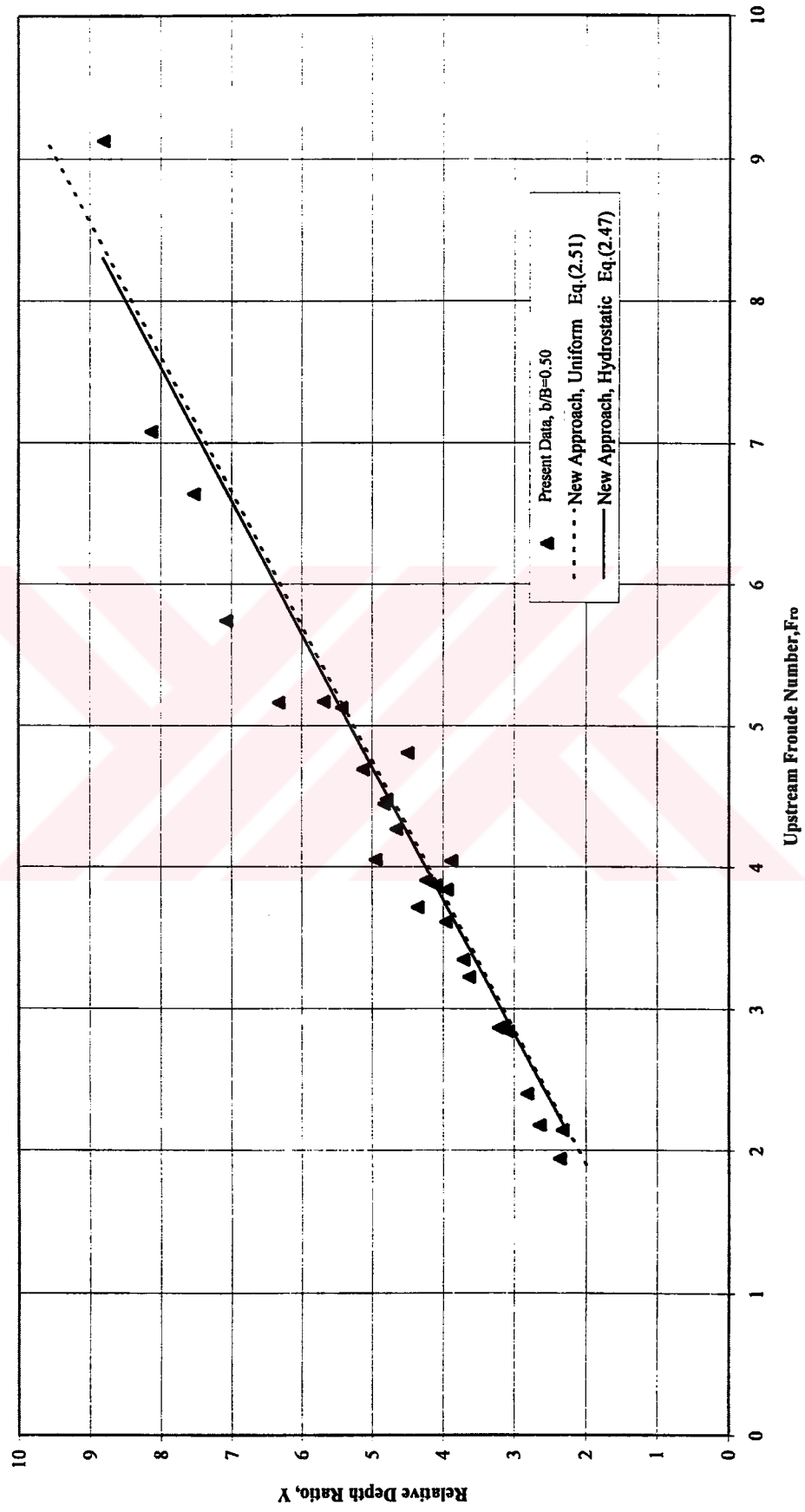
Fig. 4.20.b Comparison of Present Data With New Approaches, α=0.50
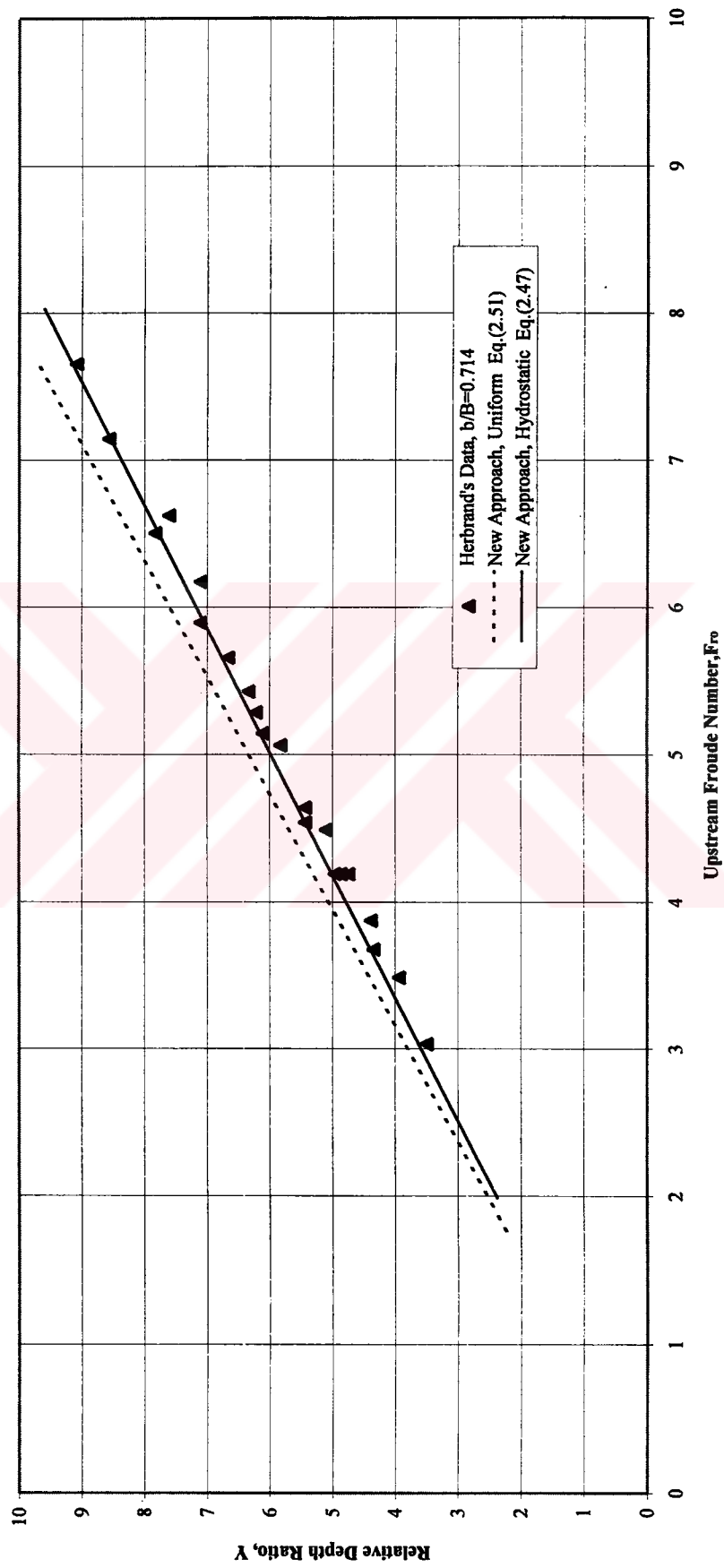
Fig. 4.21.a Comparison of Herbrand's Data With New Approaches,   α=0.714.
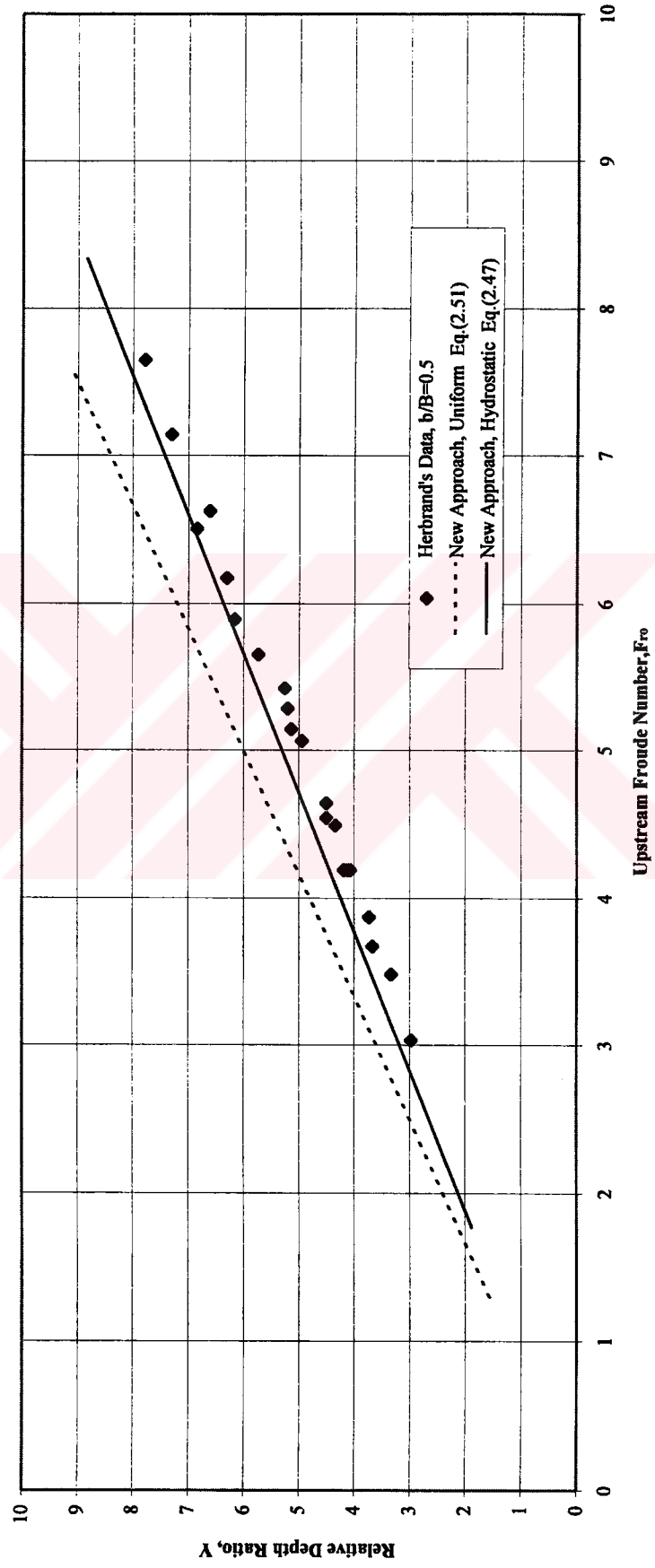
Fig. 4.21.b Comparison of Herbrand's Data With New Approaches,   α=0.50.
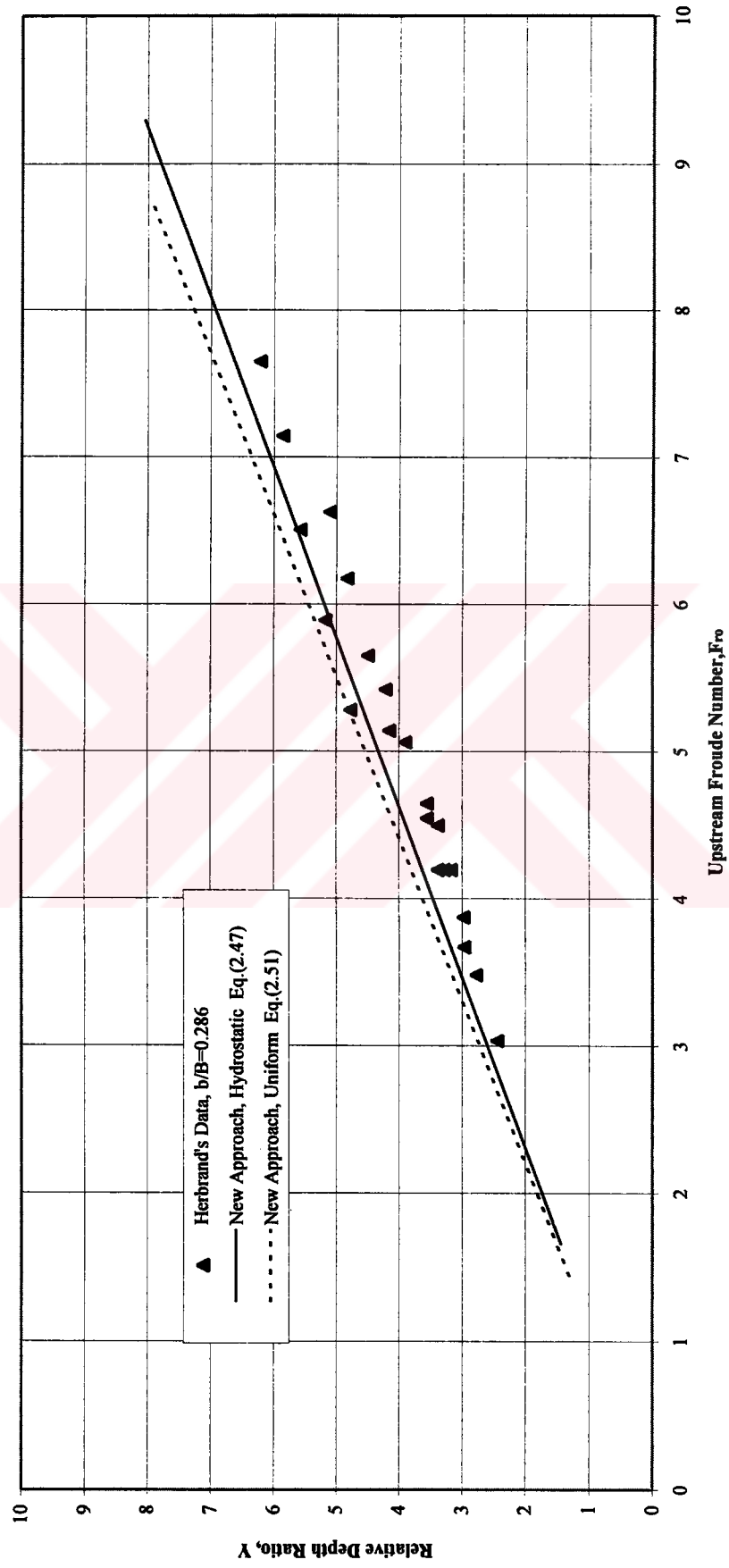
Fig. 4.21.c Comparison of Herbrand's Data With New Approaches, $\alpha=0.286$.

83
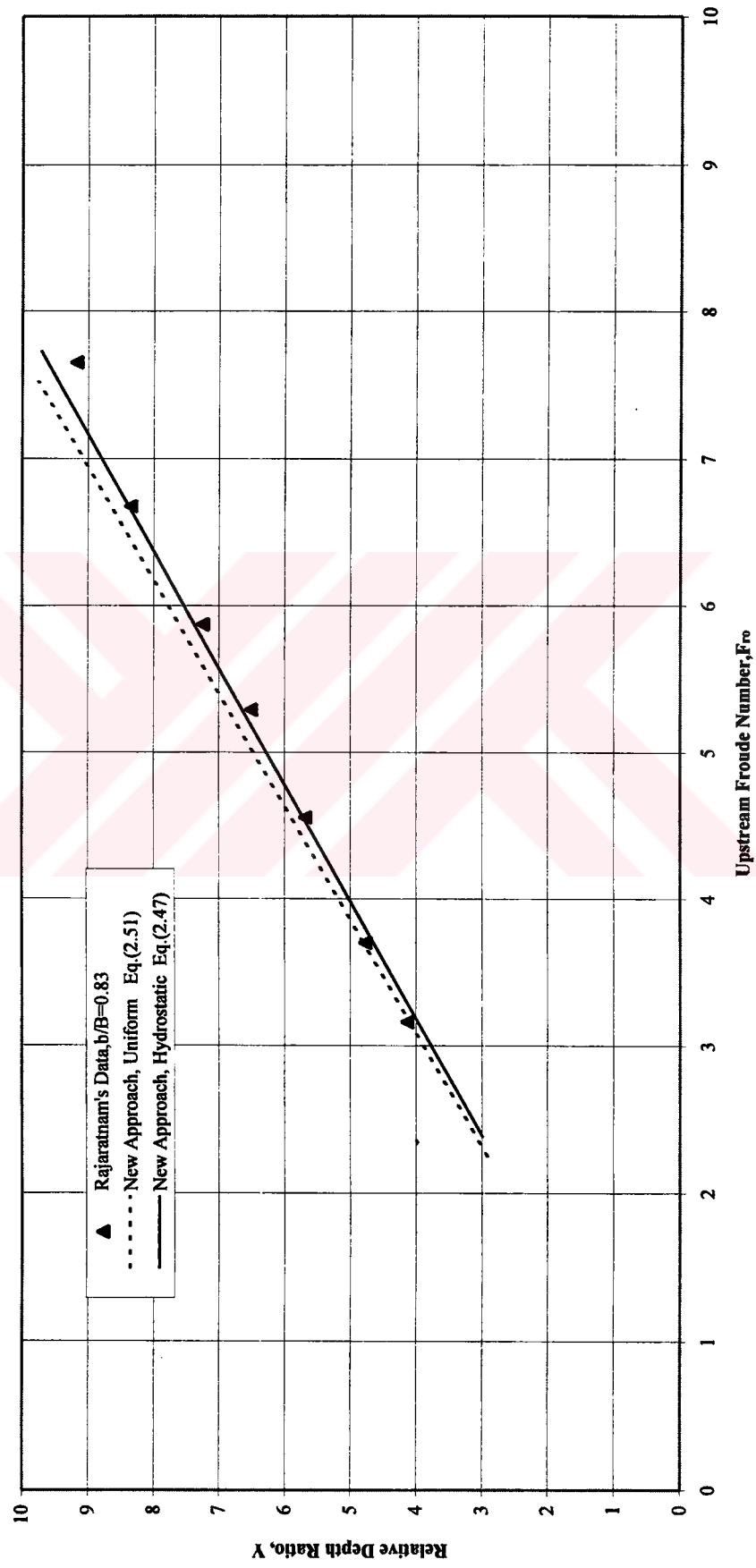
Fig. 4.22.a Comparison of Rajaratnam's Data With New Approaches, $\alpha=0.83$

84
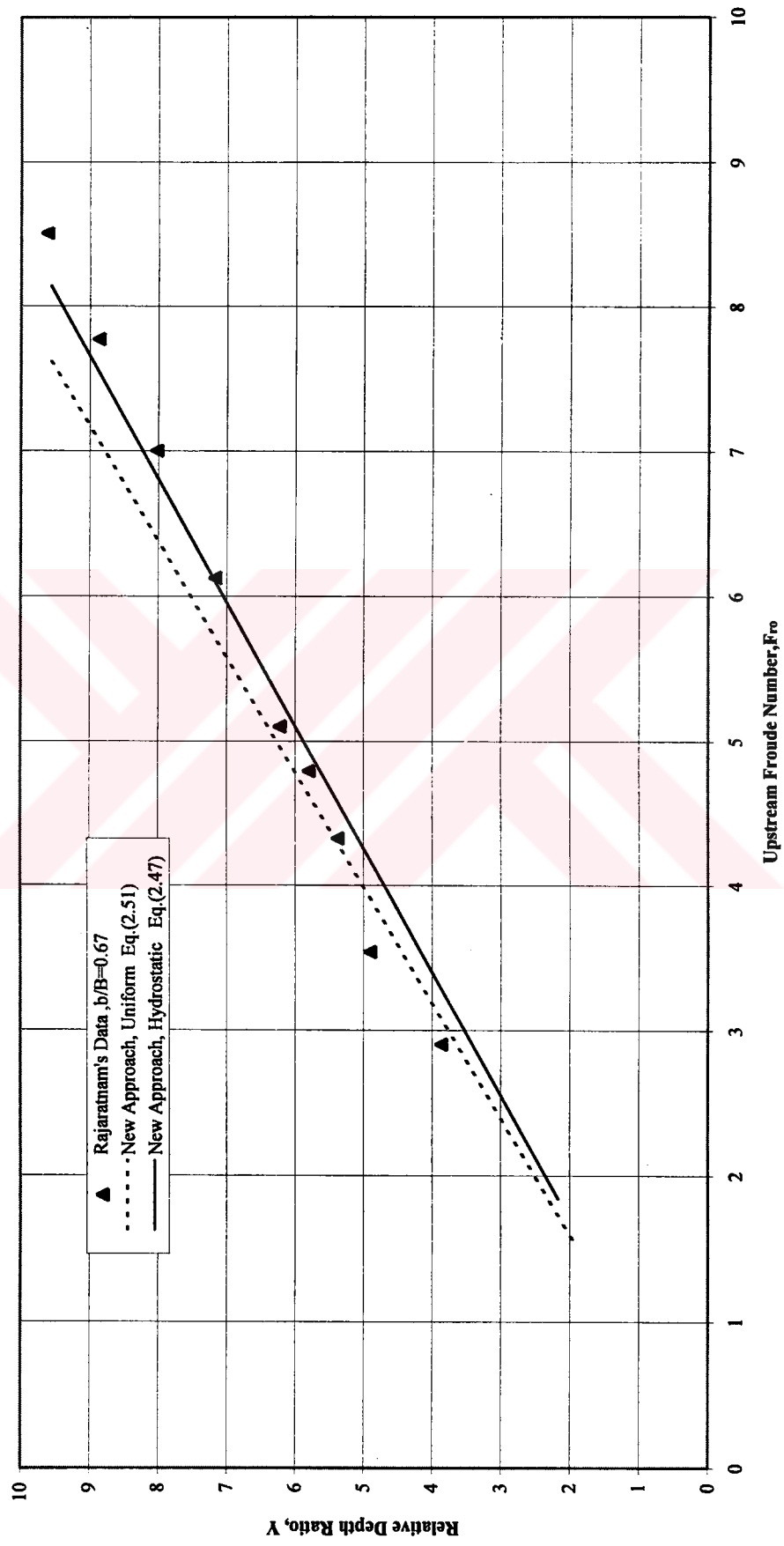
Fig. 4.22.b Comparison of Rajaratnam's Data With New Approaches, $\alpha=0.67$

85

Fig. 4.22.c Comparison of Rajaratnam's Data With New Approaches, α=0.50

Legend:
- ▲ Rajaratnam's Data, b/B=0.5
- —·—·— New Approach, Uniform Eq.(2.51)
- ——— New Approach, Hydrostatic Eq.(2.47)

Upstream Froude Number, F_{ro}

Relative Depth Ratio, Y
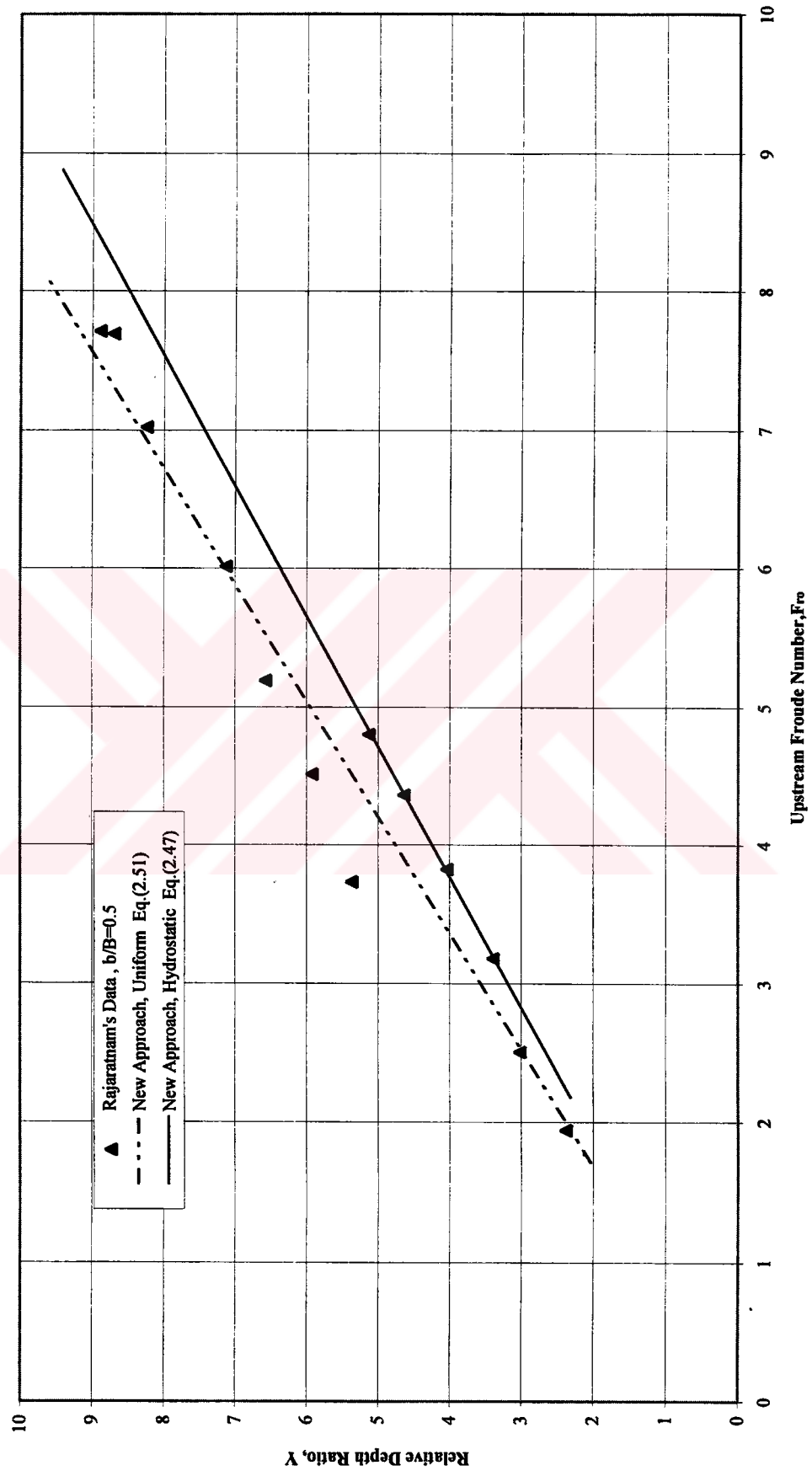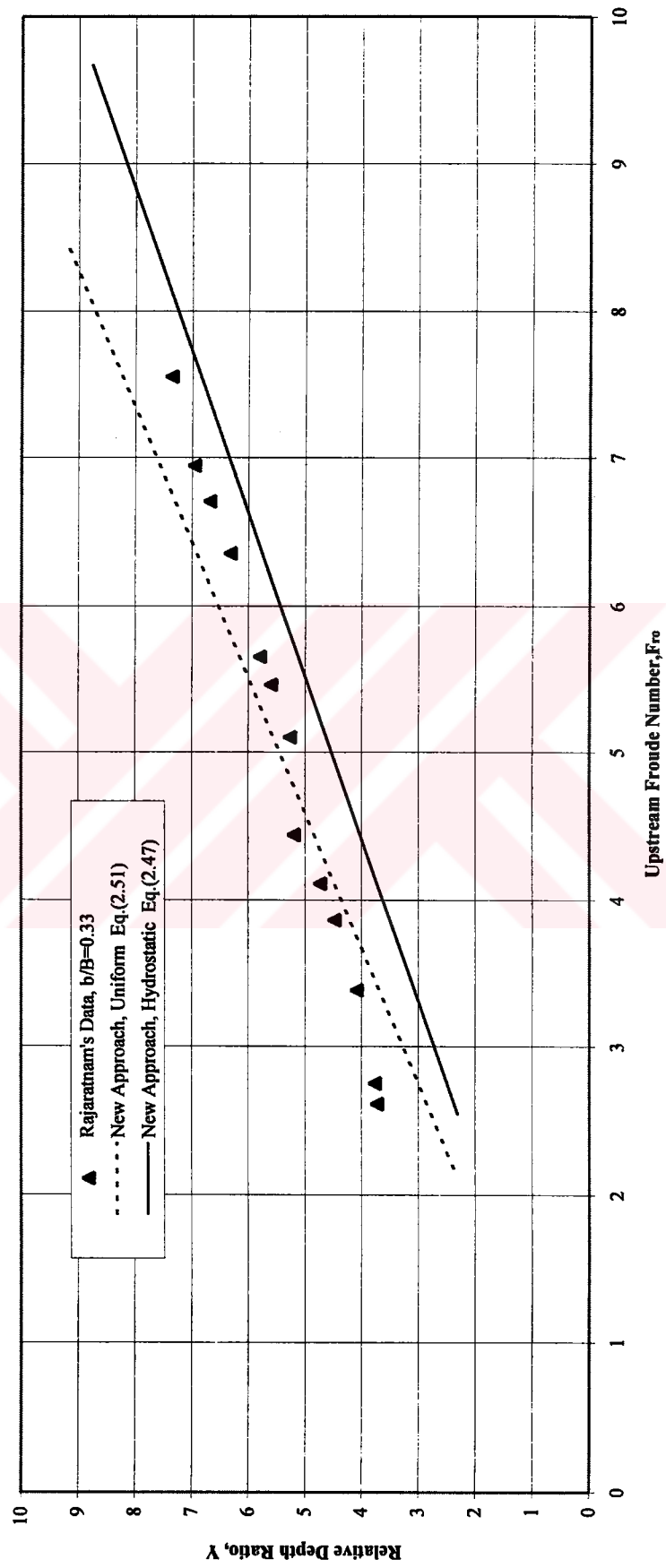
Fig. 4.22.d Comparison of Rajaratnam's Data With New Approaches, $\alpha=0.33$
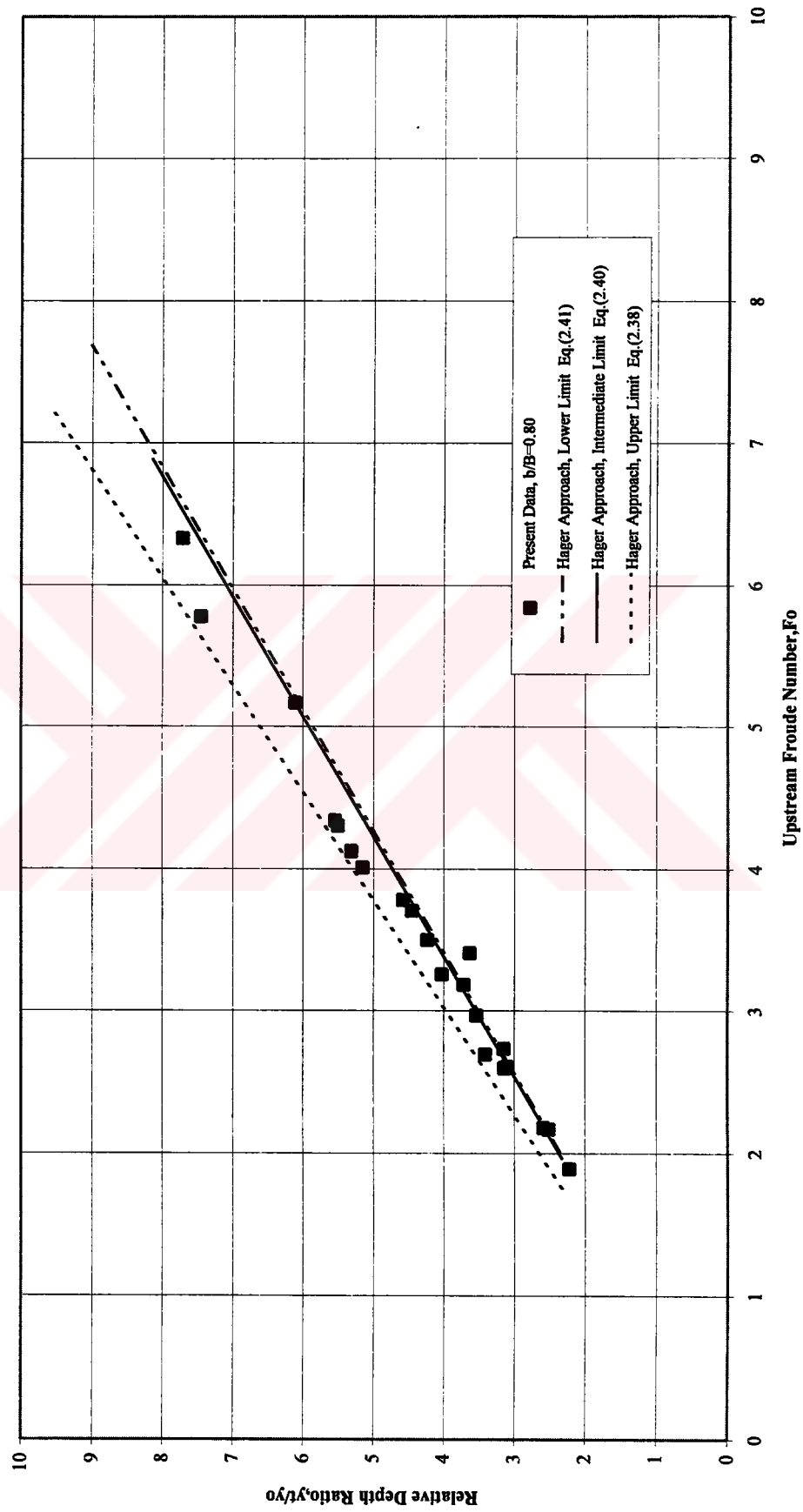
Fig. 4.23 . a Comparison of Present Data With The Approaches in The Literature, α=0.80

Legend:
- ■ Present Data, b/B=0.80
- — ·· — Hager Approach, Lower Limit Eq.(2.41)
- ——— Hager Approach, Intermediate Limit Eq.(2.40)
- ······ Hager Approach, Upper Limit Eq.(2.38)

X-axis: Upstream Froude Number,Fo

Y-axis: Relative Depth Ratio,yt/yo
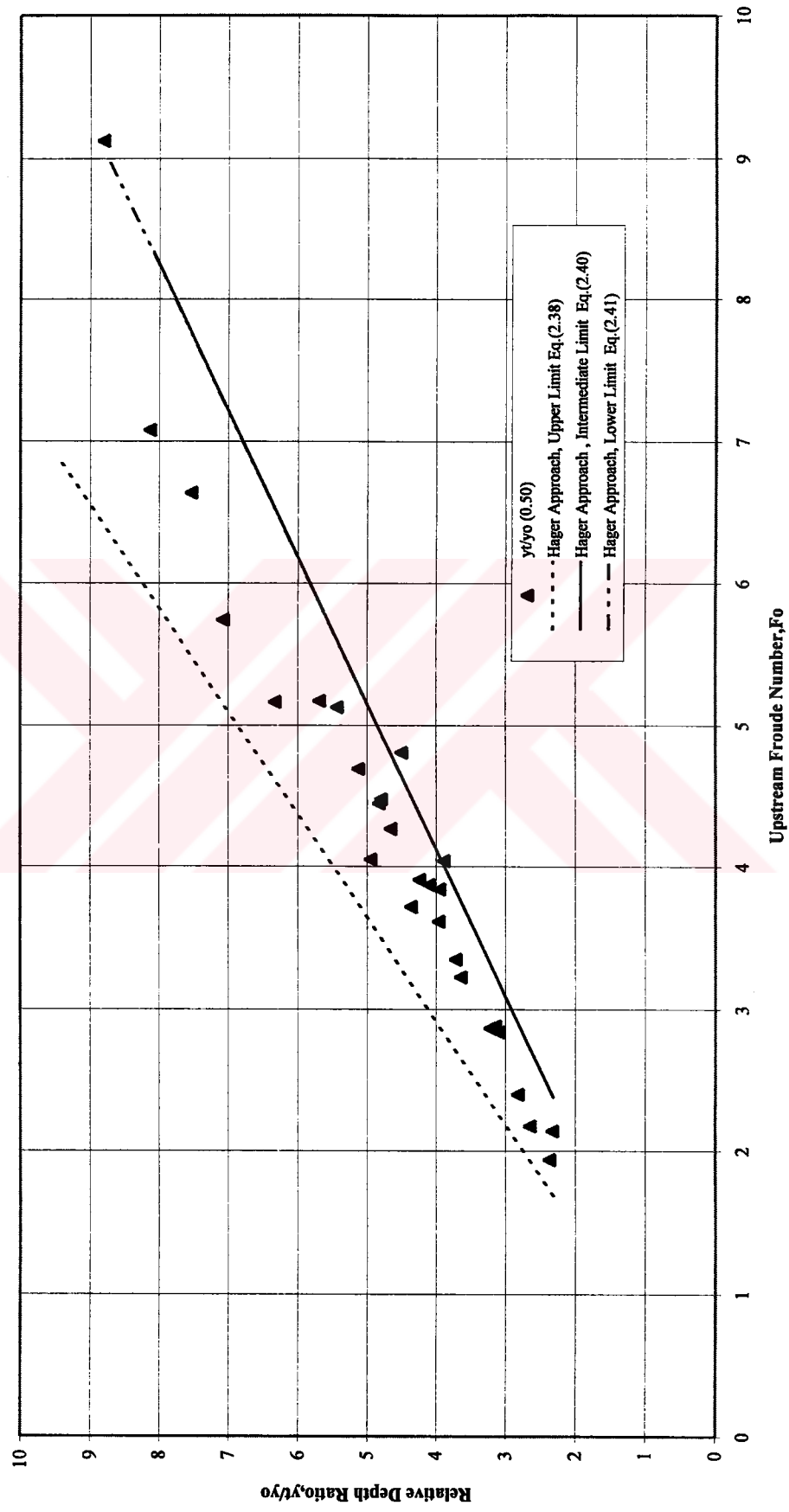
Fig. 4.23.b Comparison of Present Data With The Approaches In The Literature, α=0.50
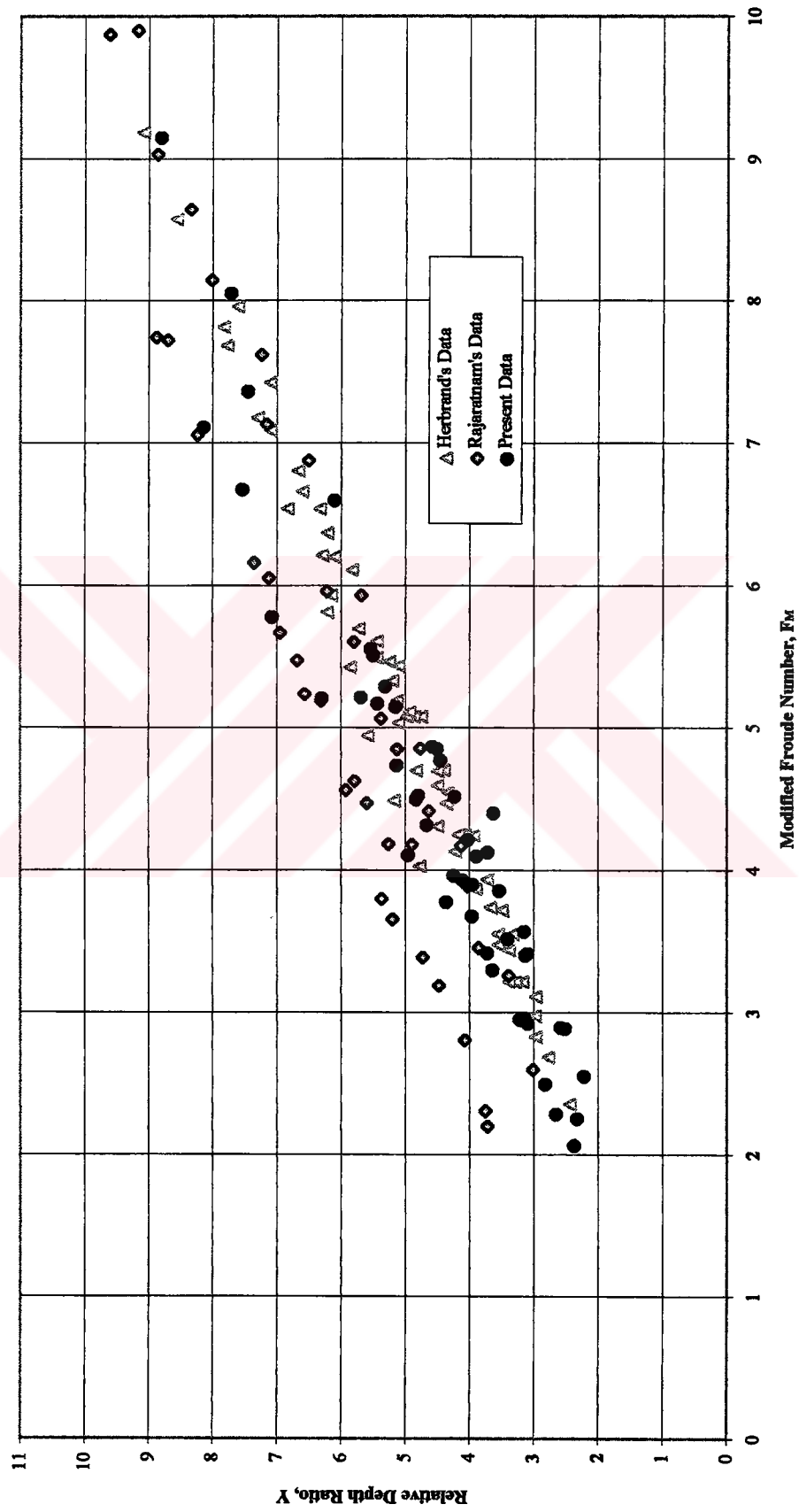
Fig. 4.24   Variation of The Relative Depth Ratio, Y With F_M For S-Jump
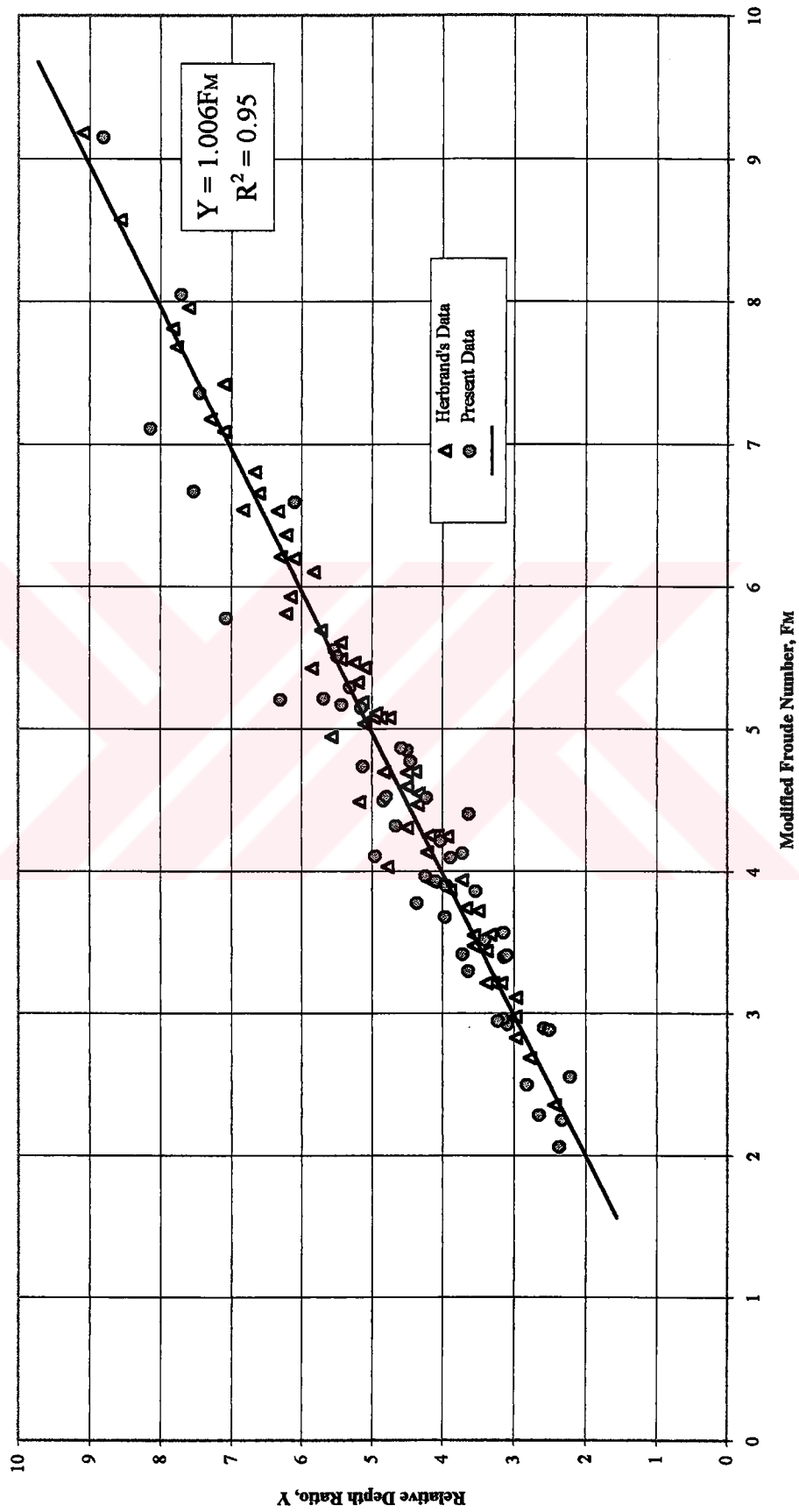
Fig. 4.25   Variation of The Relative Depth Ratio, Y With F_M For S-Jump
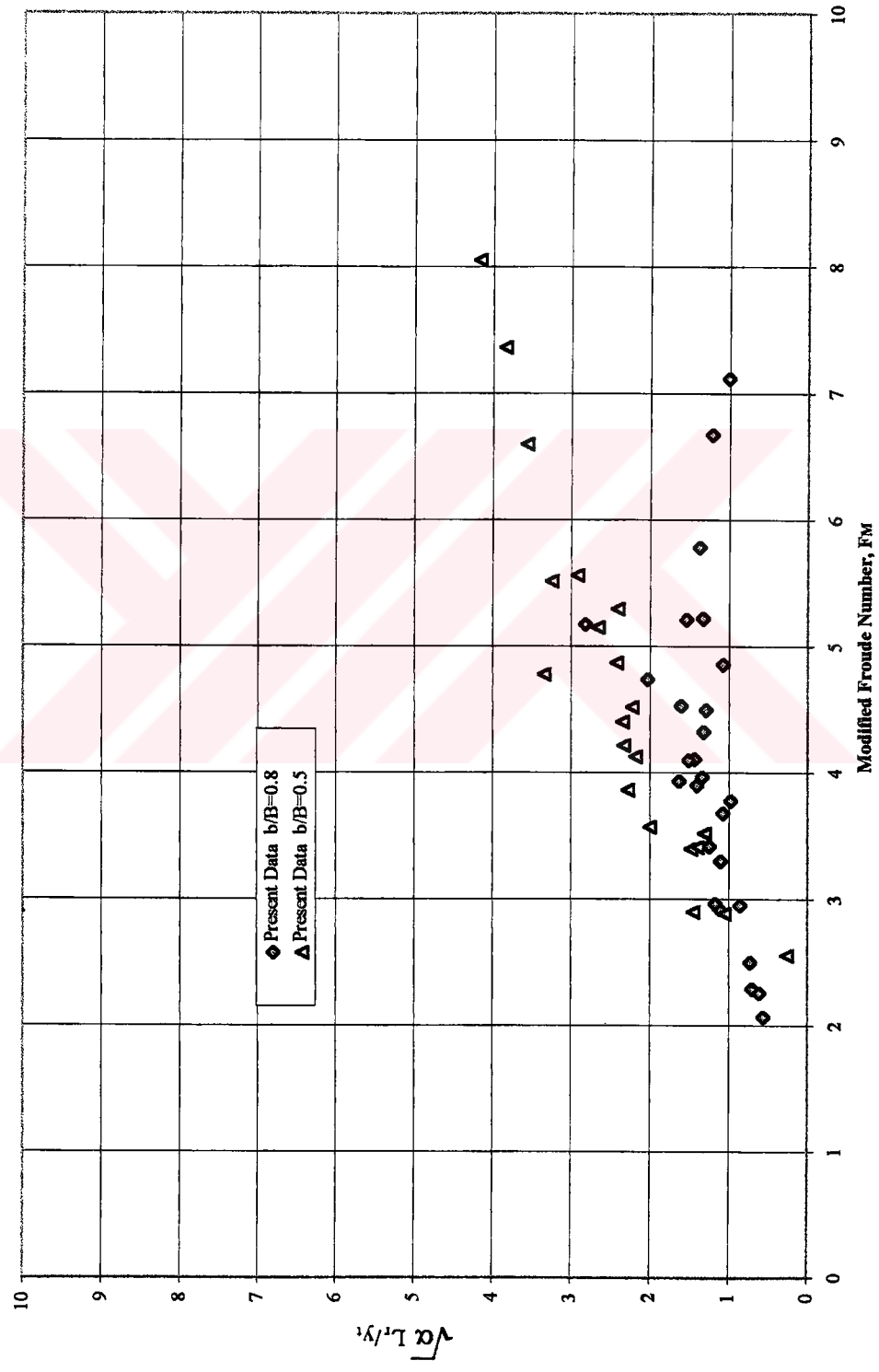
Fig. 4.26   Variation of The Length of Surface Roller of S-Jump
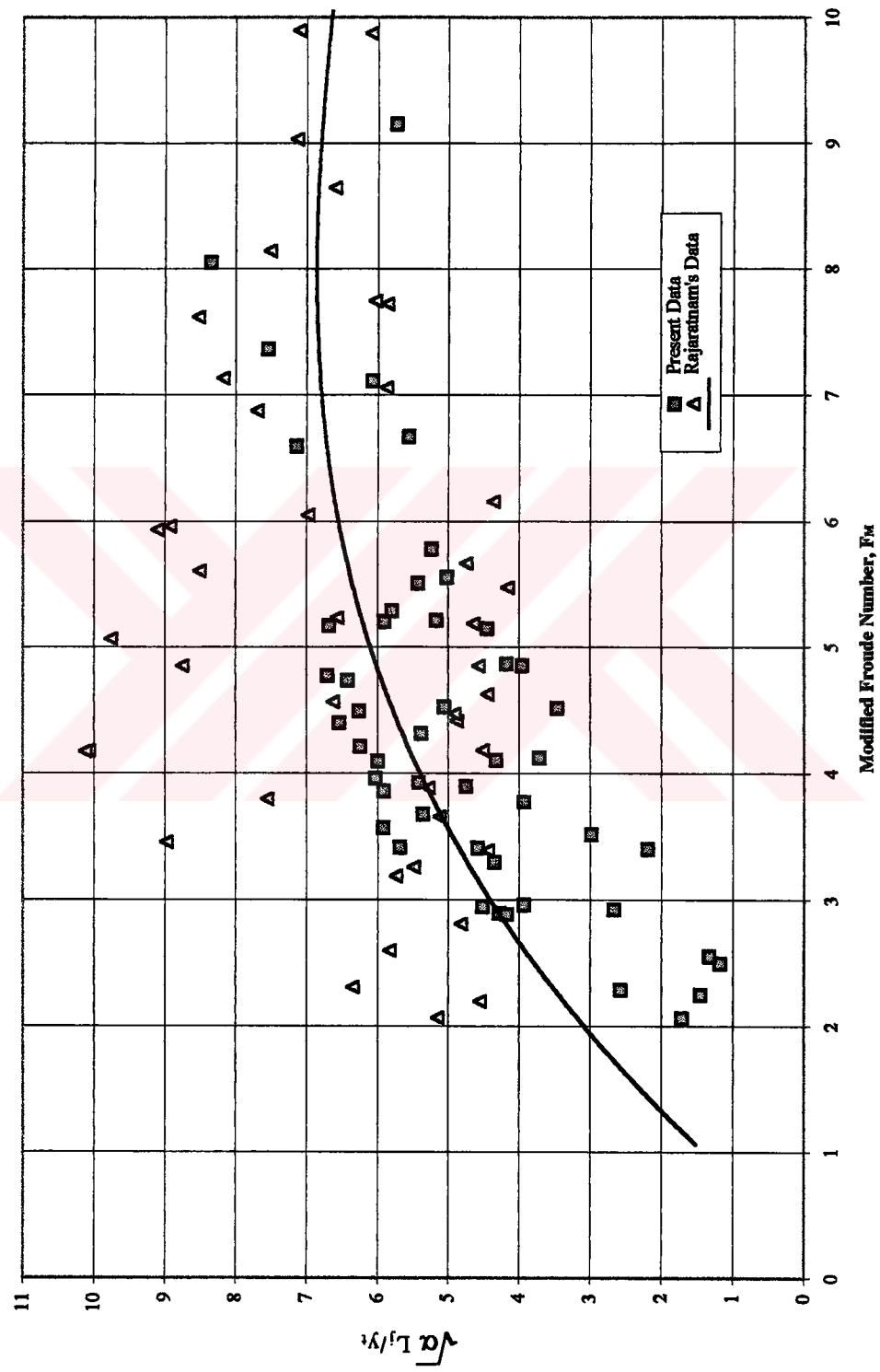
Fig. 4.27   Variation of The Length of S-Jump
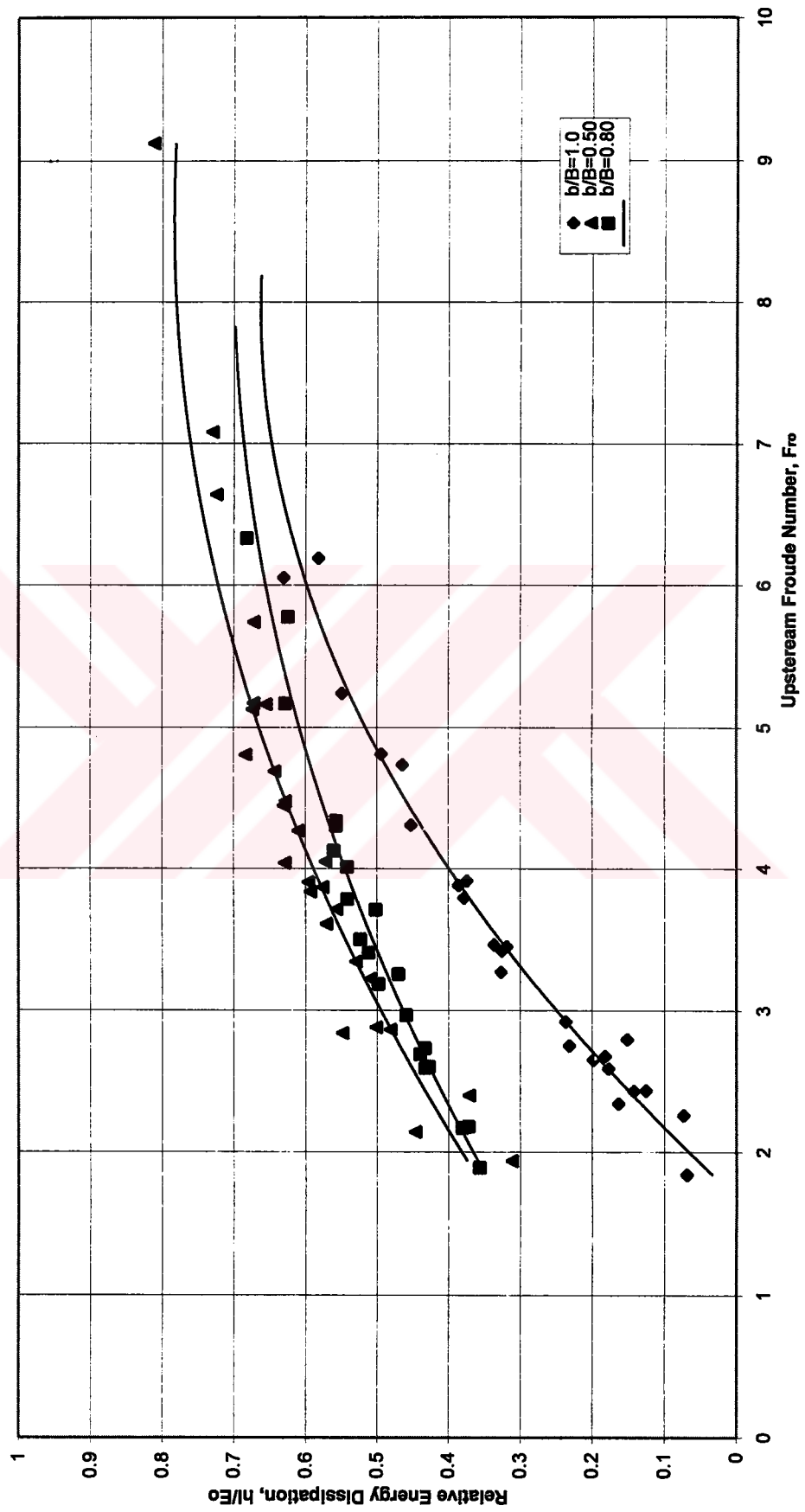
Fig. 4.28   Energy Dissipation Characteristics For S-Jump

94

CHAPTER V

CONCLUSIONS and RECOMMENDATIONS

Conclusions

The following conclusions can be drawn from the present study:

1) Hydraulic jumps at an abrupt enlargement have smaller tailwater depths than the simple hydraulic jump with the same inflow conditions, hence requires shallower stilling basins.

2) Hydraulic jumps at abrupt enlargements possess substantially higher relative energy dissipation than that of a simple hydraulic jump for equal F_{ro}. Consequently, the stilling basins with abrupt enlargements are powerful energy dissipaters.

3) Modified Froude number introduced as $\sqrt{\alpha(1+2F_{ro}^2)}$ is an important factor for scaling hydraulic jumps occurring at abrupt enlargements.

4) For R-jumps, the relative depth ratio can be obtained from $Y = 0.83\sqrt{\alpha(1+2F_{ro}^2)}$ for the range of α tested, $0.30 \leq \alpha \leq 0.83$.

5) For S-jumps, the relative depth ratio can be obtained from $Y = \sqrt{\alpha(1+2F_{ro}^2)}$ for the range of α tested, $0.286 \leq \alpha \leq 0.80$.

Recommendations for future research

1) The hydraulic jump at an abrupt enlargement should be studied numerically.

2) The unstable nonuniform flow between R-jump and S-jump may be studied.

REFERENCES

1)   CHOW, V. T., (1958), 'Open Channel Hydraulics', Mc Graw Hill Book Company, Inc. New York.

2)   HENDERSON, F. M., (1966), 'Open Channel Flow', Mc Millan Publishing C. O. New York.

3)   UNNY, T. E.,(1961), 'The Spatial Hydraulic Jump', Proceedings, 10th International Association for Hydraulic Congress, Belgrade, Yugoslavia, pp.32-42.

4)   RAJARATNAM, N. and SUBRAMANYA, K.,(1968), 'Hydraulic Jumps Below Abrupt Symmetrical Expansions', Proc. ASCE , J. Hydraulic Division , Vol. 94 , HY3 , pp. 481-503.

5)   HERBRAND, K.,(1972), 'The Spatial Hydraulic Jump', Journal Of Hydraulic Research , no. 3 , pp.205-218.

6)   HAGER, W. H.,(1985), 'Hydraulic Jump In Non Prismatic Rectengular Channels', Journal Of Hydraulic   Research, Vol. 23, no. 1 , pp. 21-35.

7)   KUSNETSOW, S. K., (1964), 'Free Horizontal Spread of the Stream Flow in the Tail Water of Hydro Structures', Soviet Hydro Engineering (English Translation) , Israel Program for Scientific Translations, Jerusalem, pp. 346-349.

8)   MAGALHAES, L. E. DE M., and MINTON, P., (1975), 'Design Implications of Hydraulic Jumps At Sudden Enlargements', Proc. Instn. Civ. Engrs., Part 2 , 59 , pp. 169-174.

9)   SMITH, CLIFF D.,(1989), ' The Submerged Hydraulic Jump In An Abrupt Lateral Expansion', Journal Of Hydraulic   Research , Vol. 27, no. 2 , pp. 257-266.

10) ARBHABHIRAMA A.,and ABELLA A.U., (1971),
'Hydraulic Jump Within Gradually Expanding Channel',
Journal of Hydraulic Division,Proc. of ASCE, Vol 97,
HY1, pp. 31-42.

11) FRANCE, P. W., (1981), 'Analysis of the Hydraulic Jump
Within a Diverging Rectengular Channel', Proc. Inst.
Civil Engrs.,Vol 71 , Part II, pp. 369-378.

12) LAWSON , J. D., and PHILLIPS , B.C., (1983), 'Circular
Hydraulic Jump', Proc. ASCE., J. Hydraulic Engineering
Vol. 109, Nr. 4, pp. 505-518.

13) KOLOSEUS, H.J. and AHMAD, D., (1969), 'Circular
Hydraulic Jump', Proc. ASCE., J. Hydraulic Division,
Vol. 95, HY1 , pp. 1065-1078.

14) GÜR, ZERRİN, (1988), ' The Hydraulic Jump At An Abrupt
Drop', A Master's Thesis In Civil Engineering Middle East
Technical University.

APPENDIX

Table A.1   Classical Jump Data Taken In This Study.   α=1.0

yo (cm)	yt (cm)	yt/yo	Q (lt/s)	Fro	L1 (cm)	Lj (cm)	Lr (cm)	Eo (cm)	Et (cm)
1.8	5.7	3.17	4.6	2.43	72	20	13	0.071	0.062
1.7	5.6	3.29	4.6	2.65	37	20	13	0.077	0.062
1.7	6.64	3.91	4.9	2.79	35	28	18	0.083	0.071
1.75	6.03	3.45	4.9	2.68	61	28	18	0.080	0.066
1.6	8.2	5.13	6.2	3.91	52	40	28	0.138	0.087
1.6	10	6.25	7.5	4.73	70	50	35	0.195	0.105
1.5	12.2	8.13	8.9	6.19	50	70	50	0.302	0.126
1.9	11.8	6.21	9.0	4.39	122	68	46	0.202	0.123
1.45	12.8	8.83	9.0	6.58	50	70	50	0.329	0.132
2.1	11.6	5.52	10.0	4.20	120	50	30	0.206	0.122
1.8	13.3	7.39	11.0	5.82	65	75	55	0.323	0.139
1.8	13.6	7.56	11.2	5.92	60	80	55	0.334	0.142
1.75	13.6	7.77	11.2	6.18	55	75	55	0.352	0.142
2	7.85	3.93	6.2	2.80	60	24	13	0.098	0.084
2.4	8.9	3.71	8.5	2.92	135	55	20	0.126	0.096
2.7	12	4.44	12.0	3.45	210	100	45	0.188	0.128
2.5	12.3	4.92	12.0	3.88	170	75	50	0.213	0.131
2.4	14.5	6.04	14.0	4.81	140	100	70	0.301	0.153
1.9	15.05	7.92	13.4	6.05	21	95	55	0.425	0.157
2.2	13.9	6.32	13.4	5.24	127	63	45	0.325	0.147
2.2	11.65	5.30	11.0	4.31	110	40	30	0.226	0.124
2.26	9.73	4.31	9.1	3.42	114	41	26	0.155	0.104

Table A.1 'Continued'

Yo (cm)	Yt (cm)	Yt/yo	Q (lt/s)	Fro	L1 (cm)	Lj (cm)	Lr (cm)	Eo (cm)	Et (cm)
2.3	7.65	3.33	7.5	2.75	113	25	15	0.110	0.084
2.2	6.76	3.07	6.2	2.43	40	15	8	0.087	0.074
2.7	15.55	5.76	16.0	4.61	130	80	50	0.313	0.164
2.6	14.8	5.69	15.0	4.57	112	68	47	0.297	0.156
2.7	10.9	4.04	11.0	3.17	140	39	26	0.162	0.117
2.8	11	3.93	12.0	3.27	130	50	30	0.178	0.120
3.2	15.3	4.78	17.0	3.79	180	100	60	0.262	0.163
2.8	9.15	3.27	9.5	2.59	60	30	20	0.122	0.100
3.5	9.7	2.77	12.0	2.34	110	30	20	0.131	0.109
3.4	14.7	4.32	17.0	3.46	140	80	50	0.238	0.158
4.25	12.8	3.01	15.5	2.26	145	55	40	0.151	0.140

Table A.2 R-Jump Data Taken In This Study For α=0.80

yg (cm)	b/B	Q (lt/s)	Fro	yo (cm)	y3 (cm)	yt (cm)	yt/yo	Lo (cm)	L1 (cm)	Lt (cm)	Lj (cm)	Eo (cm)	Et (cm)
2	0.8	7.50	6.33	1.53	0.06	10.30	6.73	8	85	35	85	0.321	0.107
2	0.8	7.50	6.33	1.53	0.06	10.55	6.90	8	60	38	80	0.321	0.110
2	0.8	6.85	5.78	1.53	0.06	9.80	6.41	8	38	33	74	0.271	0.102
2	0.8	5.23	4.13	1.60	0.06	7.70	4.81	5	40	23	48	0.152	0.081
3	0.8	11.00	5.17	2.26	0.12	12.40	5.49	9	111	45	85	0.324	0.130
3	0.8	11.00	5.17	2.26	0.12	12.80	5.66	9	49	41	66	0.324	0.134
3	0.8	9.60	4.34	2.32	0.13	11.45	4.94	7	82	35	78	0.241	0.120
3	0.8	8.00	3.78	2.25	0.14	9.33	4.15	6	66	23	40	0.184	0.099
3	0.8	5.50	2.64	2.23	0.24	6.13	2.75	3	50	15	26	0.100	0.068
4	0.8	14.00	4.30	3.00	0.09	14.20	4.73	10	110	45	80	0.307	0.150
4	0.8	14.00	4.30	3.00	0.10	14.40	4.80	10	80	45	85	0.307	0.152
4	0.8	14.00	4.30	3.00	0.10	15.30	5.10	10	30	59	85	0.307	0.160
4	0.8	12.60	4.01	2.93	0.10	13.35	4.56	9	108	40	85	0.265	0.141
4	0.8	12.60	4.03	2.92	0.10	13.90	4.76	9	62	44	77	0.266	0.146
4	0.8	11.00	3.50	2.93	0.09	11.20	3.82	9	78	30	47	0.209	0.120
4	0.8	11.00	3.48	2.94	0.09	11.60	3.95	9	50	31	50	0.208	0.123
4	0.8	9.60	3.19	2.85	0.09	9.96	3.49	6	45	25	43	0.173	0.107
4	0.8	7.90	2.59	2.87	0.36	7.65	2.67	4	45	16	24	0.125	0.085
6	0.8	20.00	3.71	4.20	0.10	17.00	4.05	9	95	52	140	0.331	0.181
6	0.8	18.00	3.26	4.27	0.10	15.00	3.51	8	110	42	90	0.269	0.162
6	0.8	18.00	3.26	4.27	0.10	15.50	3.63	8	45	40	90	0.269	0.166
6	0.8	16.00	2.97	4.20	0.16	12.45	2.96	7	132	32	83	0.227	0.138
6	0.8	16.00	2.97	4.20	0.16	13.10	3.12	7	105	34	85	0.227	0.143
6	0.8	16.00	2.97	4.20	0.15	13.45	3.20	7	48	38	86	0.227	0.146
6	0.8	13.54	2.60	4.10	0.50	11.17	2.72	5	43	28	65	0.180	0.124
6	0.8	11.13	2.18	4.05	1.20	9.40	2.32	7	21	22	55	0.137	0.105
7	0.8	23.16	3.41	4.90	0.10	17.80	3.63	9	102	50	124	0.334	0.192
7	0.8	11.50	1.89	4.55	2.20	8.90	1.96	5	35	14	35	0.127	0.103
7	0.8	13.85	2.17	4.70	1.95	10.40	2.21	5	31	22	55	0.158	0.118
7	0.8	18.00	2.73	4.80	0.15	13.50	2.81	7	100	32	86	0.227	0.149

Table A.3   R-Jump Data Taken In This Study, α=0.50

y_B (cm)	b/B	Q (lt/s)	Fr_o	y_o (cm)	y_3 (cm)	y_t (cm)	y_t/y_o	L_o (cm)	L_i (cm)	L_r (cm)	L_j (cm)	E_o (cm)	E_i (cm)
1.5	0.5	3.85	6.63	1.30	0.16	6.60	5.08	15	82	22	78	0.2991	0.0688
1.5	0.5	3.33	5.74	1.30	0.20	6.15	4.73	14	70	19	56	0.2270	0.0639
1.5	0.5	3.00	5.17	1.30	0.20	5.45	4.19	10	54	15	48	0.1867	0.0570
1.5	0.5	2.82	4.80	1.31	0.20	4.20	3.21	9	60				0.0457
2.0	0.5	4.88	5.16	1.80	0.18	7.67	4.26	17	69	24	60	0.2578	0.0800
2.0	0.5	4.20	4.44	1.80	0.12	6.75	3.75	15	65	19	57	0.1956	0.0707
2.0	0.5	3.08	3.71	1.65	0.15	4.75	2.88	10	65	13	35	0.1302	0.0509
2.0	0.5	2.08	2.40	1.70	0.21	3.40	2.00	8	46	8	10	0.0658	0.0371
3.0	0.5	7.00	5.13	2.30	0.13	9.50	4.13	17.5	105	33	82	0.3251	0.0994
3.0	0.5	7.00	5.13	2.30	0.13	9.90	4.30	17.5	62	34	83	0.3251	0.1031
3.0	0.5	6.50	4.76	2.30	0.16	8.65	3.76	17	95	27	70	0.2835	0.0911
3.0	0.5	6.50	4.76	2.30	0.16	8.90	3.87	17	72	27	72	0.2835	0.0933
3.0	0.5	5.10	4.05	2.18	0.15	6.93	3.18	13	74	21	56	0.2003	0.0737
3.0	0.5	3.70	2.84	2.23	0.20	5.32	2.39	9	28	15	29	0.1121	0.0571
4.0	0.5	9.10	4.47	3.00	0.14	11.60	3.87	18	50	37	107	0.3301	0.1210
4.0	0.5	8.50	4.26	2.96	0.20	10.75	3.63	17	43	34	90	0.2986	0.1126
4.0	0.5	7.35	3.90	2.85	0.20	9.00	3.16	14	75	28	75	0.2455	0.0954
4.0	0.5	6.62	3.61	2.80	0.24	8.30	2.96	12	43	23	72	0.2103	0.0882
4.0	0.5	5.45	2.88	2.86	0.35	6.81	2.38	9	27	18	45	0.1471	0.0733
4.0	0.5	4.20	2.14	2.93	0.33	4.70	1.60	7	59	9	18	0.0963	0.0535
5.0	0.5	11.25	4.04	3.70	0.18	11.35	3.07	17	95	35	115	0.3386	0.1215
5.0	0.5	10.00	3.83	3.54	0.21	10.75	3.04	15	77	28	85	0.2957	0.1146
5.0	0.5	10.00	3.83	3.54	0.21	11.30	3.19	15	28	32	82	0.2957	0.1194
5.0	0.5	8.50	3.34	3.48	0.30	10.10	2.90	13	33	26	70	0.2294	0.1068
5.0	0.5	7.50	2.86	3.55	0.30	8.00	2.25	11	74	16	66	0.1811	0.0872
5.0	0.5	7.50	2.86	3.55	0.30	8.60	2.42	11	23	17	57	0.1811	0.0922
5.0	0.5	5.33	1.94	3.67	0.38	6.00	1.63	6	21	12	32	0.1055	0.0664
6.0	0.5	13.50	3.87	4.30	0.13	13.70	3.19	18	87	45	130	0.3645	0.1449
6.0	0.5	10.86	3.22	4.20	0.30	10.70	2.55	13	91	25	90	0.2601	0.1154
6.0	0.5	7.20	2.18	4.15	0.43	6.95	1.67	6	67	13	45	0.1397	0.0783

Table A.4 R-Jump Data Taken In This Study, $\alpha=0.30$

y_g (cm)	b/B	Q (lt/s)	Fr_o	y_o (cm)	y_3 (cm)	y_t (cm)	y_t/y_o	L_o (cm)	L_1 (cm)	L_r (cm)	L_j (cm)	E_o (cm)	E_t (cm)
2	0.30	2.7	3.11	2.35		5.6	2.38	10	70	10	20	0.137	0.076
3	0.30	2.8	1.80	3.47		4.8	1.38	10	60	8	15	0.091	0.077
3	0.30	4.0	3.00	3.10		6.6	2.11	14	60	18	35	0.171	0.097
3	0.30	4.5	3.20	3.24		7.4	2.27	18	79	21	35	0.198	0.106
3	0.30	4.5	3.20	3.24		7.7	2.37	18	39	26	40	0.198	0.106
3	0.30	4.8	2.83	3.67		7.1	1.93	18	88	16	31	0.184	0.110
3	0.30	4.5	3.03	3.36		8.0	2.39	16	40	28	40	0.188	0.107
4	0.30	4.8	3.12	3.44		7.2	2.08	10	50	17	32	0.202	0.110
4	0.30	6.0	3.03	4.07		9.0	2.21	19	56	30	44	0.228	0.128
5	0.30	7.4	3.21	4.50		10.0	2.21	19	73	31	59	0.277	0.147
5	0.30	7.4	3.21	4.50		9.8	2.17	19	95	23	40	0.277	0.147
5	0.30	7.4	3.21	4.50		10.9	2.42	19	20	49	37	0.277	0.149
5	0.30	6.0	2.70	4.40		7.6	1.73	15	95	15	30	0.204	0.129
5	0.30	6.0	2.70	4.40		8.3	1.89	15	43	24	41	0.204	0.128
5	0.30	6.0	2.70	4.40		8.6	1.95	13	20	33	47	0.204	0.128
5	0.30	4.0	1.80	4.40		5.4	1.22	9	36	11	18	0.115	0.102
5	0.30	4.0	1.80	4.40		5.6	1.27	9	28	14	20	0.115	0.100
5	0.30	2.7	1.53	3.77		4.4	1.17	8	13	11	17	0.082	0.076
6	0.30	8.5	2.96	5.21	0.21	10.4	2.00	17	85	35	75	0.281	0.161
6	0.30	8.5	2.97	5.20	0.21	11.0	2.12	17	52	36	78	0.282	0.161
6	0.30	8.5	2.96	5.21	0.21	11.3	2.16	17	25	50	70	0.281	0.162
6	0.30	7.0	2.52	5.10	0.24	8.6	1.69	14	74	20	38	0.213	0.143
6	0.30	7.0	2.52	5.10	0.24	9.0	1.76	14	40	26	50	0.213	0.142
6	0.30	6.7	2.52	4.95	0.23	7.6	1.54	13	75	21	34	0.207	0.143
6	0.30	6.7	2.52	4.95	0.23	8.4	1.69	13	34	26	39	0.207	0.139
6	0.30	4.7	1.60	5.25	0.63	6.2	1.18	10	41	14	25	0.120	0.110
6	0.30	4.7	1.60	5.25	0.63	6.6	1.26	10	15	18	28	0.120	0.109
7	0.30	4.7	1.74	4.97	1.10	5.9	1.18	10	40	10	17	0.125	0.113
7	0.30	3.8	1.45	4.90	1.20	5.0	1.02	8	23	8	12	0.101	0.100
7	0.30	10.0	2.89	5.90	0.19	11.9	2.02	19	42	45	62	0.306	0.180
7	0.30	10.0	2.89	5.90	0.19	11.4	1.93	19	85	40	65	0.306	0.180
7	0.30	7.4	2.09	6.00	0.33	7.9	1.32	12	77	17	25	0.191	0.154

Table A.5   S-Jump Data Taken In This Study, $\alpha=0.80$

y_B (cm)	b/B	Q (lt/s)	F_{ro}	y_2 (cm)	y_3 (cm)	y_1 (cm)	y_1/y_o	L_r (cm)	L_j (cm)	E_o (cm)	E_t (cm)
2	0.8	7.50	6.33	1.53	7.5	11.8	7.71	55	110	0.381	0.121
2	0.8	6.85	5.78	1.53	5.6	11.4	7.45	49	96	0.311	0.117
2	0.8	5.23	4.13	1.60	6.4	8.5	5.31	23	55	0.200	0.088
3	0.8	11.00	5.17	2.26	8.3	13.8	6.11	55	110	0.385	0.143
3	0.8	9.60	4.34	2.32	8.2	12.9	5.54	42	72	0.300	0.133
3	0.8	8.00	3.78	2.25	7.4	10.3	4.58	28	48	0.235	0.108
3	0.8	5.50	2.69	2.20	6.2	7.5	3.41	11	25	0.142	0.079
4	0.8	14.00	4.30	3.00	10.8	16.5	5.50	60	100	0.385	0.171
4	0.8	12.60	4.01	2.93	10.6	15.1	5.15	45	75	0.342	0.157
4	0.8	11.00	3.50	2.93	9.4	12.4	4.23	31	48	0.274	0.130
4	0.8	9.60	3.19	2.85	8.0	10.6	3.72	26	44	0.225	0.113
4	0.8	7.90	2.59	2.87	7.3	9.0	3.14	15	22	0.170	0.096
6	0.8	20.00	3.71	4.20	10.5	18.7	4.45	70	140	0.394	0.196
6	0.8	18.00	3.26	4.27	11.5	17.2	4.03	45	120	0.341	0.181
6	0.8	16.00	2.97	4.20	10.7	14.9	3.54	38	98	0.292	0.158
6	0.8	13.54	2.60	4.10	9.9	12.7	3.10	20	65	0.238	0.136
6	0.8	11.13	2.18	4.05	8.5	10.5	2.58	17	50	0.181	0.114
7	0.8	23.16	3.41	4.90	10.8	17.8	3.63	47	130	0.393	0.192
7	0.8	11.50	1.89	4.55	9.2	10.1	2.22	3	15	0.173	0.112
7	0.8	13.85	2.17	4.70	9.8	11.8	2.51	14	55	0.209	0.129
7	0.8	18.00	2.73	4.80	10.8	15.1	3.15	34	100	0.287	0.163

Table A.6 S-Jump Data Taken In This Study, $\alpha=0.50$

y_g (cm)	b/B	Q (l/s)	F_{r0}	y_2 (cm)	y_3 (cm)	y_t (cm)	y_t/y_0	L_r (cm)	L_j (cm)	E_0 (cm)	E_x (cm)
1	0.5	2.75	9.12	0.84	5.0	7.4	8.81	10	60	0.400	0.075
1	0.5	2.21	7.08	0.86	4.7	7.0	8.14	10	60	0.262	0.071
1.5	0.5	3.85	6.63	1.30	7.4	9.8	7.54	17	77	0.360	0.099
1.5	0.5	3.33	5.74	1.30	7.0	9.2	7.08	18	68	0.284	0.093
1.5	0.5	3.00	5.17	1.30	5.6	7.4	5.69	14	54	0.230	0.075
1.5	0.5	2.82	4.80	1.31	4.1	5.9	4.50	9	33	0.192	0.061
2	0.5	4.88	5.16	1.80	9.5	11.4	6.33	25	95	0.335	0.115
2	0.5	4.20	4.44	1.80	6.3	8.7	4.83	16	77	0.241	0.089
2	0.5	3.08	3.71	1.65	5.2	7.2	4.36	10	40	0.166	0.073
2	0.5	2.08	2.40	1.70	3.0	4.8	2.82	5	8	0.079	0.050
3	0.5	7.00	5.13	2.30	8.9	12.5	5.43	50	118	0.391	0.128
3	0.5	6.40	4.69	2.30	8.5	11.8	5.13	34	107	0.338	0.120
3	0.5	5.10	4.05	2.18	7.8	10.8	4.95	22	66	0.257	0.110
3	0.5	3.70	2.84	2.23	6.8	6.9	3.09	11	26	0.158	0.071
4	0.5	9.10	4.47	3.00	9.6	14.4	4.80	33	103	0.396	0.147
4	0.5	8.50	4.26	2.96	9.3	13.8	4.66	26	105	0.362	0.141
4	0.5	7.35	3.90	2.85	9.0	12.1	4.25	23	103	0.307	0.124
4	0.5	6.62	3.61	2.80	8.3	11.1	3.96	17	84	0.265	0.114
4	0.5	5.43	2.88	2.86	6.8	9.0	3.15	15	50	0.186	0.093
4	0.5	4.20	2.14	2.93	6.2	6.8	2.33	6	14	0.129	0.071
5	0.5	11.25	4.04	3.70	10.0	14.4	3.89	31	122	0.402	0.149
5	0.5	10.00	3.83	3.54	9.4	14.0	3.95	28	94	0.354	0.144
5	0.5	8.50	3.34	3.48	8.8	13.0	3.72	23	104	0.283	0.133
5	0.5	7.50	2.86	3.55	8.2	11.5	3.23	14	73	0.228	0.118
5	0.5	5.33	1.94	3.67	6.2	8.7	2.37	7	21	0.131	0.090
6	0.5	13.50	3.87	4.30	10.6	17.7	4.10	41	135	0.428	0.181
6	0.5	10.86	3.22	4.20	10.2	15.3	3.64	24	94	0.320	0.157
6	0.5	7.20	2.18	4.15	8.4	11.0	2.65	11	40	0.182	0.113

Table A.7   Rajaratnam's Data For R-Jump

b/B	F$_{ro}$	y$_t$, in inches	Y	L$_j$, in inches	L$_r$, in inches
0.5	4.13	3.7	3.43	26	14
0.5	5.45	4.9	4.54	26	17
0.5	6.33	5.7	5.28	35	17
0.5	7.02	6.6	6.11	53	19
0.5	8	7.3	6.76	56	20
0.5	8.88	8.2	7.6	70	28
0.5	2.4	2.4	2.22	15	6
0.5	2.94	2.7	2.5	15	9
0.5	4.6	4.2	3.89	32	15
0.33	3.38	2.9	2.32	44	9
0.33	4.52	3.8	3.04	65	11
0.33	5.78	4.6	3.68	41	14
0.33	6.97	5.8	4.64	47	22
0.33	8	6.4	5.11	43	24
0.33	8.22	6.7	5.35	41	26
0.33	5.02	4.2	3.36	46	16
0.33	3.88	3.2	2.56	23	10
0.33	2.53	5.5	1.78	36	12
0.33	3.14	6.9	2.22	34	14
0.33	3.73	8.3	2.68	38	21
0.33	4.32	9.3	3	55	24
0.33	2.2	2.5	1.54	30	6
0.33	3.22	3.6	2.21	34	10
0.33	4.29	4.9	3.01	30	14
0.33	5.25	5.8	3.56	32	19
0.33	6.91	7.3	4.48	49	24
0.33	6.01	6.4	3.92	47	20
0.67	2.56	2.4	2.26	21	4
0.67	3.86	3.8	3.59	35	8
0.67	4.84	4.9	4.62	70	15
0.67	5.58	5.6	5.28	56	19
0.67	6.11	6.2	5.85	58	22
0.67	6.76	6.9	6.5	57	22.5
0.67	7.54	7.7	7.26	60	30
0.67	8.61	8.7	8.2	68	28
0.67	3.44	3.4	3.2	26	8
0.83	2.77	3.2	2.93	16	8
0.83	3.67	4.2	3.85	43	12
0.83	4.56	5.4	4.95	53	17
0.83	5.24	6.2	5.69	48	20
0.83	6.05	7.2	6.6	50.5	26
0.83	7.02	8.3	7.62	70	36
0.83	7.9	9.6	8.8	77.5	42

Table A.8   Rajaratnam's Data For S-Jump

b/B	F_{ro}	y_o, in inches	y_3, in inches	y_t, in inches	Y	L_j, in inches
0.50	4.51	1.08	4.60	6.40	5.93	60
0.50	5.19	1.08	4.80	7.10	6.57	66
0.50	6.01	1.08	4.70	7.70	7.13	76
0.50	7.02	1.08	5.40	8.90	8.24	74
0.50	7.71	1.08	5.40	9.60	8.89	82
0.50	3.73	1.08	4.50	5.80	5.37	62
0.50	7.69	1.08	5.50	9.40	8.70	78
0.50	1.94	2.65	4.50	6.30	2.38	46
0.50	2.50	2.65	5.60	8.00	3.02	66
0.50	3.18	2.65	5.80	9.00	3.40	70
0.50	3.82	2.65	7.50	10.70	4.04	80
0.50	4.36	2.65	8.80	12.30	4.64	85
0.50	4.80	2.65	8.90	13.60	5.13	88
0.33	2.75	1.25	4.00	4.70	3.76	52
0.33	3.86	1.25	4.50	5.60	4.48	56
0.33	4.44	1.25	5.15	6.50	5.20	58
0.33	5.46	1.25	4.90	7.00	5.60	60
0.33	6.35	1.25	5.50	7.90	6.32	64
0.33	6.94	1.25	5.60	8.70	6.96	72
0.33	7.55	1.25	5.90	9.20	7.36	70
0.33	2.61	1.69	5.40	6.30	3.73	50
0.33	3.38	1.69	5.70	6.90	4.08	58
0.33	4.11	1.69	5.90	8.00	4.73	62
0.33	5.10	1.69	6.00	8.90	5.27	70
0.33	5.65	1.69	6.60	9.80	5.80	76
0.33	6.70	1.69	7.60	11.30	6.69	82
0.67	3.54	1.06	3.60	5.20	4.91	64
0.67	4.32	1.06	3.50	5.70	5.38	68
0.67	5.10	1.06	3.70	6.60	6.23	72
0.67	6.12	1.06	3.90	7.60	7.17	76
0.67	7.00	1.06	4.00	8.50	8.02	78
0.67	7.77	1.06	4.20	9.40	8.87	82
0.67	8.50	1.06	4.70	10.20	9.62	76
0.67	2.90	1.06	2.75	4.10	3.87	45
0.67	4.79	1.06	3.60	6.15	5.80	64
0.83	3.16	1.09	2.50	4.50	4.13	50
0.83	3.70	1.09	2.60	5.20	4.77	50
0.83	6.67	1.09	3.80	9.10	8.35	66
0.83	4.55	1.09	3.00	6.20	5.69	62
0.83	5.29	1.09	3.30	7.10	6.51	60
0.83	5.87	1.09	3.50	7.90	7.25	74
0.83	7.65	1.09	3.60	10.00	9.17	78

Table A.9   Herbrand's Data For S-Jump

F_{ro}	b/B	Y	b/B	Y	b/B	Y	b/B	Y
3.03	1	3.78	0.714	3.5	0.5	2.97	0.286	2.44
3.48	1	4.33	0.714	3.94	0.5	3.33	0.286	2.78
3.67	1	4.78	0.714	4.35	0.5	3.67	0.286	2.97
3.87	1	4.86	0.714	4.39	0.5	3.73	0.286	2.98
4.19	1	5.25	0.714	4.75	0.5	4.07	0.286	3.18
4.19	1	5.39	0.714	4.87	0.5	4.12	0.286	3.29
4.19	1	5.47	0.714	4.97	0.5	4.18	0.286	3.39
4.49	1	5.61	0.714	5.11	0.5	4.34	0.286	3.39
4.54	1	6.08	0.714	5.44	0.5	4.5	0.286	3.56
4.64	1	6.01	0.714	5.44	0.5	4.5	0.286	3.56
5.06	1	6.51	0.714	5.83	0.5	4.94	0.286	3.9
5.14	1	6.84	0.714	6.11	0.5	5.13	0.286	4.16
5.28	1	7.06	0.714	6.22	0.5	5.2	0.286	4.78
5.42	1	7.01	0.714	6.34	0.5	5.25	0.286	4.22
5.65	1	7.54	0.714	6.67	0.5	5.73	0.286	4.5
5.89	1	8.01	0.714	7.11	0.5	6.16	0.286	5.18
6.17	1	8.1	0.714	7.11	0.5	6.3	0.286	4.83
6.62	1	8.74	0.714	7.61	0.5	6.61	0.286	5.11
6.5	1	8.87	0.714	7.83	0.5	6.84	0.286	5.58
7.14	1	9.57	0.714	8.57	0.5	7.3	0.286	5.86
7.65	1	10.37	0.714	9.09	0.5	7.78	0.286	6.22